

**SYNTHESIS AND CHARACTERIZATION OF NOVEL POLYURETHANE DRUG
DELIVERY SYSTEMS**

by

Wesley N. Sivak

BS, University of Dayton, 1999

Submitted to the Graduate Faculty of
School of Engineering in partial fulfillment
of the requirements for the degree of
Doctor of Philosophy

University of Pittsburgh

2007

UNIVERSITY OF PITTSBURGH
SCHOOL OF ENGINEERING

This dissertation was presented

by
Wesley N. Sivak

It was defended on

July 6, 2007

and approved by

Xinyan Tracy Cui, PhD, Assistant Professor, Bioengineering Department

William R. Wagner, PhD, Professor, Bioengineering, Chemical & Petroleum Engineering,
and Surgery Departments

William C. Zamboni, PharmD, PhD, Assistant Professor, Pharmaceutical Sciences
Department

Dissertation Director: Eric J. Beckman, PhD, Bayer Professor, Chemical & Petroleum
Engineering Department

Copyright © by Wesley N. Sivak

2007

SYNTHESIS AND CHARACTERIZATION OF NOVEL POLYURETHANE DRUG DELIVERY SYSTEMS

Wesley N. Sivak, PhD

University of Pittsburgh, 2007

Selective delivery of drugs to localized regions of tissue within the body is a complex problem, representing one path through which the efficacy of many pharmaceutical compounds can be enhanced. Many pharmaceutical compounds show excellent activity *in vitro*, but their uses are severely limited *in vivo*. Unstable active conformations, limited membrane diffusion, rapid metabolism and/or clearance, decreased solubility, and dose-limiting systemic toxicity are just a few areas in which potential problems exist, halting drug development. Compounds exist possessing ideal pharmacologic activity for treating specific disease states, but they are simply unable to be delivered in adequate quantities or in the proper active conformation to the target site in the body. The following dissertation details the synthesis, characterization, and performance of a series of polyurethane drug delivery systems based on amino acids and the simple carbohydrates. The materials were synthesized from lysine diisocyanate (LDI) and glycerol with the aid of various tertiary amine and organometallic urethane catalysts. Candidate drugs were incorporated into the materials by way of labile urethane and urea linkages; subsequent drug release relied on the passive hydrolysis of the tethering bonds. Drug release from the materials correlated to material morphology, urethane catalyst, and chemical functionality of the incorporated drug. A single-phase polyurethane material was designed, synthesized, and shown capable of simultaneously releasing multiple pharmacologic agents at different rates. Finally, naturally occurring ionic ligands were incorporated into the LDI-glycerol polyurethanes to alter their swelling characteristics and release kinetics. This endeavor has resulted in the formulation of a series of polyurethane materials, capable of long-term controlled release of pharmacologic agents within the body. The structure-function relationships elucidated provide key design criteria, which can ultimately be used to develop such advanced degradable polyurethane materials.

TABLE OF CONTENTS

PREFACE	XX
1.0 INTRODUCTION.....	1
1.1 POLYURETHANES.....	5
1.1.1 Polyurethane synthesis.....	6
1.1.2 Polyurethane catalysis.....	9
1.2 DRUG DELIVERY	12
1.2.1 Systemic delivery.....	14
1.2.2 Localized delivery.....	17
1.2.3 Biodegradable systems	20
2.0 LDI-GLYCEROL POLYURETHANE IMPLANTS EXHIBIT CONTROLLED RELEASE OF DB-67 AND ANTI-TUMOR ACTIVITY <i>IN VITRO</i> AGAINST MALIGNANT GLIOMAS.....	24
2.1 ABSTRACT.....	24

2.2	INTRODUCTION	25
2.3	MATERIAL AND METHODS	27
2.3.1	Materials.....	27
2.3.2	Reaction of DB-67 with LDI	27
2.3.3	Synthesis of the LDI-glycerol Polyurethane containing DB-67	27
2.3.4	Distribution of DB-67.....	28
2.3.5	Stability of DB-67 in Aqueous Solution	29
2.3.6	In vitro Release of DB-67	29
2.3.7	Effect of Polyurethane Tablets on Cellular Proliferation.....	30
2.4	RESULTS AND DISCUSSION	30
2.4.1	Reaction of DB-67 and LDI.....	30
2.4.2	Characterization of LDI-Glycerol Tablets	32
2.4.3	In vitro Drug Release	37
2.4.4	Cytotoxicity Assays	39
2.5	CONCLUSIONS	41

3.0	LDI-GLYCEROL POLYURETHANE FOAMS DEMONSTRATE CATALYST-DEPENDENT CONTROLLED RELEASE PROFILES AND EXHIBIT ANTI-TUMOR ACTIVITY AGAINST MALIGNANT GLIOMA CELLS	42
3.1	ABSTRACT.....	42
3.2	INTRODUCTION.....	43
3.3	MATERIAL AND METHODS.....	44
3.3.1	Materials.....	44
3.3.2	Urethane Catalyst Toxicity	45
3.3.3	Reaction of LDI with DB-67: DMDEE vs. DABCO.....	46
3.3.4	Synthesis of LDI-glycerol polyurethane foams	46
3.3.5	Distribution of DB-67 within the polyurethane foams.....	47
3.3.6	Release of DB-67 from LDI-glycerol Foams.....	47
3.3.7	Effect of Polyurethane Foams on Cellular Proliferation	47
3.4	RESULTS	48
3.4.1	Urethane Catalyst Toxicity	48
3.4.2	Reactivity of DB-67 and LDI with DMDEE or DABCO	50
3.4.3	Characterization of LDI-Glycerol Foams	52

3.4.4	DB-67 Release from Polyurethane Foams.....	54
3.4.5	Polyurethane Foam Cytotoxicity	57
3.5	DISCUSSION.....	59
3.6	CONCLUSIONS	61
4.0	CHEMICAL STRUCTURE AND FUNCTIONALITY OF A DRUG DICTATES ITS CONTROLLED-RELEASE PROFILE FROM DEGRADABLE LDI-GLYCEROL POLYURETHANE FOAMS: A STUDY ON NAPHTHALENE AND RELATED COMPOUNDS	63
4.1	ABSTRACT.....	63
4.2	INTRODUCTION.....	64
4.3	MATERIALS AND METHODS	65
4.3.1	Materials.....	65
4.3.2	Excitation-emission spectra of naphthalene compounds	66
4.3.3	Naphthalene fluorescence stability	66
4.3.4	Synthesis of Naphthalene Foams	66
4.3.5	Evaluation of foam architecture by SEM.....	67
4.3.6	Distribution of naphthalene compounds within polyurethane	67

4.3.7	Naphthalene Release	68
4.4	RESULTS	68
4.4.1	Excitation-emission spectra of naphthalene compounds	68
4.4.2	Naphthalene fluorescence stability	70
4.4.3	Polyurethane foams: SEM Analysis and Distribution	71
4.4.4	Naphthalene release	75
4.5	DISCUSSION	78
4.6	CONCLUSIONS	82
5.0	RELEASE OF DB-67, DOXORUBICIN AND PACLITAXOL OCCURS SIMULTANEOUSLY AT DIFFERING RATES FROM SINGLE-PHASE LDI- GLYCEROL POLYURETHANE FOAMS	83
5.1	ABSTRACT.....	83
5.2	INTRODUCTION.....	84
5.3	MATERIALS AND METHODS	85
5.3.1	Materials.....	85
5.3.2	Synthesis of drug-loaded polyurethane foams	85

5.3.3	Drug Reactivity with LDI	86
5.3.4	Excitation-emission spectra and fluorescence stability.....	86
5.3.5	Evaluation of foam architecture by SEM.....	87
5.3.6	Distribution of DB-67 and doxorubicin within polyurethane.....	87
5.3.7	DB-67 and doxorubicin release.....	87
5.4	RESULTS	88
5.4.1	DB-67 and Doxorubicin Reactivity with LDI.....	88
5.4.2	Excitation-emission spectra and fluorescent stability.....	89
5.4.3	Polyurethane Foams: SEM analysis and Drug Distribution	92
5.4.4	Drug release.....	96
5.5	DISCUSSION	99
5.6	CONCLUSIONS	101
6.0	INCORPORATION OF INCORPORATION OF CATIONIC AND ANIONIC CONSTITUENTS ACCELERATES THE RELEASE OF DB-67 FROM LDI- GLYCEROL POLYURETHANE IMPLANTS.....	102
6.1	ABSTRACT.....	102
6.2	INTRODUCTION.....	103

6.3	MATERIALS AND METHODS	105
6.3.1	Materials.....	105
6.3.2	Synthesis of Ionic Films and Foams.....	105
6.3.3	ISE Reactivity with LDI.....	106
6.3.4	Swelling studies	107
6.3.5	SEM Evaluation of Polymer Architecture	107
6.3.6	DB-67 Distribution throughout the Polyurethanes.....	108
6.3.7	Drug Release.....	108
6.4	RESULTS	109
6.4.1	ISE Reactivity with LDI.....	109
6.4.2	Swelling Studies.....	110
6.4.3	SEM analysis and DB-67 distribution	111
6.4.4	Drug release.....	116
6.5	DISCUSSION.....	119
6.6	CONCLUSIONS	123

7.0	GENERAL DISCUSSION	124
7.1	INTRODUCTION.....	124
7.2	OLD COMPOUNDS, NEW APPROACHES.....	126
7.3	CONTROLLED RELEASE VIA COVALENT INCORPORATION	127
7.4	CONTROLLED RELEASE VIA ALTERATIONS IN MATERIAL MORPHOLOGY.....	128
7.5	CONTROLLED RELEASE VIA CATALYST MECHANISM.....	129
7.6	CONTROLLED RELEASE VIA DRUG STRUCTURE	130
7.7	CONTROLLED RELEASE VIA IONIC LIGANDS	132
7.8	CONCLUSION.....	133
	BIBLIOGRAPHY	135

LIST OF TABLES

Table 1 - Structure of some common biodegradable polymers.....	20
Table 2 - DB-67, lysine and glycerol content of LDI-glycerol polymer discs.....	35
Table 3 - <i>In vitro</i> cytotoxicity of DB-67 loaded LDI-glycerol polyurethanes	40
Table 4 - Polyurethane catalyst structures and toxicities	50
Table 5 - Release characteristics of the LDI-glycerol polyurethane foams.....	57
Table 6 - <i>In vitro</i> cytotoxicity of DB-67 loaded LDI-glycerol polyurethane foams	59
Table 7 - Naphthalene compounds – structure, functionality and fluorescent wavelengths.....	70
Table 8 – Release characteristics naphthalene compounds from LDI-glycerol polyurethane foams	77
Table 9 – Chemical structure and fluorescent properties of DB-67, doxorubicin, and taxol.....	91
Table 10 - Release characteristics of DB-67 and Doxorubicin from single and multi-drug LDI-glycerol polyurethane foams.....	98

Table 11 - Release characteristics of DB-67 from ionic and control LDI-glycerol polyurethane
films and foams..... 119

Table 12 – Newly approved therapeutics available on the US market..... 125

LIST OF FIGURES

Figure 1 - Structure of DB-67 - lactone and hydroxy acid.....	2
Figure 2 - Urethane formation.....	7
Figure 3 - Urea formation.....	7
Figure 4 - Some reactions that occur during the formation of polyurethanes.....	8
Figure 5 - Structures of some commonly used urethane amine catalysts	10
Figure 6 – Molecular structure of DB-67, LDI, glycerol and the LDI-glycerol polyurethane	31
Figure 7 - IR Data depicting 1:1 molar reactions between DB-67 and LDI after 48 hours: (A) without tin(II) 2-ethylhexanoate, (B) with 10 μ l tin(II) 2-ethylhexanoate.....	32
Figure 8 – Scanning electron microscope images of an LDI-glycerol drug delivery system: (A) Top surface of tablet which was exposed to non-solvent during the curing process, (B) View of bottom surface in contact with Teflon surface during curing, (C) Cross-sectional image of tablet demonstrates pore distribution, (D) Examination at 8000x magnification (only bottom surface is shown).....	33
Figure 9 - FT-IR spectrum of an LDI-glycerol polyurethane disc containing DB-67.....	34

Figure 10 - Fluorescence decay profiles of 200 nM DB-67 solutions in PBS (pH 7.4) left unprotected from light at 4, 22 and 37 °C. Error bars represent one standard deviation from the mean.....	36
Figure 11 - Excitation-emission fluorescence spectra of a 1.0 mg/ml DB-67 solution in 1N NaOH.....	37
Figure 12 - <i>In vitro</i> release characteristics of DB-67 from LDI-Glycerol tablets incubated at 10 mg/ml in PBS at 4, 22, and 37 °C (pH 7.4). Error bars represent one standard deviation from the mean	38
Figure 13 - <i>In vitro</i> cytotoxicity results of (A) 3-day and (B) 5-day treatments on malignant gliomal cell lines. Error bars represent one standard deviation from the mean	39
Figure 14 - Dose-response profiles for various organometallic and tertiary amine urethane catalysts: (A) baseline studies (B) extended profile for DABCO and DMDEE.....	49
Figure 15 - FT-IR data assessing the reactivity of DB-67 with LDI in the presence of (A) DMDEE and (B) DABCO	51
Figure 16 - Viscosity data for LDI-glycerol pre-polymer prior to initiation of the blowing reaction: (A) 1 st run at 5.0 Pa shear stress and (B) 2 nd run at 50.0 Pa shear stress	52
Figure 17 - Scanning electron micrographs of the LDI-glycerol polyurethane foams: (A) DABCO foam @ 25X (B) DMDEE foam @ 25X (C) DABCO foam @ 10,000X (D) DMDEE foam @ 10,000X	53
Figure 18 - Fluorescent and non-fluorescent images of the LDI-glycerol polyurethane foams ...	54
Figure 19 - Temperature dependent DB-67 release profiles for the LDI-glycerol foams	55

Figure 20 - Comparison of DB-67 release by DABCO and DMDEE foams at 37 °C56

Figure 21 - Comparison of DB-67 Release by DABCO and DMDEE foams at 70 °C56

Figure 22 - In vitro cytotoxicity results of (A) 3-day and (B) 5-day treatments on malignant gliomal cell lines. Error bars represent one standard deviation from the mean58

Figure 23 - Fluorescence excitation and emission spectra for naphthalene compounds in aqueous media69

Figure 24 - Fluorescence decay profiles for the naphthalene analogs in PBS buffer (pH 7.4) solution 71

Figure 25 - Low-magnification scanning electron micrographs (25X) of the LDI-glycerol polyurethane foams containing the various naphthalene analogs.....72

Figure 26 - High-magnification SEM image of 1,5-diaminonaphthalene: (A) before and (B) after a threshold was applied to determine the porosity of the foam 73

Figure 27 - Fluorescent images depicting the distribution of select naphthalene analogs in the LDI-glycerol polyurethane foam 74

Figure 28 - Concentration profiles depicting the release of the naphthalene analogs from the LDI-glycerol polyurethane foams.....75

Figure 29 - Profiles depicting the mol% of the naphthalene analogs released from the LDI-glycerol polyurethane foams.....76

Figure 30 - Functional group comparison of the mol% and normalized release of naphthalene analogs from the LDI-glycerol foams81

Figure 31 – FT-IR spectra depicting the reactivity of DB-67 and doxorubicin with LDI in the presence of a tertiary amine urethane catalyst	89
Figure 32 – Fluorescent excitation and emission spectra of DB-67 and doxorubicin.....	90
Figure 33 – Fluorescent decay profiles of DB-67 and doxorubicin at 70 °C over a 2-week period	92
Figure 34 – Scanning electron micrographs demonstrating the morphological features of LDI-glycerol polyurethane drug foams.....	93
Figure 35 – Fluorescent microscope images showing the distribution of DB-67 and doxorubicin through the LDI-glycerol polyurethane foam.....	94
Figure 36 – Fluorescent microscope images showing the distribution of DB-67 and doxorubicin through multi-drug LDI-glycerol polyurethane foams.....	95
Figure 37 – DB-67 release profiles for single and multi-drug LDI-glycerol polyurethane foams	96
Figure 38 - Doxorubicin release profiles for single and multi-drug LDI-glycerol polyurethane foams	97
Figure 39 – Comparison of DB-67 and doxorubicin release from multi-drug LDI-glycerol polyurethane foams at 37 and 70 C°	99
Figure 40 – Structure of CC, ISE and DMB	103
Figure 41 - FT-IR data depicting the reaction of LDI with ISE at 1 NCO : 1OH and 1LDI : 1 ISE molar ratios	109

Figure 42 - Swelling studies for the 6 mol% CC, ISE, DMB, and control foam and film LDI-glycerol polyurethanes loaded with DB-67	110
Figure 43 - SEM images of the 6 mol% CC, ISE, DMB, and control LDI-glycerol polyurethane films loaded with DB-67	112
Figure 44 - SEM images of the 6 mol% CC, ISE, DMB, and 0 control LDI-glycerol polyurethane foams loaded with DB-67.....	113
Figure 45 - Fluorescent microscope images demonstrating DB-67 distribution through the CC, ISE, DMB and control LDI-glycerol polyurethane film samples.....	114
Figure 46 - Fluorescent microscope images demonstrating DB-67 distribution through the CC, ISE, DMB and control LDI-glycerol polyurethane foam samples	115
Figure 47 - Concentration profiles for the release of DB-67 from the CC, ISE, DMB, and control LDI-glycerol polyurethane films and foams.....	117
Figure 48 - Release profiles showing the mol% of DB-67 retrieved from the CC, ISE, DMB, and control LDI-glycerol polyurethane films and foams.....	118
Figure 49 - Release of DB-67 from the ionic films and foams at 37 °C.....	121
Figure 50 - Release of DB-67 by the ionic materials at 70 °C.....	122
Figure 51 – Structure and attachments of DB-67 and doxorubicin.....	131

PREFACE

Thank you to all of my family, friends, and colleagues for their support over the years. Without it, I certainly would not be where I am today.

Portions of this manuscript have been published in part or whole or are currently under review.

1.0 INTRODUCTION

Many pharmaceutical compounds show excellent activity in vitro, but their uses are severely limited in vivo. Unstable active conformations, limited membrane diffusion, rapid metabolism and/or clearance, decreased solubility, and dose-limiting systemic toxicity are just a few areas in which potential problems exist that can halt drug development [1]. Indeed compounds exist that possess ideal pharmacologic activity for treating specific disease states, but they are simply unable to be delivered in adequate quantities or in the proper active conformation to the target site in the body. The camptothecins are one such family of compounds and one member in particular, *7-tert*-butyldimethylsilyl-10-hydroxycamptothecin (DB-67), displays potent anti-tumor activity but is plagued with delivery obstacles such as poor solubility and poor active-state stability[2].

Chemotherapy has played a central role in the management and sometimes the elimination of hematological malignancies and solid tumors. Despite reduced clinical morbidity and mortality, virtually all chemotherapeutics cause unacceptable damage to normal tissues when used in doses required to eradicate cancer cells [3]. Improved selectivity in the delivery of anti-cancer drugs to tumor tissues offers one possible solution. Therapeutic efficacy could be markedly enhanced and dose-limiting toxicity could be greatly diminished if high concentrations of anti-cancer agents could be selectively administered to only malignant cells.

The majority of current cancer chemotherapeutic agents are low molecular weight (MW) chemicals, possessing a high pharmacokinetic volume of distribution, which leads to the presence of cytotoxic compounds throughout the entire patient. The exposure of normal tissues to the drug is manifested in the many well-known side effects to rapidly dividing cells, e.g., bone marrow suppression, alopecia, sterility, and the sloughing of gut epithelial cells [4]. Low MW anticancer compounds are also rapidly removed by renal excretion and can be subject to deactivation by chemical processes or enzymatic degradation. Chemotherapeutic drugs

invariably have a very narrow therapeutic index that separates the toxic dose from the clinically effective dose. Furthermore, the development of multi-drug resistance (MDR) pumps in tumor cells exacerbates the problem of achieving selective toxicity [5].

Camptothecins are a special class of anticancer agents that act as topoisomerase I (topo I) inhibitors and appear to be quite active in human cancers previously reported resistant to chemotherapy [6]. These agents are analogs of the plant alkaloid 20(S)-camptothecin and interact with topo I and DNA to form cleavage complexes – preventing the resealing of the topo I-mediated DNA single strand breaks [7]. This interaction eventually leads to double-strand DNA breaks and apoptosis.

The pharmaceutical development and clinical utility of the camptothecins are limited by the distinctive dynamics of these agents in the blood stream. All of the camptothecins now in clinical development contain a α -hydroxy- δ -lactone moiety, and they exist in two distinct forms at the physiological pH of 7.0 and above. The biologically active “lactone-closed” form reacts with water to form a biologically inactive “lactone-opened” (carboxylate) form [8, 9] as shown in Figure 1.

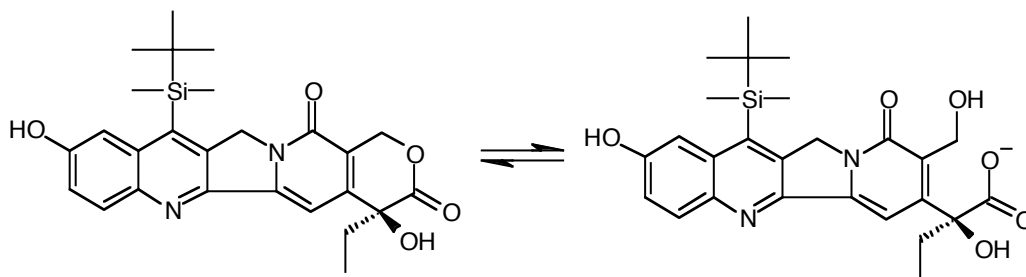


Figure 1 - Structure of DB-67 - lactone and hydroxy acid

This simple chemical hydrolysis dynamically inactivates the parent drug. Furthering the problem, the predominant human blood serum protein, albumin (HSA), preferentially binds the carboxylate form – shifting the equilibrium towards the inactive moiety [10-12]. Because camptothecins are S-phase specific drugs, optimal topo I inhibitory activity is only obtained when the tumors of a patient are continuously exposed to the drug. Accordingly, establishing conditions where a therapeutically relevant concentration of the lactone-closed form of a

camptothecin is present over a suitable period of time for tumor cells to cycle through the S-phase is a major challenge.

Surgically implantable polymer matrices loaded with chemotherapeutic agents provide a successful approach to localized drug delivery. The matrix is loaded with the desired agent and then implanted within the tumor site, following as complete a surgical resection as clinically possible. The matrix releases its drug load over a period determined by the characteristics of the encapsulating polymer, delivering drug to the neoplastic cells existing in the peritumoral region that otherwise would give rise to recurring tumor. The advantage of polymer-based delivery over current catheter technology is that the polymers are not subject to clogging and blockage of tissue debris; in addition, drugs can be more accurately delivered to a specific site within the body and there are no concerns with respect to patient compliance [13]. Our goal is to develop a biodegradable polyurethane matrix capable of delivering DB-67 intratumorally or to remaining tumor cells within the resection margins following surgical removal.

Numerous modalities for selective delivery of anti-tumor compounds to cancer cells have been described, with the most successful of these systems largely based on degradable synthetic polymers. These systems have shown limited efficacy in combating the growth and spread of metastatic tumors, yet a systematic approach to their design and synthesis has not yet been undertaken. Beginning with a degradable polyurethane drug delivery system based on lysine diisocyanate (LDI) and glycerol, we propose to begin a thorough analysis of the system's drug delivery capabilities. This study should result in the design, synthesis and implementation of highly effective drug delivery systems for the DB-67 compound that can later be applied to other suitable therapeutics. The specific aims of the series of studies detailed in this manuscript are summarized below.

Specific Aim 1: Develop and characterize an LDI-glycerol polyurethane film for delivery of a pharmacological agent. Polyurethane films incorporating DB-67 through labile urethane linkages were synthesized with use of an organometallic catalyst. Drug content and release from the films was assessed. The cytotoxicity profile of these films against a panel of malignant glioma cell lines was compared to polyurethane alone.

Hypothesis 1.1 LDI-glycerol polyurethanes can be fashioned into degradable films suitable for drug delivery applications.

Hypothesis 1.2 The pharmacologic agent DB-67 can be incorporated into polyurethane films.

Hypothesis 1.3 Polyurethane films containing a pharmacologic agent will exhibit cytotoxicity *in vitro*.

Specific Aim 2: Develop and characterize an LDI-glycerol polyurethane foam for delivery of a pharmacological agent. Polyurethane foams incorporating DB-67 through labile urethane linkages were synthesized with use of two tertiary amine catalysts. Drug content and release from the foams was assessed. The cytotoxicity profile of these foams against a panel of malignant glioma cell lines was compared to polyurethane alone.

Hypothesis 2.1 LDI-glycerol polyurethanes can be fashioned into degradable foams suitable for drug delivery.

Hypothesis 2.2 A pharmacologic agent DB-67 can be incorporated into LDI-glycerol polyurethane foams.

Hypothesis 2.3 LDI-glycerol polyurethane foams containing a pharmacologic agent will exhibit cytotoxicity *in vitro*.

Specific Aim 3: Analyze how the functional groups present on a drug affect its release from LDI-glycerol polyurethane foams. A series of LDI- glycerol polyurethane foams incorporating naphthalene and some of its functionalized derivatives was prepared. The naphthalene analogs were incorporated into the polyurethane network via labile urethane linkages with use of a tertiary amine catalyst. Content and release from the foams was assessed.

Hypothesis 3.1 Naphthalene and its various analogs can be incorporated into LDI-glycerol polyurethane foams.

Hypothesis 3.2 Release of the analogs from the foams will occur at differing rates.

Hypothesis 3.3 The release rates will correlate to the functional groups present on the various naphthalene analogs.

Specific Aim 4: Develop LDI-glycerol polyurethane foams capable of the controlled release of multiple anti-cancer compounds at different rates. Polyurethane foams incorporating DB-67, doxorubicin and paclitaxol – alone and in combination – were prepared. The drugs were

incorporated into the polyurethane foam via labile urethane linkages via a tertiary amine catalyst. Content and release of the drugs from the foams was assessed.

Hypothesis 4.1 DB-67, doxorubicin, and paclitaxol can be incorporated alone and in combination into LDI-glycerol polyurethane foams.

Hypothesis 4.2 Release of the drugs from the foams will occur at different rates.

Hypothesis 4.3 The release rates can be correlated to the pendant functional groups present on each drug.

Specific Aim 5: Incorporate cationic and anionic ligands into LDI-glycerol polyurethane films and foams to alter their rates of drug release. A series of polyurethane foams and films incorporating choline chloride (CC) and isethionic acid (DMB), was prepared. The non-ionic species 3,3-dimethylbutanol was used as a control. DB-67 was incorporated into the polyurethane films and foams via labile urethane linkages via a tertiary amine catalyst. Content and release of DB-67 from the films and foams was assessed.

Hypothesis 4.1 Ionic ligands can be incorporated into LDI-glycerol polyurethane foams.

Hypothesis 4.2 Release of the drugs from the films and foams will occur at different rates.

Hypothesis 4.3 The release rates can be correlated to the ionic ligands present in each polyurethane material.

1.1 POLYURETHANES

Polyurethanes are used often in medical device applications, and their use continues to grow. Compared with other polymers, polyurethanes often require sophisticated manufacturing processes and are more expensive on a price-per-pound basis. For example, the average flexible PVC compound sells for 85 cents per pound, while the typical polyurethane sells for 10–20 times that amount [14]. So, what is it that motivates medical device developers to use them? The answer is quite simple: polyurethanes can be used in applications where other materials fail. Polyurethanes are among the most versatile construction materials that can be formulated for medical devices. By controlling the components in the formulation, one can produce

polyurethanes in the form of flexible foams, rigid foams, and elastomers. They are tough, biocompatible, and hemocompatible, and they can be processed using extrusion, injection molding, film blowing, solution dipping, and two-part liquid molding.

Polyurethanes' unique chemistry gives them this versatility. The vast majority of polyurethanes are segmented polymers, meaning they have a soft segment that provides flexibility and a hard segment that provides strength. These polyurethanes are made from three basic building blocks: the backbone, the diisocyanate, and the chain extender. The backbone, usually a long chain molecule, provides flexibility to the polymer. The diisocyanate and the chain extender combine to form the hard segment, which acts as a cross-link. It provides the polymer with high tensile strength and high elongation threshold. Generally, the diisocyanate is to blame the majority of the toxicity associated with the production of polyurethane materials [15, 16].

Polyurethanes are made from either aromatic or aliphatic diisocyanates. Aromatic diisocyanates contain benzene rings, which create polyurethanes that are generally tougher, stronger, and less costly than the aliphatics. The aromatics generally have tougher hard segments, which are more chemically resistant and give rise to higher tensile strength and elongation than aliphatics. Aliphatic diisocyanates contain hydrocarbon backbones without any benzene rings. Aliphatic polyurethanes make strong polymers but lack the chemical resistance of aromatics. They are more expensive than aromatics and are used primarily in applications that require good light stability. There are thousands of possible combinations of the basic building blocks used to create aromatic and aliphatic polyurethanes, thereby providing device engineers with a myriad of options for their products.

1.1.1 Polyurethane synthesis

The term polyurethane is broadly used to describe materials that contain urethane, urea or isocyanurate linkages as part of the polymer backbone. Urethane, urea and isocyanurate bonds are formed via the reaction of isocyanate with hydroxyl, amine or other isocyanates, respectively. Isocyanates are essentially carbonyl compounds with multiple double bonds, and the reaction mechanisms closely corresponds to the reaction mechanisms observed for common carbonyl compounds [17]. The first reaction step of carbonyl compounds is the addition between the

electrophilic carbonyl carbon of the carbonyl compound and the nucleophilic center of the nucleophilic compound. Similarly, the urethane formation starts with the reaction between the carbonyl carbon of the isocyanate and the alcohol oxygen (Figure 2).

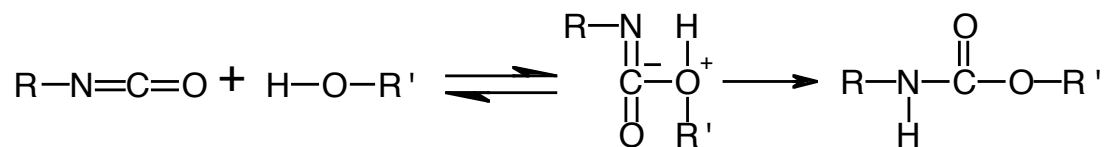


Figure 2 - Urethane formation

The nucleophile, in this case the alcohol, attacks the electrophile, the carbonyl carbon of the isocyanate, generating an intermediate species. Proton transfer from the alcohol carbon to the isocyanate nitrogen accompanies electron transfer from the isocyanate's carbonyl carbon to its nitrogen, producing a urethane bond. The greater the electrophilicity or nucleophilicity of the reacting centers is, the higher is the rate of carbonyl reaction. Accordingly, the rate of urethane formation increases with these reactivity factors.

Similar to urethane formation, an isocyanate can also react with an amine to generate a urea bond (Figure 3).

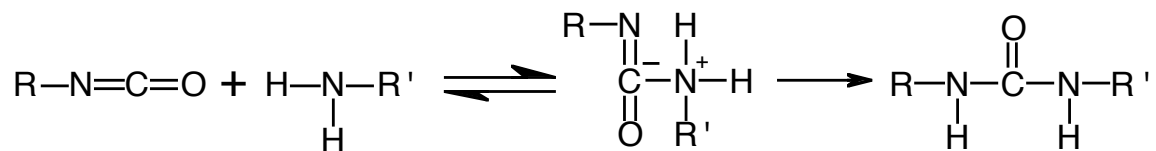


Figure 3 - Urea formation

In this case, the primary amine functions as the nucleophile and the carbonyl carbon of the isocyanate still functions as the electrophile. Proton and electron transfer occur in an analogous manner, generating a urea bond. Other important reactions occur during the formation of polyurethanes, and they are shown in Figure 4. For simplicity, the reactants are depicted as monofunctional, although polyurethanes will be generated from di- or multi-functional reactants.

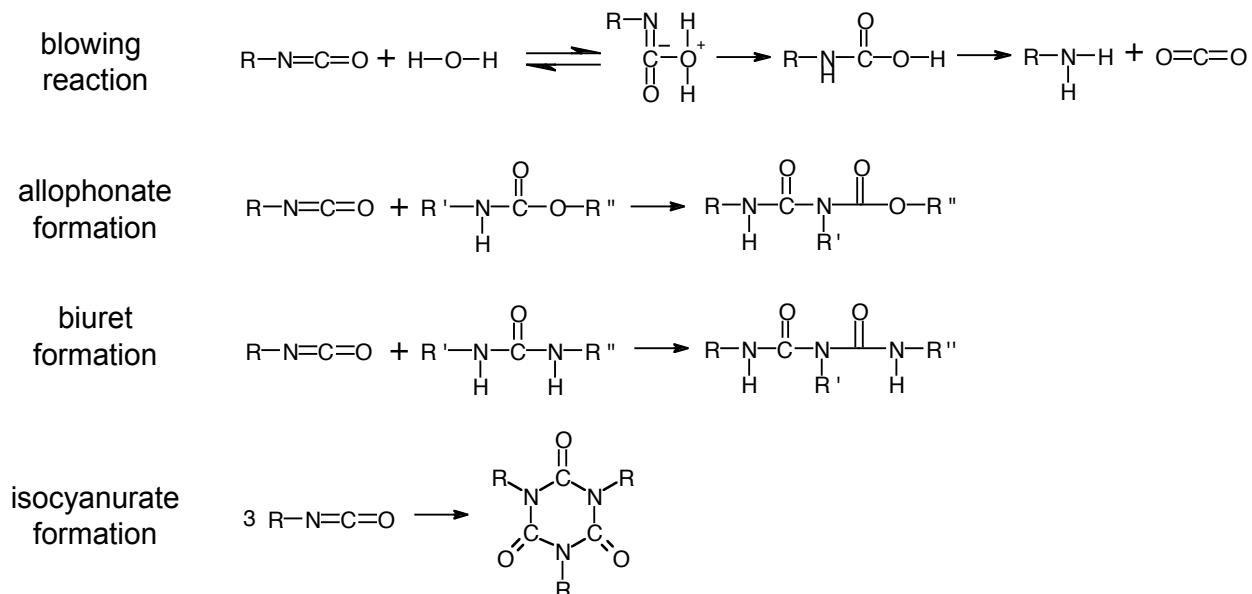


Figure 4 - Some reactions that occur during the formation of polyurethanes

All of the aforementioned isocyanate reactions can be broken into three categories: gelling, cross-linking and blowing. The gelling reactions refer to those that do not produce a volatile product, such as urethane or urea formation, and yield linear polymers (assuming difunctional reactants). The cross-linking reactions function via the active hydrogen in the urethane and urea groups, and these species crosslink the polyurethane by reaction with another isocyanate to form allophonate and biuret, respectively. The isocyanurate linkage, also formed via a cross-linking reaction, provides rigidity and thermal stability. Isocyanates can also form dimers, called uretidiones, that also result in cross-linked polymer, but this is far less common than the trimerization reaction.

The blowing reaction, or the reaction between isocyanate and water, is of fundamental importance to urethane chemistry. The reaction produces carbamic acid as an intermediate. As the carbamic acid readily decomposes into an amine and carbon dioxide gas, the polyurethane expands into foam. The amine generated in this process is then free to react with another isocyanate to form a urea linkage, curing the foam as it expands. Physical blowing agents such as chlorofluorocarbons and methylene chloride can also be used to produce foams, but these foams

are generated by the vaporization of these liquids and not by a chemical reaction. The blowing reaction is used to manufacture foam cushioning for a variety of commercial applications in the auto and home industries.

It is the precise control and sequencing of the blowing, gelling, and cross-linking reactions that determine the final properties of the polyurethane [18]. For example, if the blowing reaction occurs too quickly in a water-blown foam, the foam will expand rapidly and will not have sufficient mechanical strength to prevent a collapse. Conversely, if the gelling reactions occur too rapidly, the gas resulting from the blowing reaction will not be able to expand the polyurethane matrix. Thus, the precise balance of these reactions determines the resulting physical properties; this balance is primarily controlled by the amount and type of catalyst present.

1.1.2 Polyurethane catalysis

For polyurethanes, the catalyst is most responsible for controlling the reaction time and for defining polymer architecture that influences the ultimate mechanical properties. Specifically, it is the catalyst's activity and selectivity towards each of the many reactions occurring in the formation of polyurethanes that determine the structure of the resulting material. It is possible to accelerate the reactions of carbonyl compounds via Lewis acids and bases, and many urethane catalysts function in this manner [19]. The myriad of catalyst choices available to the polyurethane chemist presents a significant challenge, and often a blend of catalysts is used to obtain the desired results.

There are three major classes of polyurethane catalysts: tertiary amines, organometallics, aprotic salts; only tertiary amine and organometallic catalysts will be discussed. Amine catalysts, especially tertiary amines, form the largest class of catalysts used in the manufacture of polyurethanes. Tertiary amines catalyze both the gelling and blowing reactions to different extents, but they are generally not very active isocyanurate catalysts. Increased catalyst basicity generally increases activity, and steric hindrance plays a significant role too. Triethylene-diamine or 1,4-diazobicyclo[2.2.2]-octane (DABCO) is the most widely employed tertiary amine catalyst used in the production of polyurethanes. Its unusually high activity in spite of decreased basicity is due to a lack of steric hindrance. While DABCO is generally regarded as a powerful gelling

catalyst, it is also a powerful catalyst of the blowing reaction [20]. In contrast, the catalyst 4,4'-(oxydi-2,1-ethane-diyl)bismorpholine or dimorpholino-diethylether (DMDEE) is another tertiary amine catalyst that is highly specific for the blowing reaction [21]. The structures of some of the more commonly used tertiary amine catalysts are shown in Figure 5.

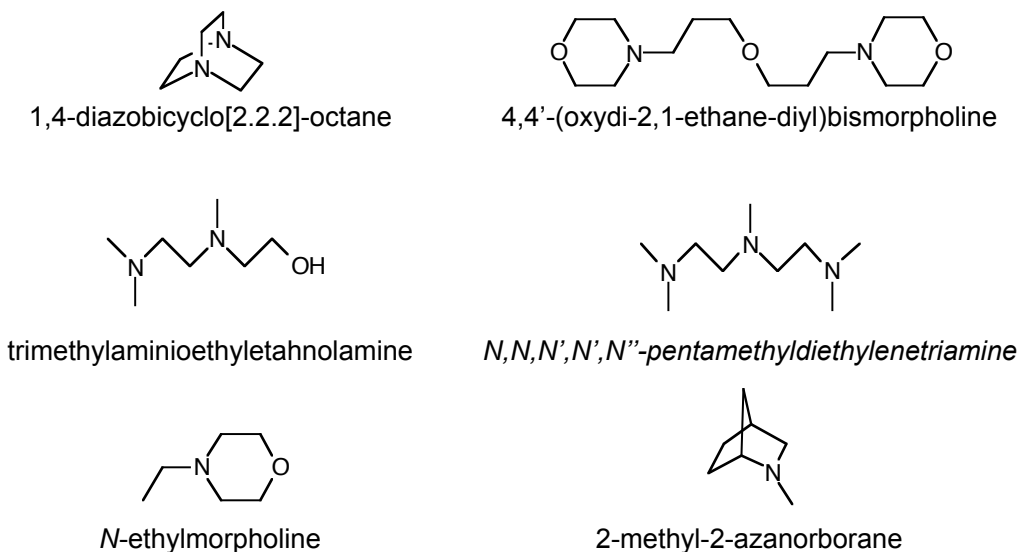


Figure 5 - Structures of some commonly used urethane amine catalysts

Several mechanisms have been invoked to explain the observed rate data in amine-catalyzed isocyanate and isocyanate trimerization reactions. Most of the mechanisms are variations of two mechanisms proposed by Baker and for the tertiary amine catalyzed formation of urethane [22-24]. The first mechanism consists of the formation of an isocyanate-amine complex followed by reaction with an alcohol. The second consists of the formation of an activated amine-alcohol complex followed by reaction with the isocyanate. The former mechanism suggests that the nucleophilicity of the amine is the dominant factor; the latter implies that the amine basicity is dominant. Experimental evidence, as well as shortcomings, for both methods exists, although a mechanism based on an isocyanate-amine complex is generally more accepted.

Organometallic compounds are another large class of catalysts used in the synthesis of polyurethanes. The most common of these catalysts are organotin compounds, which are salts of

organic acids, especially the dialkyltin dicarboxylates. Among the more common organometallic catalysts are dibutyltin dilaurate ($[\text{CH}_3(\text{CH}_2)_3]_2\text{Sn}[\text{OCO}(\text{CH}_2)_{10}\text{CH}_3]_2$), stannous octoate ($\text{Sn}(\text{OCOC}_7\text{H}_{15})_2$), dibutyltin diacetate ($[\text{CH}_3(\text{CH}_2)_3]_2\text{Sn}[\text{OCOCH}_3]_2$), and dibutyltin dimercaptide ($[\text{CH}_3(\text{CH}_2)_3]_2\text{Sn}(\text{SC}_{12}\text{H}_{25})_2$). The organometallic catalysts tend to be more selective for the gelling reactions than the tertiary amines. A few of the limitations of organotin compounds are their high toxicity and their tendency to lose activity in the presence of water. Since polyurethanes are generally synthesized under anhydrous conditions, only the latter generally poses a problem. A synergy in catalytic activity has been observed when tertiary amines are used in combination with organotin compounds [25].

Other varieties of metal-based catalysts are also available. These include mercury-, lead-, iron-, bismuth-, and cobalt-based compounds that are routinely used for coating and elastomers applications. These catalysts generally exhibit a higher degree of selectivity for the gelling reactions relative to the amine and organotin catalysts [18]. However, many of these heavy metal catalysts face uncertain futures due to toxicological and environmental concerns. However, bismuth salts are an exception and possess decreased toxicological concerns, as they are routinely employed in the medical field as diagnostic imaging dyes and as anti-diarrhea medications [26, 27].

Several mechanisms have been proposed for the organometallic catalysis of isocyanate-hydroxyl reactions [28-30]. The most prevalent mechanism is that of a ternary complex of isocyanate, hydroxyl, and the organometallic catalyst. It has been proposed that the organometallic catalyst can first complex with either the isocyanate or alcohol followed by complexation with the other reactant. Others favor the formation of a Lewis acid-isocyanate complex followed by complexation with the alcohol. Still others claim that the organometallic catalyst increases the electrophilic character of the isocyanate group and brings the alcohol and isocyanate in close proximity. Indeed there is still an ongoing debate regarding the exact mechanisms governing the organometallic catalysts, but lack of a true and definite mechanism of action has not impeded their use in the commercial production of polyurethanes.

Catalysts play a vital role in reducing reaction times and in controlling the polymer properties in the synthesis of polyurethane materials. Each catalyst has a unique activity and selectivity for the reactions that occur during the formation of polyurethane. Of the many types of polyurethane catalysts, the most important and most widely used are the tertiary amines and

the organotin compounds. The combinations of catalysts are often required to provide the proper balance between ease of processing and physical property requirements. A variety of approaches have also been made to meet the changing environmental and manufacture concerns, such as toxicity, odor and delayed activity [20].

1.2 DRUG DELIVERY

Over the past three decades, significant advances have been made in drug delivery technology. This realization has come about and been accelerated in recent years due to the substantial decline in the development of new pharmaceutical compounds [31]. Drug delivery has now truly become a multidisciplinary endeavor. Emerging technologies now rely on new discoveries in all fields of science. Drug delivery, which takes into consideration the carrier, the route, and the target, has evolved into a strategy of processes or device designs to enhance the efficacy of therapeutic agents through controlled release. This may involve enhanced bioavailability, improved therapeutic index, or improved patient compliance. Drug delivery, or controlled release, has been defined by Flynn as “the use of whatever means possible, be it chemical, physiochemical, or mechanical, to regulate a drug’s access rate to the body’s central compartment, or in some cases, directly to the involved tissues” [32].

Countless attempts have been made over the years in attempts to formulate a truly selective delivery strategy as envisioned by Flynn. In the beginning of the 20th century, P. Erlich first described this idea in his concept of “magic bullets” [33], consisting of haptophore (binding component to target) and toxophore (cytotoxic part). As a haptophore, he proposed the use of an antibody. Nevertheless, it took another 70 years for drug delivery and drug targeting to become areas of active research, arousing the interest of many people.

When looking back on the history of drug delivery and targeting, several keystone discoveries are noticeable in the period of the 1960s and 1970s. Erlich’s concept of using an antibody as a haptophore was experimentally proven in the treatment of several tumors inoculated into experimental animals. Toxophores used in these experiments were radiotherapeutic agents (radioactive iodine) [34, 35], cytotoxic drugs (e.g., chlorambucil) [36], and diphtheria toxin [37]. The concept of biodegradable polymers for sustained drug release was

first introduced in the early 1970's, following the introduction of bio-resorbable sutures [38]. The first drug to be delivered from a biodegradable drug-delivery system was cyclazocine, an opioid antagonist that has been used as an analgesic and in the treatment of narcotic dependence; it was reported in 1971 and delivered drug via a poly(DL-lactide) implant [39]. Since then, biodegradable polymers have become increasingly popular, and numerous new polymers have been synthesized and employed for drug delivery applications.

On the other hand, it was also discovered that conjugating a drug to an appropriate polymeric carrier could modulate drug uptake by cells, and Ringsdorf presented the first clear concept of targetable polymeric drugs [40]. Because polymers follow different cellular uptake mechanisms than their low-molecular weight analogs, they are introduced into the cell neither by permeation through the plasma membrane nor by means of transport proteins. Polymers are internalized into the cellular compartment through a process called endocytosis [41]. Endocytosis begins with the enclosure of the polymer by a part of the plasma membrane to form an intracellular vesicle. The intracellular vesicles with ingested polymers are transferred to organelles called endosomes, which are eventually carried to lysosomes. Ringsdorf envisioned that drug delivery could further be improved by tailoring polymers that could not only incorporate drugs, but also molecules that could guide the drugs to cells.

These early discoveries paved the way for the development of many technologies aimed at limiting the systemic exposure of therapeutics, while increasing their availability to select tissues. Site-selective drug delivery has been proven successful in the laboratory with strategies such as liposomes, hydrogels, synthetic peptides, synthetic polymers, and nanoparticles just to name a few. Among the diverse applications of macromolecular drug formulations, the treatment of solid tumors is one in which intensive research has been devoted. However, there has been limited clinical impact because of these advances. With continued technological advances and re-tailoring of currently available systems, the drug delivery field will continue to move toward its goal of improving therapeutic efficacy through site-specific release strategies.

Drug delivery strategies can be divided into two categories based upon their method of administration – systemic and local delivery strategies. Although there exists some crossover between the two divisions, most modern drug delivery systems can be categorized in this manner. Systemic drug delivery formulations are generally introduced into the body's vascular space, relying on selective mechanisms to reach and affect the diseased tissues. Local

administration strategies place the drug in a particular body compartment and passive release mechanisms dictate the rate and time course of administration of the therapeutic compound to the diseased tissue. Many advances have been made over the years in both of these types of systems, and a review of their progress is certainly warranted here.

1.2.1 Systemic delivery

Although the technologies underlying systemic drug delivery formulations vary to a considerable degree, they all rely on three basic tenants. First, a protective carrier mechanism limits the drug's exposure in extraneous tissues, protects it from inactivation, and inhibits premature release. Second, a targeting moiety is associated with the carrier mechanism and it is able to recognize and remain at the targeted tissues. Third, a site-specific or time-delayed release strategy is employed to deliver the drug only once it has reached and invaded the targeted tissue.

Water-soluble polymers were first applied in the biomedical field as plasma expanders. Compounds such as poly(glutamic acid), dextran, poly(vinyl alcohol), poly[N-(2-hydroxypropyl)methacrylamide] (HPMA), and poly(ethylene glycol) (PEG) had been shown to exhibit increased circulation times relative to their low-molecular weight counterparts. This is because renal clearance is significant for molecules with relatively small molecular weights. Proteins with MW lower than 40,000 show a very short plasma half-life because of rapid renal clearance [42]. However, it was demonstrated that the urinary excretion of soybean trypsin inhibitor (MW ~20,000) could be significantly reduced through conjugation to water-soluble polymers including PEG and dextran [43]. In a rational manner water-soluble plasma expanders became used as starting components to design polymer-drug conjugates.

Another important aspect of drug targeting is the modulation of distribution and disposition of drugs by binding with appropriate carrier systems. After administration of macromolecular drug formulations via the intravenous route, their transport in the body compartment is principally governed by diffusion and convection. Even if effective homing moieties are installed in the conjugate, they are of no use unless the conjugates reach the vicinity of the target cell to ensure close contact. So how is it that macromolecular drug conjugates are able to reach specific targets when administered systemically to the vasculature compartment?

Solid tumor masses exist outside of the vascular space and are one indication in which site-specific delivery of macromolecular therapeutics has found some success. This is due to the unique biology of tumor masses and that changes in vasculature architecture that this biological profile promotes. It is now well accepted that because of activation of kinin-generating cascade and the secretion of vascular permeability factor, blood capillaries in tumor tissues develop considerably high density with enhanced permeability due to loose interendothelial junctions. This process leads to enhanced passive transport of macromolecular substances, such as proteins and polymeric drugs, across the blood vessel into the interstitial spaces of the tumor tissues.

On the other hand, the development of a lymphatic drainage system is insufficient in tumorous tissues, resulting in poor tissue drainage of macromolecular substances. Consequently, macromolecular substances may exhibit a considerable accumulation in the tumor due to the synergistic effect of the increased vascular permeability and the decreased tissue drainage. This effect has been systematically studied by the Maeda group at Kumamoto University, Japan, and is termed “enhanced permeability and retention” (EPR) effect [42, 44]. EPR has become one of the major guiding principles in drug targeting using macromolecular carriers. However, it should be noted that this effect also takes place in sites of increased inflammatory reaction as a result of several causes, including microbial infections.

Obviously, the EPR is a great advantage of using macromolecular drugs for targeting. Low-molecular weight analogs readily suffer from glomerular excretion from the bloodstream, whereas macromolecular drugs are expected to achieve a prolonged half-life in the bloodstream because of decreased glomerular filtration and renal excretion. Obviously, extended circulation is a requisite for sufficient EPR effect. However, prolonged circulation is not always achieved for macromolecular carrier systems. An increase in hydrophobic character or induction of cationic charges in the carrier significantly alters the distribution, resulting in significant accumulation in the liver, resulting in rapid clearance from the blood stream. In terms of prolonged circulation and a resulting increase in plasma half-life, conjugation of drugs to macromolecular carriers with neutral or slightly anionic character generally gives good results.

Tumor invasion, metastasis, and resistance to chemotherapeutic drugs remain as major obstacles to the successful treatment of cancer, even in light of these findings. To further overcome some of these limitations, therapeutics that further increase the specificity and efficacy, while at the same time reduce the toxicity of the therapeutics are being explored.

Features unique to malignant human tumor cells can be exploited in the development of targeting therapeutic agents. For example, cancer cells often over-express specific tumor-associated antigens, carbohydrate structures, or growth factor receptors on their cell surface. Incorporation of a recognizable moiety into the macromolecular carrier structure allows for actively targeted drug delivery systems. Potential targeting moieties include monoclonal, polyclonal antibodies and their fragments, carbohydrates (galactose, mannose), peptides/proteins (melanocyte stimulating hormone, transferrin, growth factors), glycolipids, vitamins, and other ligands. Active macromolecular conjugates can first utilize EPR effect to arrive within the solid tumorous tissues, and then use active targeting moieties to be selectively transported into tumor tissues at much higher rates.

Macromolecules without a specific affinity to plasma membrane components are taken up through a non-selective process called “fluid-phase endocytosis” in which polymers are engulfed into endosomes along with liquid components. This process is a result of normal immune surveillance and antigen presentation common to the immune system. On the other hand, when macromolecules show an affinity for a plasma membrane and adsorb onto it, they are internalized into the cell by “adsorptive endocytosis”, which can have uptake rates 10-fold higher compared to fluid-phase endocytosis.

Studies on endocytic uptake of HPMA copolymers bearing tyrosineamide (Tyr-NH₂) residues have shown there is an intense increase in uptake rate into rat visceral yolk sacs when 10 mol% of the copolymer side groups were terminated with Tyr-NH₂ [45]. This result was considered to be due to an increase in the contribution of nonspecific adsorptive endocytosis with an increase in the hydrophobic character of the copolymer chain owing to the increased number of the hydrophobic aromatic residue, tyrosine. Nonspecific adsorptive endocytosis is also significant for the cellular uptake of cationic polymers because of the negatively charged features of cellular plasma membranes. Results showing the increased hepatic uptake of charged dextran in a rat *in vivo* model have been obtained and also demonstrate the feasibility of the strategy [46].

In the case of endocytosis through receptors expressed on the surface of the target cell plasma membrane (receptor mediated endocytosis), the uptake rate reaches even 1,000 fold higher values than those observed with fluid-phase endocytosis. Receptor mediated endocytosis is quite common for many kinds of cell species. For example, low-density lipoprotein (LDL), a natural vehicle for cholesterol, known to be taken up by liver parenchymal cells through LDL receptors

expressed on these cellular surfaces. Receptor mediated endocytosis is not only extremely efficient, but also highly specific. Cellular-specific targeting has been made possible through these discoveries and can be used as a route to deliver a drug into a particular cell population in a particular site in the body. Incorporation of site-specific ligands onto the surface of macromolecular carrier systems should enable highly specific carrier systems for therapeutics capable of treating selected tissues in the body.

1.2.2 Localized delivery

Many technologies exist for localized delivery of drugs to select regions of the body. The driving force for the deliver can function via a variety of mechanisms such as diffusion, dissolution, osmotic pressure, biodegradation, and even micro-magnetic, mechanical, and electrical systems. With these types of systems, a body compartment can be selected and considered an isolated system. Various release strategies can then be employed to deliver drug to only the local tissues within a desired region. Subsections of the body compartment can even be selected for treatment via this strategy. Since the target organ system remains isolated from the remainder of the body, many dose-limiting systemic toxicities can be avoided entirely. Localized delivery systems also give the physician much tighter control on the extent and duration of therapeutic exposure.

Catheter technology has found many uses in both systemic and local drug delivery systems. Implantable drug delivery devices can be designed to transmit drugs and fluid directly into the bloodstream without the repeated insertion of needles. These systems are particularly well suited to the delivery of insulin, steroids, chemotherapeutics, antibiotics, analgesics, total parental nutrition and heparin. These types of devices are placed completely under the skin – usually in a convenient but inconspicuous location. The patient is aware of only a small bump under the skin. Because the device is subcutaneous, with no opening in the skin, there is little chance of infection or interference with daily activities. These devices can even be refilled by simple injection through the skin and a septum into the pump reservoir.

A catheter can also be attached to the exit port of an implantable pump to perfuse a discrete location distant from the site of implantation. In this manner, drug solutions may be delivered into solid tissues. The miniature pump is capable of changing local drug concentrations around the catheter tip without influencing the rest of the body. Flows of 0.5 – 1.0 $\mu\text{l/hr}$ appear to

be low enough that hydraulic damage or edema is minimal in the micro-perfused region [31]. This strategy has proven successful in the treatment of many neurological malignancies, where the size of the pump prohibits spinal and cranial implantation [47-49]. However, catheters are often subject to blockage and clogging by tissue debris, which can seriously hinder the performance of the device.

Implanted polymer matrices loaded with a therapeutic provide another approach to localized drug delivery. The typical polymers that are used in medicine can be divided into two groups: those that are introduced for a chronic period of time and polymers whose presence is transient. The former includes the use of polymeric materials in cardiovascular surgery, orthopedics, plastic surgery, and otolaryngology. Such applications impose high demands on the stability of the materials used. The latter includes the use of polymers for drug delivery applications, where the material is no longer needed after the drug supply has been exhausted. The matrix is loaded with the desired agent and then implanted at the treatment site. If degradable polymers are not used, one is often required to harvest the implant. The major disadvantage to implantable polymer systems is that they are not refillable, as is the pump system. If a further dose is required, another implant must be placed at the treatment site, often requiring repeated surgical intervention.

Currently available polymers for site-specific controlled release can be classified into four major categories: diffusion controlled systems, solvent-activated systems, magnetically controlled systems, and chemically controlled systems. Diffusion controlled systems involve either a reservoir or a matrix. In reservoir type systems, a layer of non-biodegradable polymeric material, through which a drug slowly diffuses, surrounds a core reservoir. The properties of the drug and the encapsulating polymer govern the diffusion rate of the drug out of the system. One of the problems with such reservoir systems is that it must be removed from the body when the drug load has been depleted. Another potentially life-threatening problem may be encountered when the reservoir accidentally ruptures and a large amount of drug is suddenly released into the surrounding tissues (known as “drug dumping”) [50, 51]. In a matrix type diffusion-control system, the drug is uniformly distributed throughout the polymer matrix and is released at a predetermined rate as drug particles are displaced from the polymer network. In such a system, there is no inherent danger of drug dumping in the case of accidental rupture of and encapsulating membrane.

Solvent-activated systems can be classified as either osmotically controlled or swelling controlled. In osmotically controlled polymer systems, an external fluid containing low concentrations of drug moves across a semi-permeable membrane to a region inside the device, where the drug is in high concentration. Osmotic pressure tends to decrease the concentration gradient between one side of the membrane and the other. The inward movement of fluid forces the dissolved drug out of the device through a small orifice. In swelling controlled systems, the polymer holds a large quantity of water without dissolving. Typically, hydrogels, consisting of cross-linked hydrophilic macromolecules, are used for these types of applications [52-55]. As the system swells, the gel's permeability for low molecular weight solutes (i.e., drugs) changes and these agents are released at a controlled rate as the gel continues to swell.

Magnetically controlled drug delivery systems have been developed from proteins such as albumin and magnetic microspheres and are used in site-specific chemotherapy applications. Because of the magnetic nature of the resulting particles, they are theoretically capable of enhanced area-specific accumulation when the body is subject to an external magnetic field. Although still experimental, this carrier system has been shown capable of accommodating a wide variety of drug loads. Two advantages of this type of approach are the high efficiency for *in vivo* targeting and controllable release of drug at the microvascular level. A few electrically controlled polymers are also currently being developed for the controlled release of drugs [56].

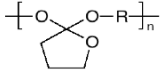
Chemically controlled systems also have two classes: the "pendant chain" system and the biodegradable system. The pendant chain system is one in which the drug molecule is chemically linked to the backbone of a polymer. In the presence of enzymes or fluids, chemical or enzymatic hydrolysis occurs with concomitant release of the drug at a controlled rate. The drug may be linked directly to the polymer or can be linked via a "spacer" group. In the biodegradable system, polymers gradually decompose and bring about a controlled release of drug. The drug is dispersed uniformly throughout the polymer and is slowly released as the polymer disintegrates. The two major advantages to this type of system are that polymers do not have to be removed from the body after the drug supply is exhausted, and the drug does not need to be water-soluble. In fact, because of these factors future use of biodegradable polymers is likely to increase more than any other type of polymer in the future. The LDI-glycerol polyurethanes discussed within this dissertation are essentially a blend of the pendant chain and

biodegradable system technologies, incorporating compounds via labile chemical bonds into a degradable polyurethane matrix.

1.2.3 Biodegradable systems

Biodegradable polymers may be synthetic or natural in origin. Some of the widely used synthetic biodegradable polymers in drug delivery technology are summarized in Table 1.

Table 1 - Structure of some common biodegradable polymers

Polymer	Structure
polyester	$\left[\left(\text{C}_{\text{H}_2} \right)_n \text{C}_{\text{H}} \begin{array}{c} \text{O} \\ \parallel \\ \text{C} \\ \\ \text{R} \end{array} \text{O} \right]_n$
poly(orthoester)	$\left[\text{O} \begin{array}{c} \text{R} \\ \\ \text{C} \\ / \quad \backslash \\ \text{O} \quad \text{O} \\ \quad \\ \text{C} \quad \text{C} \\ / \quad \backslash \\ \text{O} \quad \text{O} \\ \quad \\ \text{R} \quad \text{R}' \end{array} \right]_n$ 
poly(caprolactone)	$\left[\text{C}_{\text{H}_2} \begin{array}{c} \text{O} \\ \parallel \\ \text{C} \\ \\ \text{O} \end{array} \text{C}_{\text{H}_2} \text{C}_{\text{H}_2} \text{C}_{\text{H}_2} \text{C}_{\text{H}_2} \right]_n$
poly(α-amino acids)	$\left[\text{NH} \begin{array}{c} \text{H} \\ \\ \text{C} \\ \\ \text{R} \end{array} \text{C}_{\text{O}} \right]_n$
pseudo-poly(amino acids)	$\left[\text{O} \text{C}_6\text{H}_4 \text{C}_{\text{H}_2} \begin{array}{c} \text{H} \\ \\ \text{C} \\ \\ \text{NH} \\ \\ \text{Cbz} \end{array} \text{C}_{\text{O}} \text{NH} \begin{array}{c} \text{H}_2 \\ \\ \text{C} \\ \\ \text{O} \\ \\ \text{R} \end{array} \text{C}_{\text{H}_2} \text{C}_6\text{H}_4 \text{O} \text{NH} \right]_n$
polydepsipeptides	$\left[\text{NH} \begin{array}{c} \text{H} \\ \\ \text{C} \\ \\ \text{R} \end{array} \text{C}_{\text{O}} \text{O} \begin{array}{c} \text{H} \\ \\ \text{C} \\ \\ \text{R}' \end{array} \text{C}_{\text{O}} \right]_n$
polyphosphazene	$\left[\text{NH} \begin{array}{c} \text{R} \\ \\ \text{P} \\ \\ \text{R} \end{array} \text{O} \right]_n$
polyphosphoester	$\left[\text{O} \begin{array}{c} \text{O} \\ \parallel \\ \text{P} \\ \\ \text{R} \end{array} \text{O} \text{C}_{\text{H}_2} \text{C}_{\text{H}_2} \text{C}_{\text{H}_2} \right]_n$
polyanhydrides	$\left[\text{O} \begin{array}{c} \text{O} \\ \parallel \\ \text{R} \\ \parallel \\ \text{O} \end{array} \right]_n$
polycyanoacrylates	$\left[\text{C}_{\text{H}_2} \begin{array}{c} \text{C} \equiv \text{N} \\ \\ \text{C} \\ \\ \text{O} \\ \\ \text{R} \end{array} \right]_n$

Natural degradable polymers include human serum albumin, low-density lipoproteins (LDLs), bovine serum albumin, gelatin, collagen, hemoglobin, polysaccharides, etc. [57]. Use of the natural polymers is often limited by difficulties in purification and large-scale manufacture, in addition to the potential to cause immunogenic and adverse reactions. With advances in polymer science over the past 30 years in the synthesis, handling and degradation mechanisms, many synthetic and natural polymers are being successfully employed in drug delivery applications. Irrespective of their source, all biodegradable polymers share some common characteristics: (1) stability and compatibility with the drug molecule, (2) biocompatible and biodegradable, (3) ease of manufacture on a large scale, (4) amenability to sterilization, and (5) flexibility to yield multiple release profiles [38]. Among the polymers listed in Table 1, polyesters, polylactones, poly(amino acids), and polyphosphazenes, predominantly undergo bulk erosion; polyorthoesters and polyanhydrides predominantly undergo surface erosion.

Temporal drug release, delivering drug over an extended period of time and/or at a specific time, is advantageous for types of drugs such as chemotherapeutics, anti-inflammatory agents, antibiotics, opioid antagonists just to name a few [3, 4, 53, 58-60]. In general, drug release from biodegradable polymeric devices is controlled by diffusion of drug and/or polymer erosion. In practice, both of these mechanisms play a role in controlling the release rate; one dominates the other depending on the drug, morphology of the carrier, and other physiochemical characteristics. Release of small drug molecules from polymeric systems is largely governed by diffusion; diffusion closely follows Fick's diffusion equation. In contrast, release of macromolecules such as proteins and peptides from polymer systems is more complex because it depends largely on polymer degradation.

Biodegradable polymers generally undergo three types of degradation [61]. Type I degradation refers to the polymer where the degradation occurs along the main chain of the polymer. The cleavage of linkages between monomers results in a continuous decrease in molecular weight. Most of the linear biodegradable polymers follow this degradation pattern. Type II degradation occurs when water-soluble polymer is made insoluble by ubiquitous cross-linking with a hydrolysable covalent bond. As the cross-links erode, polymer fragments become soluble and diffuse away from the bulk material mass. Type III degradation involves a degradation of a polymer side chain. This type of degradation has been observed with partially esterified maleic anhydride copolymers [62, 63]. The polymer becomes water-soluble as the side

chain carboxylate groups are ionized. Often times, polymer drug delivery systems will function via various combinations of the aforementioned degradation types.

The desire to build into polymers precise zero-order surface erosion substrates, without alteration of the integrity of the inner structures, has been difficult to achieve. Although surface erosion can account for a significant portion of the release process, diffusion of the drug out of the device or solvent into the polymer ultimately contributes to the drug-release process and causes unpredictable changes in release rate that may not be desirable. However, a variety of factors has been identified that allow for the design of controlled release delivery systems.

Changes in molecular weight and co-polymerization are two parameters that can be used to alter the degradation rates of controlled release systems. To date, the largest body of literature exists on polyesters such as poly(DL-lactide) or poly(DL-lactide-co-glycolide). These polyesters are commercially available with varied molecular weights and monomer ratios of lactide and glycolide. They are also available with acid end groups to impart higher hydrophilicity. Addition of low-molecular-weight poly(DL-lactide) (MW 2000 Da) increases drug release from a biodegradable poly(DL-lactide) (MW 120,000 Da) drug delivery system [64]. It was found that the duration of action could be varied over a range of several hours to months by changing the amount of low-molecular-weight poly(DL-lactide).

The molecular weight of the drug species can also be varied to control the release profile. In the case of macromolecular drugs, major portions are released by polymer degradation and erosion, and a small portion is released by the diffusion mechanism. For instance, polypeptides usually have limited solubility in a polymer matrix of the aqueous channels present in the delivery system could be tortuous and narrow to facilitate diffusion. Reports from the literature indicate that the release of macromolecular drugs is tri-phasic, characterized by a high initial or “burst” release, a lag phase, and finally the release of drug at a higher rate until depletion. Physiologically, this may mean a brief period of therapeutic activity or even acute toxicity, a period of no activity corresponding to the lag phase, and finally sustained activity.

Many classes of polymers are hydrophobic and crystalline in nature and need certain modifications in order to have acceptable biodegradation and drug release. As an example, polycaprolactone is crystalline and hydrophobic, and it can take years for complete dissolution in the body. Similar to polylactides, the biodegradation rates of polycaprolactones can be hastened by blending with polymers such as PLA and PGA or alkylamines [65, 66]. Plasticizers can also

be added to polymeric systems to alter their degradation properties in addition to their mechanical properties. Addition of the plasticizer has been reported to reduce the glassy nature of the polymers, reduces the porosity, and may deform the surface owing to dehydration, all resulting in altered drug release [67, 68].

The method of preparation and processing used to manufacture the release system can have significant effects on the ultimate release rates observed. Degradation of the polymer matrix and as well as the stability of the drug should be considered before selecting a manufacturing process. Vapreotide, a somatostatin analogue, incorporated PLGA implants formulated by two different manufacturing techniques, extrusion and injection molding, and the influence of processing methods on the *in vitro* degradation of the polymer was studied [69]. Both methods decreased the molecular weight and polydispersity index of the polymer, but there was no change in the crystalline network. The extruded implants degraded more rapidly *in vitro* than the injection molded ones and showed higher early release rates. The physicochemical properties of solvents used in the fashioning of biodegradable drug implants can affect the release profiles as well. The boiling point, volatility, and miscibility with other solvents need to be considered especially in the case of formulated micro- and nano-spheres. Solvent effects tend to alter the micro-sphere morphology, changing drug entrapment efficiency and release rates [70, 71].

Numerous synthetic biodegradable polymers are available and still being developed for sustained release and targeted drug delivery applications. An enormous amount of literature is available on various means of altering the performance of these polymers and the delivery systems they constitute. Development of such an optimized drug delivery system using biodegradable polymers can offer significant improvements in patient comfort and compliance. These systems in many cases reduce the required dose intake and limit unwanted toxicities, as well as providing better therapeutic efficacy owing to continuous availability of drug in the therapeutic ranges over an extended period.

2.0 LDI-GLYCEROL POLYURETHANE IMPLANTS EXHIBIT CONTROLLED RELEASE OF DB-67 AND ANTI-TUMOR ACTIVITY *IN VITRO* AGAINST MALIGNANT GLIOMAS

2.1 ABSTRACT

The purpose of the present study was to develop a biodegradable and biocompatible polyurethane drug delivery system based on lysine diisocyanate (LDI) and glycerol for the controlled release of 7-*tert*-butyldimethylsilyl-10-hydroxy-camptothecin (DB-67). DB-67 has yet to be implemented into any clinical due to an inability to be delivered in sufficient quantities to impact tumor growth and disease progression. To remedy this, DB-67 was covalently incorporated into our delivery system by way of an organometallic urethane catalyst, and was found dispersed uniformly throughout the LDI-glycerol polyurethane discs. Scanning electron micrographs indicate that the LDI-glycerol discs are uniform and possess a pore distribution typical of the non-solvent casting technique used to prepare them. The release rates of DB-67 from the LDI-glycerol discs were found to follow zero-order kinetics, varying with both time and temperature, and were shown capable of delivering therapeutic concentrations of DB-67 *in vitro*. Cellular proliferation assays demonstrate that empty LDI-glycerol discs alone do not significantly alter the growth of malignant human glioma cell lines (U87, T98G, LN229, SG388). DB-67 loaded LDI-glycerol polyurethane discs were found to inhibit cellular proliferation by 50% on average in all the malignant glioma cell lines tested. These results clearly demonstrate the long-term slow release of DB-67 from LDI-glycerol polyurethane discs and their potential for postoperative intra-cranial chemotherapy of cancers.

Keywords: drug delivery; polyurethane; camptothecin; glioma; lysine diisocyanate

2.2 INTRODUCTION

Camptothecin (CPT) and its numerous synthetic analogs comprise a special class of anticancer agents active in lung, ovarian, breast, pancreas, and stomach cancers previously reported resistant to chemotherapy [2, 5, 6, 72]. CPT is a naturally occurring alkaloid first isolated from the Chinese tree *Camptotheca acuminata* (Nyssaceae) by Wall and co workers in 1966 [73]. Unsuccessful results in three early Phase I studies lessened the interest in the drug for a number of years [74-76]. It was later shown that CPT inhibited the enzyme topoisomerase I, a nuclear protein essential for DNA repair during replication, and interest in the drug and its analogs was reborn [77, 78]. Currently, two CPT analogs, topotecan and irinotecan, have been approved by the FDA, and at least 10 additional CPT derivatives are in various stages of clinical trials – including 9-amino-CPT in advanced clinical trials [2, 5].

The pharmaceutical development and clinical utility of the camptothecins are limited by the distinctive dynamics of these agents in the blood stream. All of the camptothecins now in clinical development contain a α -hydroxy- δ -lactone moiety, and they exist in two distinct forms at the physiological pH of 7.0 and above. The biologically active “lactone-closed” form reacts with water to form a biologically inactive “lactone-opened” (carboxylate) form [8, 9]. This simple chemical hydrolysis dynamically inactivates the parent drug. Furthering the problem, the predominant human blood serum protein, albumin (HSA), preferentially binds the carboxylate form – shifting the equilibrium towards the inactive moiety [10-12]. Because camptothecins are S-phase specific drugs, optimal topo I inhibitory activity is only obtained when the tumors of a patient are continuously exposed to the drug. Accordingly, establishing conditions where a therapeutically relevant concentration of the lactone-closed form of a camptothecin is present over a suitable period for tumor cells to cycle through the S-phase is a major challenge.

The CPT analog, 7-*tert*-butyldimethylsilyl-10-hydroxy-camptothecin (DB-67), was synthesized in an attempt to further enhance the therapeutic performance of this class of drugs [79-81]. DB-67 displays superior stability in plasma relative to other camptothecin agents, likely due to its lipophilicity and reduced interactions with the carboxylate-binding site on serum albumin. The analog also possesses a high intrinsic potency against the topo I target enzyme with a unique DNA cleavage profile. Ultimately, the combination of its potency and stability profiles suggests that it may be more efficacious than the currently used FDA-approved CPT-based

therapies. However, the compound is largely water-insoluble, making it difficult to deliver into the body through the conventional routes such as oral, intravenous or intramuscular injection [12]. As such, DB-67 has yet to be implemented into any clinical therapies due to an inability to be delivered in adequate quantities to impact tumor growth and disease progression.

Surgically implantable polymer matrices loaded with chemotherapeutic agents are a proven approach to localized drug delivery [48, 82, 83]. The matrix is loaded with the desired agent and then implanted within the tumor site, following as complete a surgical resection as clinically possible. The matrix releases its drug load over a period pre-determined by the characteristics of the encapsulating polymer, delivering drug to neoplastic cells existing in the peritumoral region that otherwise would give rise to recurring tumor. Typically, these types of drug delivery systems have been created by dissolving drug in a polymer and processing it into the desired morphology. The drug remains physically entrapped in the polymer, but it is not anchored through chemical bonds – and a burst release of drug subsequently follows. CPTs have previously been delivered in this manner [83-86]. Because the degree of survival improvement with previous polymer-based local delivery approaches, although statistically significant, has been modest at best, there is a rationale to build on this strategy in order to further enhance therapeutic efficacy. Our goal was therefore to develop a synthetic, biodegradable matrix incorporating DB-67 through labile chemical bonds, resulting in controlled long-term delivery of the agent to tumor cells.

Our laboratory has developed a new generation of biocompatible polyurethanes composed of lysine diisocyanate (LDI) and glycerol that degrade into the non-toxic components – lysine, glycerol, and CO₂ [87, 88]. Only a handful of studies have reported the successful use of polyurethanes in drug delivery applications, and their favorable results support further examination of this approach [89-94]. Our peptide-based urethane possesses the versatility of commercial polyurethane systems, but lacks the toxicity associated with commercial urethane degradation products. The goal of this study was to develop a biodegradable polyurethane disc incorporating DB-67 through reactive isocyanate groups capable of controlled, long-term drug delivery to tumor cells through hydrolysis of urethane linkages. We hypothesized that it is possible to incorporate DB-67 into the backbone of such a polymer and impact cellular growth *in vitro* – the ultimate goal being long-term delivery of active compound over a period of months *in vivo*.

2.3 MATERIAL AND METHODS

2.3.1 Materials

Lysine diisocyanate methyl ester (LDI) was purchased from Chemical Division, Kyowa Hakko Kogyo Co. Ltd. (Tokyo, Japan). 7-*tert*-butyldimethylsilyl-10-hydroxycamptothecin (DB-67) was obtained from Dr. Dennis Curran at the University of Pittsburgh, Chemistry Dept. (Pittsburgh, PA). The human malignant glioma cell lines U87 and T98G were obtained from the American Type Tissue Culture Collection. LN229 was kindly provided by Dr. Nicolas de Tribolet (Lausanne, Switzerland). The SG388 cell line was established at Children's Hospital of Pittsburgh from a tumor specimen identified by a neuropathologist. MTS reagents were obtained from Promega. Chemicals were obtained from Sigma–Aldrich Chemical Co. and were of reagent grade unless otherwise specified (Milwaukee, WI).

2.3.2 Reaction of DB-67 with LDI

Lysine methyl-ester diisocyanate (MW 212, 4.43 mg, 0.021 mmol) was added to DB-67 (MW 479, 10.0 mg, 0.021 mmol) in a 1:1 molar ratio and dissolved in 1 ml of THF in a dry flask. Two samples were prepared and 10 μ L of tin(II) 2-ethylhexanoate (MW 405, d 1.251, 0.031 mmol) was added to one sample. Samples were sealed and stirred in the dark at room temperature for 48 hours. THF was then removed at 50 °C in a vacuum oven, and the resulting solid was incorporated into a potassium bromide (KBr) window. FT-IR spectroscopy was then used to confirm the presence or absence of isocyanate signal at 2265 cm^{-1} in the samples.

2.3.3 Synthesis of the LDI-glycerol Polyurethane containing DB-67

DB-67 (MW 479, 10 mg, 0.021 mmol), LDI (MW 212, 3.93 g, 18.52 mmol) and tin(II)-2-ethylhexanoate (MW 405, 5 μ l, 0.016 mmol) were added to a small, dry reaction vessel. The flask was then flushed with nitrogen, sealed, and the mixture was allowed to stir in the dark at room temperature for a period of 24 hours. Glycerol (MW 92, 1.13g, 12.28 mmol) and dry, HPLC

grade acetone (2.5 ml) were then added to the flask. The flask was again flushed with nitrogen, sealed, and allowed to stir vigorously in the dark at room temperature for approximately 72 hours. During this time the mixture changed from opaque to translucent and its viscosity increased.

Following a 72-hour reaction period, a non-solvent casting technique was used to cast the material into a film. The viscous pre-polymer was transferred to a 65mm PTFE dish submerged in an ethyl-acetate (EtAc) bath. The pre-polymer was allowed to cure for 5 days in the dark at room temperature and then placed into a vacuum oven at 45 °C for 24 hours to remove residual EtAc and acetone. At this time the resulting film was removed from the PTFE dish and cut into discs using a 4mm tissue biopsy punch (Sklar Instruments). The discs were placed into an ethanol bath in order to remove residual acetone from the polymerization reaction; the discs were left to soak in the dark for 7 days and the ethanol was changed daily. Following the ethanol wash, the samples were rinsed several times with deionized H₂O, and allowed to soak in the dark for 72 hours to remove any remaining ethanol. The deionized H₂O was changed twice daily. The discs were then dried overnight in a vacuum oven at 45 °C and placed into storage in the dark at 4 °C for further analysis. Control discs not containing DB-67 were prepared by adding LDI, glycerol, and tin catalyst in the same amounts as above simultaneously to a reaction vessel. The contents were then reacted and processed as previously described.

2.3.4 Distribution of DB-67

Twenty LDI-glycerol discs containing DB-67 were placed into individual sample vials. One milliliter of 1N NaOH was added to each vial, and the vials were sonicated at 45 °C for 1 hour to completely hydrolyze the polymer. In basic solution, DB-67 will exist in its ionized hydroxy-acid form, but its fluorescent properties are identical to the closed lactone form [81]. Samples were stored in the dark at 4 °C overnight and analyzed the following day.

The DB-67 content of each LDI-glycerol disc was assessed with fluorescence spectroscopy utilizing 430 nm and 550 nm for the excitation and emission wavelengths, respectively. Samples were diluted 100-fold with de-ionized water prior to being read. Each sample was read 10 times in rapid succession, and an average of the signal was used to calculate

DB-67 content from a standard curve ($R^2=0.9995$). Standards were prepared by serial dilution from a 50 $\mu\text{g}/\text{ml}$ stock solution in 1N NaOH.

Lysine content of the polymer discs was assessed using the ninhydrin colorimetric assay. Ninhydrin reagent was prepared by dissolving ninhydrin (MW 178, 2.0 g, 11.23 mmol) in 50 ml DMSO and stannous chloride (MW 190, 80 mg, 0.42 mmol) in 50 ml of 0.2 M citrate buffer (pH 5). These two solutions were mixed; the resulting solution was used the same day. Polymer samples dissolved in NaOH were diluted 20-fold with PBS (pH 7.4). 20 μL of the diluted sample was added to 1 ml of ninhydrin reagent and immersed in boiling water for 20 minutes. 200 μL from each sample was then transferred to a 96-well plate and the absorbance at 570 nm was read and used to calculate the lysine content from a standard curve ($R^2=1.0000$). Standards were prepared by serial dilution from a 10 mg/ml stock solution of lysine methyl-ester in PBS (pH 7.4) Each sample was assayed in triplicate and the average was used to determine the final lysine content.

2.3.5 Stability of DB-67 in Aqueous Solution

Previous studies have reported the fluorescence quenching of CPT in aqueous solution [95]. In order to assess the stability of DB-67's fluorescence signal in aqueous solution, 200 nM DB-67 solutions were prepared in PBS (pH 7.4) from a 10 mM stock solution prepared in DMSO. Samples were placed on rocking plates and incubated in a temperature-controlled room at 4, 22, and 37° C for 60 days. Every 7 days, 3ml of PBS was retrieved and DB-67 content was assessed using fluorescence spectroscopy.

2.3.6 In vitro Release of DB-67

LDI-glycerol polyurethane samples containing DB-67 were incubated at 10 mg/ml in PBS (pH 7.4) on rocking plates in temperature-controlled rooms at 4, 22, and 37° C for 60 days. Sample chambers were protected from light during this time. Every few days, 3 ml of PBS was retrieved from each sample. The amount of DB-67 released from the polymer was detected using fluorescence spectroscopy and a standard curve ($R^2=0.9973$), with 430 and 550 nm as the

excitation and emission wavelengths, respectively. Lysine and glycerol release from the polymer were not assessed at this time due to the extremely low concentration of these species present in the degradation media.

2.3.7 Effect of Polyurethane Tablets on Cellular Proliferation

A panel of human malignant glioma cell lines consisting of U87, T98G, SG388, and LN229 was used for the anti-proliferative analysis of our drug releasing polymer discs. For these studies, 1×10^2 cells were plated and grown for 24 hr in 100 μ l of growth medium in 96-well plates. Polymer discs were then added to the cells and they were incubated for 5 days. Positive and negative controls received a stock solution of DB-67 (100 nM final concentration) or media alone, respectively. In all cases, final concentrations of DMSO were $\leq 0.1\%$, well below the concentrations that interfere with the proliferation in the above cell lines. After the incubation period, the number of viable glioma cells were determined by measuring the bio-reduction of the tetrazolium compound MTS by intracellular hydrolases in the presence of the electron coupling reagent PMS as previously described [96]. All samples were tested in twelve separate wells and averaged.

Prior to beginning the anti-proliferative analysis described, varying numbers of cells from each of the four malignant glioma cell lines were plated, and the MTS signal was measured at 24-hour intervals over a 5 day period (data not shown). From these preliminary studies, it was found that plating 1×10^2 cells/well retained a linear MTS signal over the proposed 5-day incubation period.

2.4 RESULTS AND DISCUSSION

2.4.1 Reaction of DB-67 and LDI

Our laboratory has previously shown that polyurethanes synthesized from LDI and glycerol degrade hydrolytically into the non-toxic components lysine, glycerol, and CO_2 [87]. DB-67 was

incorporated into the LDI-glycerol polymer by way of hydrolysable urethane linkages in an attempt to retain its anti-proliferative activity. Figure 6 illustrates the chemical structure of these components and that of the proposed polymer structure.

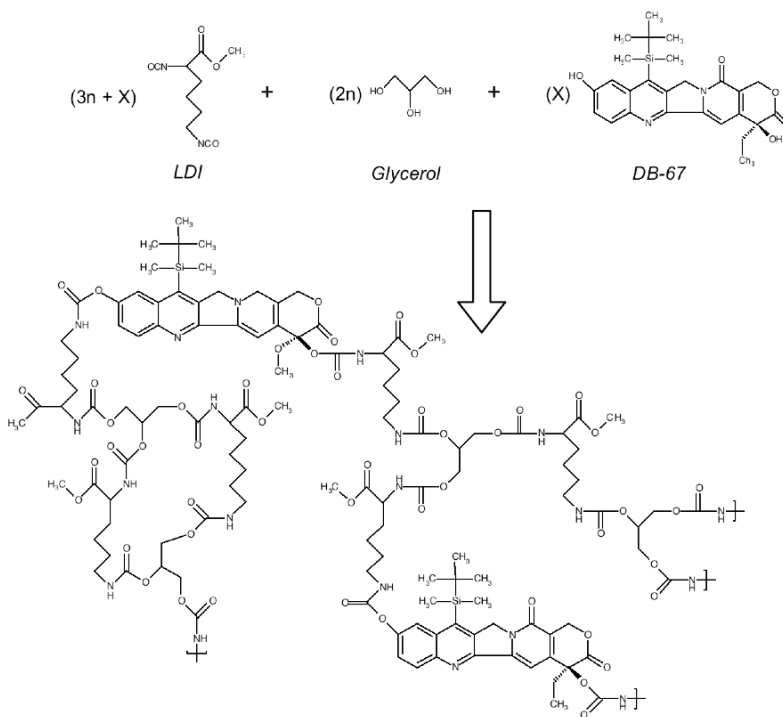


Figure 6 – Molecular structure of DB-67, LDI, glycerol and the LDI-glycerol polyurethane

FT-IR data demonstrate isocyanate signal at 2265 cm^{-1} that persists in a 1:1 molar reaction between DB-67 and LDI after 48 hours (Figure 7). When tin(II) 2-ethylhexanoate, an organometallic urethane catalyst, is present there is an absence of any isocyanate band after 48 hours. Complete disappearance of the isocyanate signal in a 1:1 molar reaction of LDI and DB-67 (1:1 NCO/OH) suggests that both of the hydroxyl groups present in DB-67 have reacted. Identification of the individual carbonyl bands representative of the newly formed urethane is not possible here, as DB-67 also contains several carbonyl structures that overlap in that particular region of the spectra. Furthermore, the FT-IR spectra of DB-67 and LDI alone demonstrates hydroxyl stretching at 3430 cm^{-1} , and a shift of that band to 3380 cm^{-1} occurred when catalyst was added – suggesting the formation of a secondary amine, and hence urethane linkages.

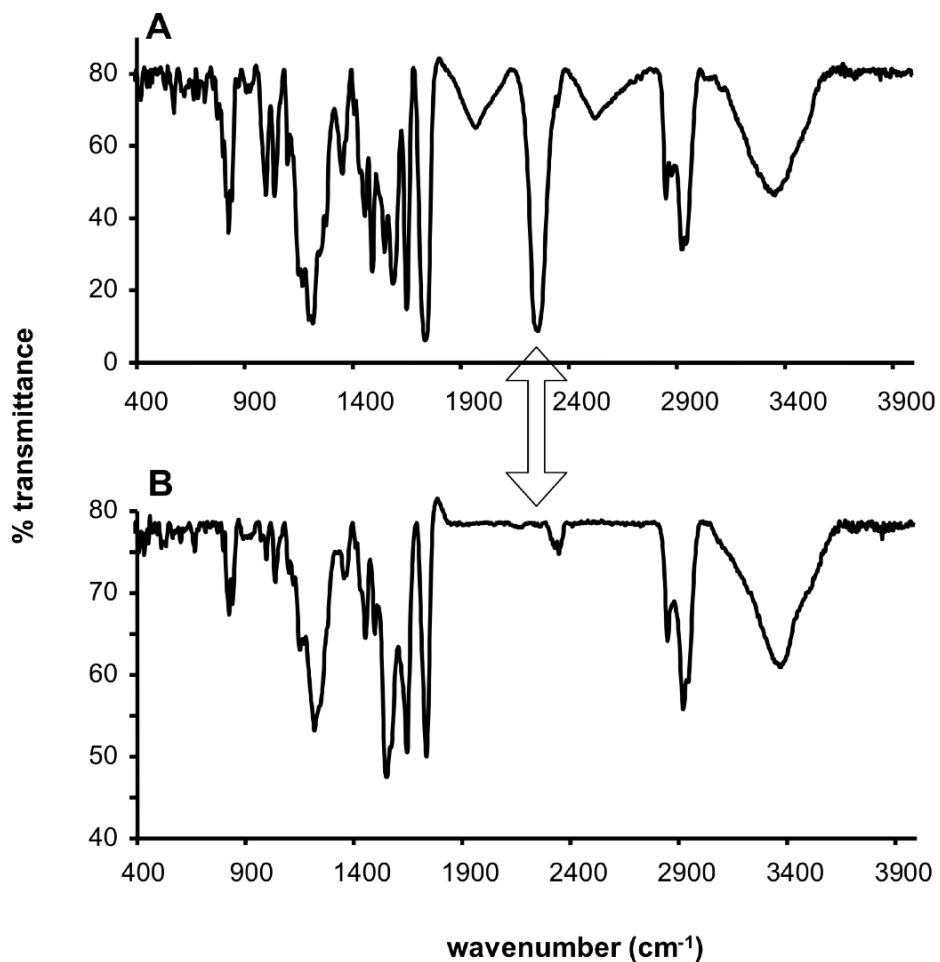


Figure 7 - IR Data depicting 1:1 molar reactions between DB-67 and LDI after 48 hours: (A) without tin(II) 2-ethylhexanoate, (B) with 10 μ l tin(II) 2-ethylhexanoate

2.4.2 Characterization of LDI-Glycerol Tablets

Our lab has previously synthesized LDI-based foams that support cellular growth and attachment [87, 88]. The polyurethane tablets fashioned in this study differ in morphology from those materials previously studied. Scanning electron micrograph images reveal polymer samples with a unique pore distribution through out the volume of the tablet (Figure 8). This morphology is artifact and is typical of non-solvent casting techniques used to form the film that was later cut

into 4mm discs. However, all surfaces of the material appeared identical under higher magnification.

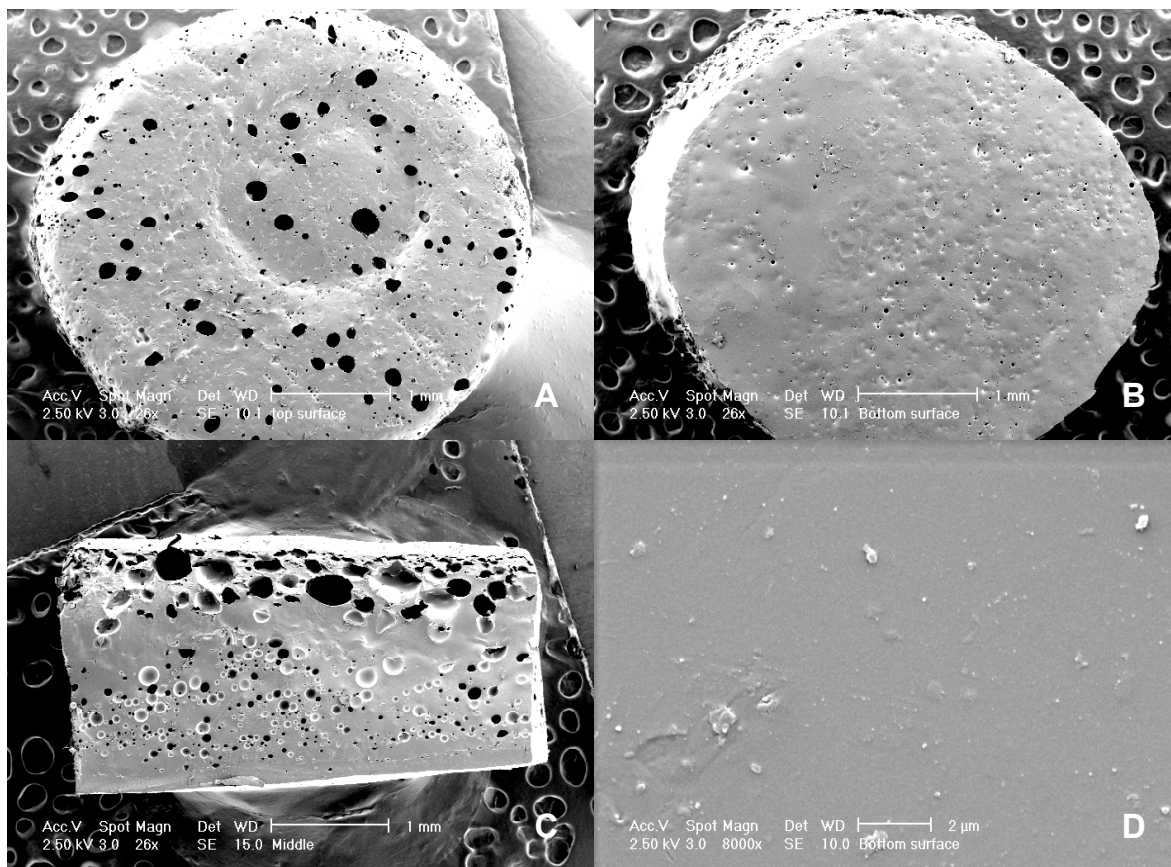


Figure 8 – Scanning electron microscope images of an LDI-glycerol drug delivery system: (A) Top surface of tablet which was exposed to non-solvent during the curing process, (B) View of bottom surface in contact with Teflon surface during curing, (C) Cross-sectional image of tablet demonstrates pore distribution, (D) Examination at 8000x magnification (only bottom surface is shown)

An FT-IR spectrum of the LDI-glycerol polyurethane disc with DB-67 was obtained through freezing a small sample in liquid nitrogen, crushing it, and then incorporating it into a KBr window (Figure 9). The spectrum does not display the characteristic isocyanate signal at 2265 cm^{-1} , while it does indicate urethane and secondary amine formation at 1720 cm^{-1} and 3400 cm^{-1} , respectively. The spectrum also displays the requisite CH_2 (2945 cm^{-1}), CH (2865 cm^{-1}), and C=O (1260 cm^{-1}) stretching frequencies, as well as the NH bending frequency (1540 cm^{-1}). All of these signals are consistent with the polymer structure shown in Figure 1. Individual

frequencies of the DB-67 moiety were not able to be resolved due to the low concentration of the species in the sample.

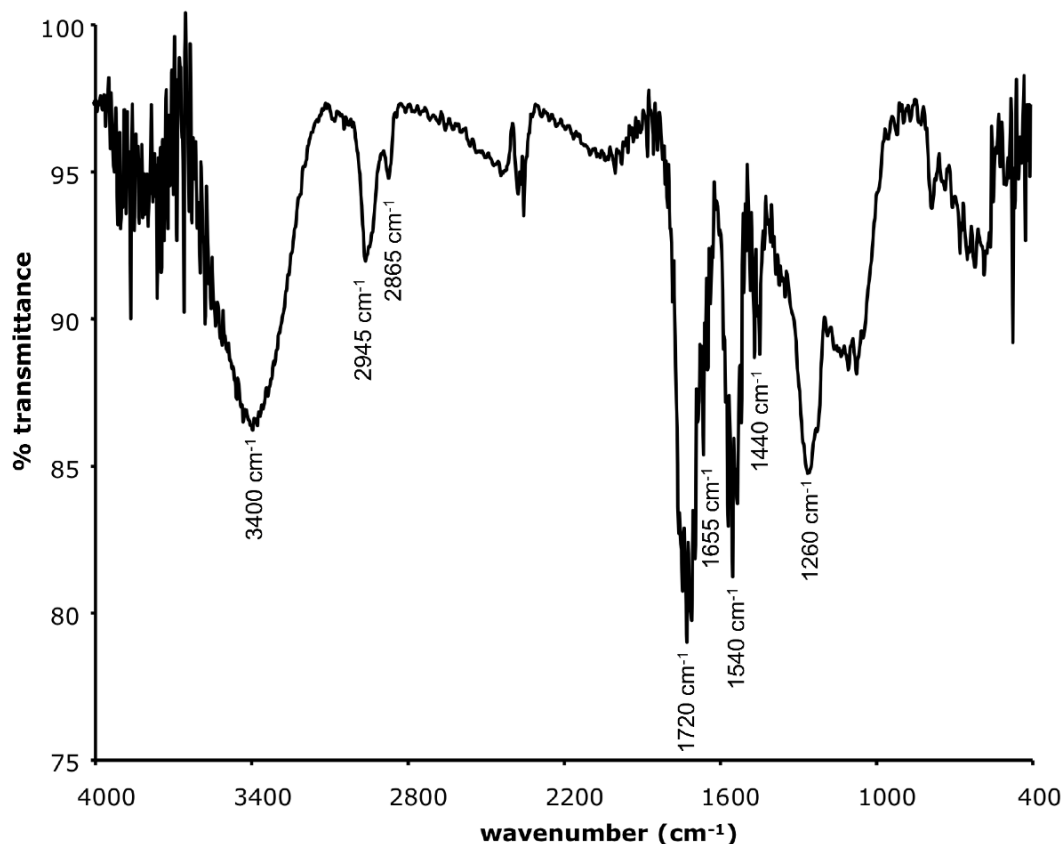


Figure 9 - FT-IR spectrum of an LDI-glycerol polyurethane disc containing DB-67

It is essential that drug delivery systems be able to be reliably reproduced in the amounts and under the conditions required for clinical use [4]. Therefore, it was important to ensure that the polymer processing techniques used in this study resulted in reproducible samples with uniform distribution of drug throughout the samples. LDI-glycerol polymer discs containing DB-67 (n=20) were produced using the aforementioned methods, and analyzed for average DB-67, lysine, and glycerol content (Table 2). The relative percentages listed are calculated from the total weight of the synthetic constituents, not the degradation products resulting from polymer hydrolysis.

Table 2 - DB-67, lysine and glycerol content of LDI-glycerol polymer discs

<i>Polymer disc (mg)</i>	<u>DB-67</u>		<u>Lysine</u>		<u>Glycerol^a</u>		<u><i>μg DB-67</i></u> <u><i>mg polymer</i></u>
	<i>μg</i>	<i>wt %</i>	<i>mg</i>	<i>wt %</i>	<i>mg</i>	<i>wt %</i>	
18.3	14.7 ± 0.1	0.08	12.5 ± 0.4	68.2	1.8	10.1	0.8
22.7	17.7 ± 0.1	0.08	13.9 ± 0.4	61.3	4.3	19.2	0.8
20.8	16.3 ± 0.1	0.08	12.9 ± 0.4	62.2	3.8	18.0	0.8
20.9	16.3 ± 0.1	0.08	13.4 ± 0.5	64.2	3.2	15.4	0.8
19.9	15.4 ± 0.1	0.08	11.9 ± 0.4	60.0	4.2	20.9	0.8
16.5	12.6 ± 0.1	0.08	11.2 ± 0.5	68.1	1.7	10.3	0.8
17.4	13.4 ± 0.1	0.08	11.2 ± 0.4	64.2	2.7	15.4	0.8
17.3	13.4 ± 0.1	0.08	11.7 ± 0.6	67.8	1.8	10.6	0.8
19.7	15.8 ± 0.1	0.08	13.0 ± 0.5	65.9	2.6	13.2	0.8
22.1	17.1 ± 0.1	0.08	13.5 ± 0.6	60.9	4.4	19.7	0.8
17.2	13.2 ± 0.1	0.08	11.4 ± 0.5	66.3	2.2	12.7	0.8
17.8	13.5 ± 0.1	0.08	11.8 ± 0.3	66.4	2.2	12.6	0.8
16.2	12.5 ± 0.1	0.08	10.5 ± 0.7	64.5	2.4	15.0	0.8
17.3	13.6 ± 0.25	0.08	11.4 ± 0.5	65.7	2.3	13.4	0.8
18.3	13.1 ± 0.1	0.07	11.0 ± 0.4	56.0	3.8	21.0	0.7
15.5	12.0 ± 0.1	0.08	10.1 ± 0.6	65.2	2.2	14.1	0.8
21.0	16.0 ± 0.1	0.08	13.4 ± 0.5	63.9	3.3	15.8	0.8
17.4	13.7 ± 0.1	0.08	10.9 ± 0.3	62.7	3.0	17.4	0.8
15.9	12.1 ± 0.1	0.08	10.1 ± 0.6	63.6	2.6	16.2	0.8
18.2	13.8 ± 0.1	0.08	11.2 ± 0.5	61.3	3.5	19.2	0.8
18.5 ± 2.1	14.32 ± 0.1	0.08	11.9 ± 0.5	64.12	2.9 ± 0.9	15.5	0.8

^aglycerol content = (total mass) – (mass of LDI and DB-67)

Samples were found to have a consistent drug load of 14.3 μg DB-67 per disc, or 0.08% (w/w). The relative percentages of lysine and glycerol were found to be 64.1% (w/w) and 15.5% (w/w), respectively. These values agree reasonably well with the nominal percentages predicted from the reaction stoichiometry of 58.7% and 22.2% lysine and glycerol, respectively. Although the weights of the discs were found to vary, the drug is evenly distributed throughout the polymer film (0.772 μg drug/mg polymer). It is clear upon inspection of these results that the processing techniques used in this study are reproducible and result in uniform distribution of DB-67 throughout the material.

Given 10 mg of DB-67 was used in our synthetic reaction and the weight of LDI and glycerol used was approximately 5 grams, we would anticipate the LDI-glycerol polyurethane discs to contain 0.2% (w/w) drug. However, the discs were found to contain 0.08 % (w/w) DB-

67, indicating that only 38.5% of the DB-67 used was successfully loaded into the polymer. We believe the decreased loading of drug results from a few key factors. First, the DB-67 fluorescence signal was found to be light sensitive and to decay significantly at 37 °C when left exposed to light in aqueous media (Figure 10).

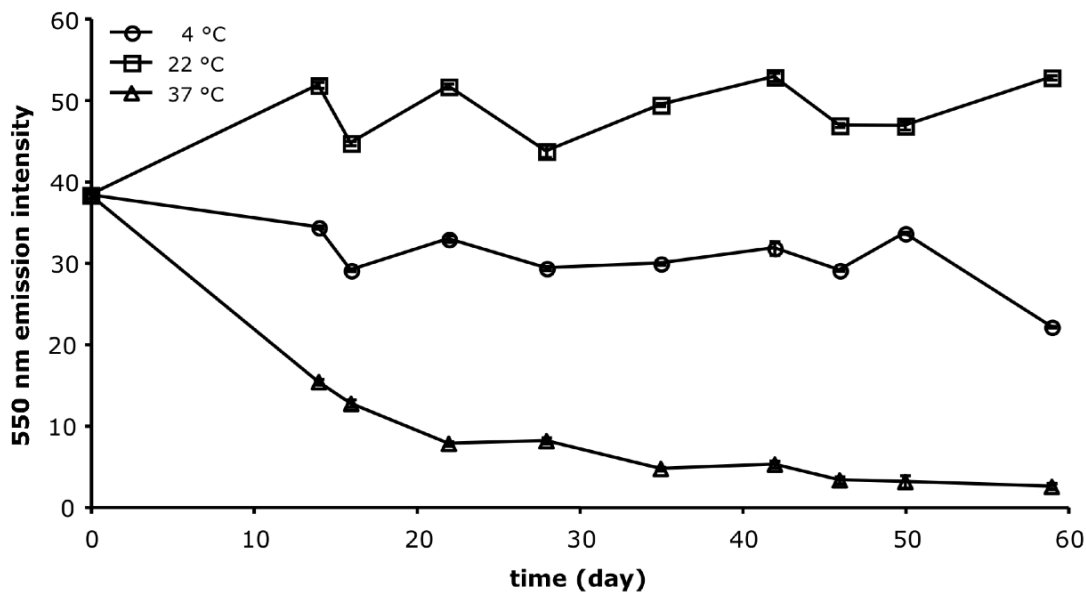


Figure 10 - Fluorescence decay profiles of 200 nM DB-67 solutions in PBS (pH 7.4) left unprotected from light at 4, 22 and 37 °C. Error bars represent one standard deviation from the mean

It is likely that the decaying fluorescence signal results in an underestimation of the total drug content in our samples as well as what was being released *in vitro*. Second, our synthetic reaction relies on the use of acetone as a polymerization solvent, and it must be removed from the discs prior to tissue culture with a series of ethanol and deionized water washes. The half-life of other CPT analogs in aqueous solution has been reported to be on the order of 20 minutes [97]. Our discs were subject to an aqueous environment for 72 hours, and this may have contributed to some of the loss DB-67 signal. Third, small oligomers if present in the viscous pre-polymer are likely to be sparingly soluble in EtAc. As a result they are then lost during the curing process. This was confirmed by FTIR of the polymer residue found on the bottom of our curing chambers after the EtAc was allowed to evaporate (data not shown). These factors when combined can

reasonably account for the “missing” DB-67 in our polyurethane films, and refinement of the processing techniques can certainly limit this loss in the future.

2.4.3 In vitro Drug Release

DB-67 possesses a characteristic, intense excitation-emission spectra that makes it easily detectable in aqueous solution at extremely low concentrations although the drug is sparingly soluble [54, 97]. The fluorescence excitation/emission spectrum of a 10 $\mu\text{g/ml}$ DB-67 solution prepared in 1N NaOH is shown in Figure 11.

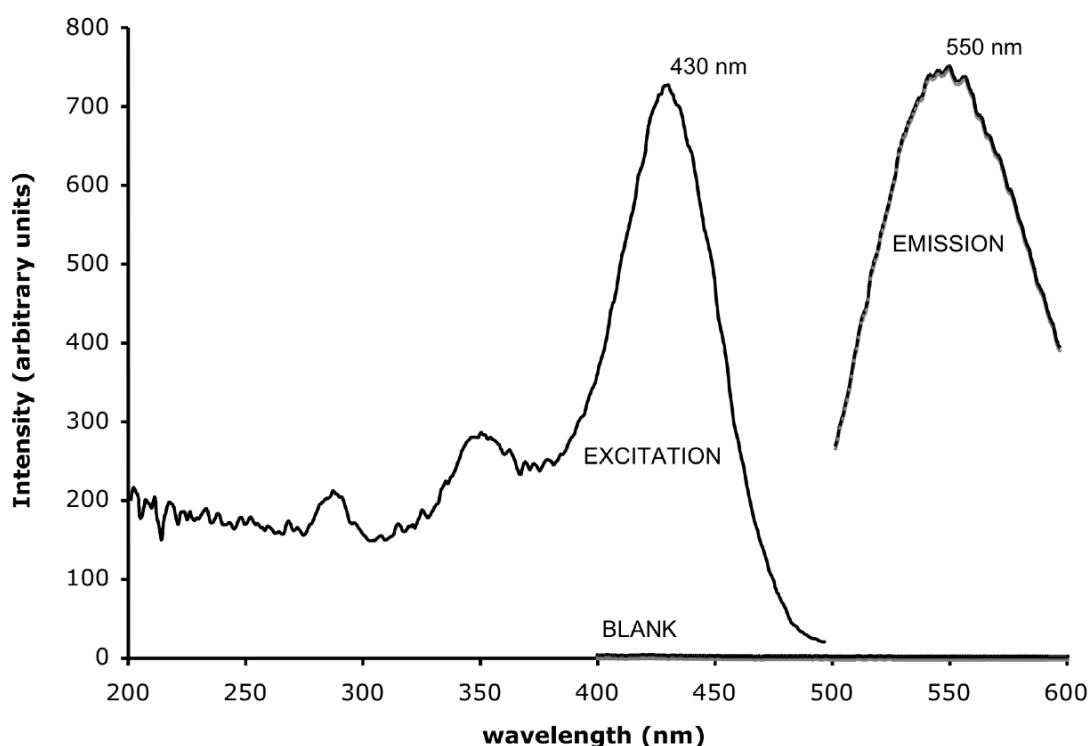


Figure 11 - Excitation-emission fluorescence spectra of a 1.0 mg/ml DB-67 solution in 1N NaOH

There was no appreciable signal present in the DB-67 emission range from the solution used to dissolve the samples and to prepare standards. The standard curve used to assess the degradation samples was linear over the concentration ranges used for detection ($R^2=0.9998$). Since the DB-67 fluorescence signal was found to be light sensitive and was shown to significantly decay over

time when left exposed to ambient light in the temperature controlled rooms, degradation samples were kept in the dark in an attempt to limit signal decay. However, it is still possible that we are underestimating the true concentration of DB-67 in solution using this method.

The small amount of DB-67 incorporated into the discs was assumed to not alter the degradative kinetics of the LDI-glycerol material. Figure 12 shows the release profiles of LDI-glycerol discs containing 0.08 % (w/w) DB-67 content.

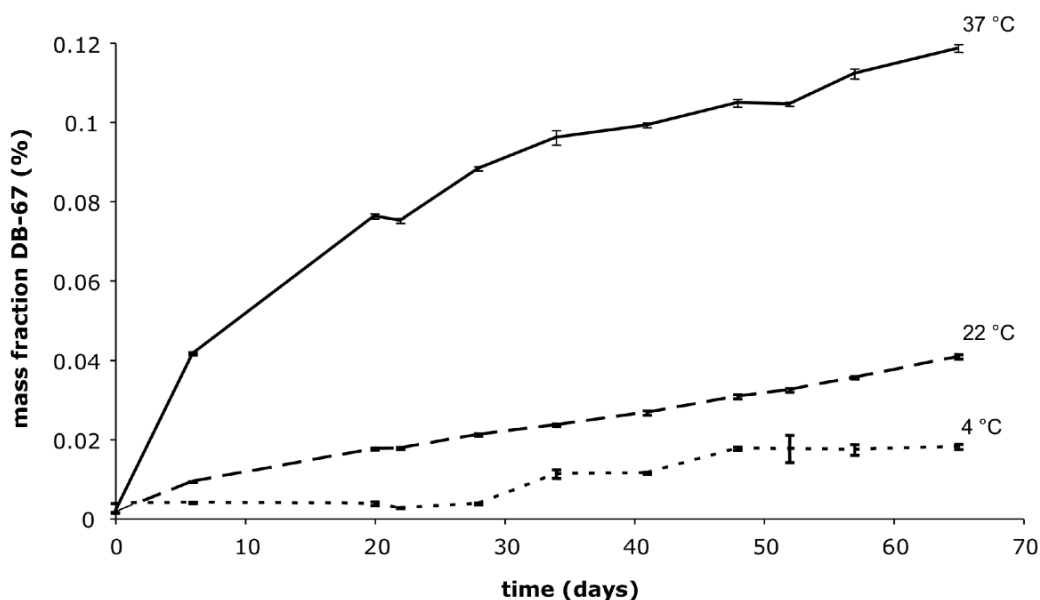


Figure 12 - *In vitro* release characteristics of DB-67 from LDI-Glycerol tablets incubated at 10 mg/ml in PBS at 4, 22, and 37 °C (pH 7.4). Error bars represent one standard deviation from the mean

Drug release was shown to vary in a temperature dependent fashion, with the highest drug loads being released at 37 °C. The release at 22 °C was observed to follow zero-order kinetics. These results agree well with the degradation profile previously observed for LDI-based polyurethanes [87]. By day 65 of the study, DB-67 concentrations of 1.4, 3.1, and 9.2 ng/ml were obtained in aqueous solution at 4, 22, and 37 °C, respectively. These values represent 0.02, 0.04, and 0.1 % of the total drug load contained in the samples. These results indicate that only a small fraction of the total drug load found its way into solution, and that slow release of drug from a polymer by way of urethane hydrolysis is indeed a successful long-term release strategy. It was not possible to assess whether the DB-67 being released was in its active lactone or inactive hydroxy-acid

form, but *in vitro* cytotoxicity assays should provide insight. It is well-known that *in vivo* degradation rates of polymers are increased relative to those seen *in vitro* [98, 99], and this effect has also been noted to occur in polyurethane materials as well [100]. Therefore, we anticipate achieving higher concentrations of DB-67 *in vivo* than were obtained *in vitro*.

2.4.4 Cytotoxicity Assays

Previous studies indicate that CPT and its many analogs are quite effective at halting the growth of malignant tumors [80, 101-104], and one study in particular has examined the *in vitro* effects of DB-67 on malignant gliomal cell lines [96]. In that study, DB-67 was found to inhibit the growth of malignant gliomal cell lines at extremely low concentrations. Specifically, the U87, SG388 and T98G cell lines were found to have decreased proliferation in the presence of DB-67 at concentrations of 2, 3, and 6 ng/ml, respectively. Our degradation assays of the LDI-glycerol discs containing 0.08 % (w/w) DB-67 have shown that by day 6 a concentration of 3.2 ng/ml was attained in PBS at 37 °C. Therefore, we anticipated that the amounts of drug being released from LDI-glycerol discs are great enough to inhibit growth in our panel of malignant glioma cell lines.

The cytotoxicities of the LDI-glycerol discs containing 0.08 % (w/w) DB-67 in each of the malignant gliomal cell line are shown in Figure 13.

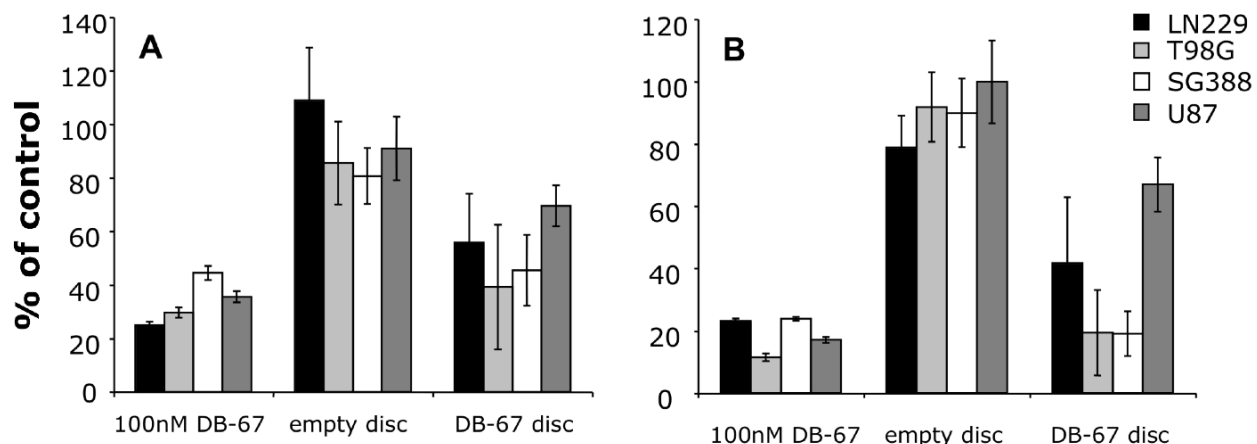


Figure 13 - *In vitro* cytotoxicity results of (A) 3-day and (B) 5-day treatments on malignant gliomal cell lines. Error bars represent one standard deviation from the mean

Empty polymer discs were found to not significantly differ from cells grown in media alone at the $\alpha=0.0001$ level of significance. In all malignant gliomal cell lines, a statistically significant difference was seen between neat polymer and “drug-loaded” polymer in both 3-day and 5-day treatment groups ($p<0.0001$). In the T98G, SG388, and LN229 malignant gliomal cell lines there was no significant difference between the 100 nM DB-67 treated cells and the 0.08% (w/w) DB-67 discs ($p<0.0001$). The cytotoxicity data has been summarized in Table 3.

Table 3 - *In vitro* cytotoxicity of DB-67 loaded LDI-glycerol polyurethanes

<i>3 Day Treatment</i>							
<i>Cell line</i>	<i>Media alone</i>	<i>100 nM DB-67</i>		<i>Empty disc</i>		<i>DB-67 disc</i>	
	MTS ^a	MTS	% control	MTS	% control	MTS	% control
LN229	0.992 ± 0.045	0.247 ± 0.012	24.9 ± 1.2	1.080 ± 0.195	108.9 ± 19.6	0.554 ± 0.179	55.9 ± 18.1
T98G	1.155 ± 0.103	0.342 ± 0.022	29.6 ± 1.9	0.986 ± 0.179	85.4 ± 15.5	0.452 ± 0.269	39.1 ± 23.3
SG388	0.938 ± 0.084	0.416 ± 0.024	44.4 ± 2.6	0.755 ± 0.098	80.6 ± 10.5	0.426 ± 0.124	45.4 ± 13.3
U87	0.625 ± 0.069	0.222 ± 0.013	35.5 ± 2.1	0.568 ± 0.074	90.9 ± 11.9	0.434 ± 0.047	69.4 ± 7.6

<i>5 Day Treatment</i>							
<i>Cell line</i>	<i>Media alone</i>	<i>100 nM DB-67</i>		<i>Empty disc</i>		<i>DB-67 disc</i>	
	MTS	MTS	% control	MTS	% control	MTS	% control
LN229	1.071 ± 0.059	0.247 ± 0.009	23.0 ± 0.8	0.844 ± 0.110	78.8 ± 10.2	0.447 ± 0.226	41.7 ± 21.1
T98G	2.486 ± 0.202	0.285 ± 0.029	11.5 ± 1.2	2.282 ± 0.278	91.8 ± 11.2	0.482 ± 0.341	19.4 ± 13.7
SG388	1.720 ± 0.163	0.410 ± 0.010	23.8 ± 0.6	1.545 ± 0.189	89.8 ± 11.0	0.328 ± 0.124	19.1 ± 7.2
U87	1.202 ± 0.144	0.205 ± 0.011	17.1 ± 0.9	1.201 ± 0.159	99.9 ± 13.3	0.804 ± 0.105	66.9 ± 8.7

^aMTS = absorbance at 490 nm

These results suggest that DB-67 is being released in its active lactone-closed structure from the LDI-glycerol discs and it is present in concentrations high enough to impact malignant glioma proliferation *in vitro*.

2.5 CONCLUSIONS

In this study, we present a novel approach to the controlled delivery of the CPT analog DB-67 employing biocompatible, biodegradable polyurethanes constructed from LDI and glycerol. Our delivery system differs from other conventional approaches in that the drug has been covalently bound into the polymer framework. We have shown that DB-67 incorporates by reacting with LDI in the presence of an organometallic urethane catalyst. The drug is then released through slow, passive hydrolysis of urethane bonds. We were able to demonstrate the ability of an LDI-glycerol polyurethane disc to steadily deliver drug over a prolonged period. Therapeutic concentrations of the potent anticancer compound on the order of nanograms/ml were attained through steady, zero-order release from the polyurethane discs over a 65-day period with the potential to continue for much longer periods of time. It has also previously been demonstrated that the lactone moiety must remain intact in order to observe any cytotoxic effect[80]. Cellular proliferation assays conclude that only LDI-glycerol discs loaded with DB-67 exhibited any cytotoxic effect. It is unclear at this time how the polymer is able to stabilize the active lactone structure during the degradative process. These results from this study clearly demonstrate the potential for long-term drug release from a surgically implantable LDI-glycerol polyurethane device.

3.0 LDI-GLYCEROL POLYURETHANE FOAMS DEMONSTRATE CATALYST-DEPENDENT CONTROLLED RELEASE PROFILES AND EXHIBIT ANTI-TUMOR ACTIVITY AGAINST MALIGNANT GLIOMA CELLS

3.1 ABSTRACT

The purpose of the present study was to develop a biodegradable and biocompatible polyurethane drug delivery system based on lysine diisocyanate (LDI) and glycerol for the controlled release of 7-tert-butyldimethylsilyl-10-hydroxy-camptothecin (DB-67). The impact of urethane catalysts on cellular proliferation was assessed in an attempt to enhance the biocompatibility of our polyurethane materials. DB-67, a potent camptothecin analogue, was then incorporated into LDI-glycerol polyurethane foams with two different amine urethane catalysts: 1,4-diazobicyclo[2.2.2]-octane (DABCO) and 4,4'-(oxydi-2,1-ethane-diyl)bismorpholine (DMDEE). The material morphologies of the polyurethane foams were analyzed via SEM. DB-67 distribution throughout the foams was assessed through fluorescence microscopy. Release rates of DB-67 from the DABCO and DMDEE foams were found to be catalyst dependent and vary with temperature. The foams were capable of delivering therapeutic concentrations of DB-67 *in vitro* over an 11-week period. Cellular proliferation assays demonstrate that empty LDI-glycerol foams do not significantly alter the growth of malignant human glioma cell lines ($p < 0.05$). DB-67 loaded LDI-glycerol polyurethane foams were found to inhibit cellular proliferation by at least 75% in all the malignant glioma cell lines tested ($p < 1.0 \times 10^{-8}$). These results clearly demonstrate the long-term, catalyst-dependent release of DB-67 from LDI-glycerol polyurethane foams and their potential for use as implantable drug-delivery devices.

Keywords: lysine diisocyanate, polyurethane, drug delivery, camptothecin; glioma

3.2 INTRODUCTION

Camptothecin (CPT) and its numerous synthetic analogs comprise a special class of anticancer agents that appear to be quite active in human lung, ovarian, breast, pancreas, and gastric cancers previously reported resistant to chemotherapy [2, 5, 6, 72]. CPT is a naturally occurring alkaloid that was first isolated from the Chinese tree *Camptotheca acuminata* (Nyssaceae) by Wall and co workers in 1966 [73]. It inhibits the enzyme topoisomerase I, a nuclear protein essential for DNA repair during replication [77, 78]. Currently, two CPT analogs, topotecan and irinotecan have been approved by the FDA, and at least 10 additional CPT derivatives are in various stages of clinical trials – including 9-amino-CPT in advanced clinical trials [2, 5]. The CPT analog 7-*tert*-butyldimethylsilyl-10-hydroxy-camptothecin (DB-67) was synthesized in an attempt to enhance the stability and performance of CPTs [79-81]. DB-67 displays superior human blood stability relative to other camptothecin agents and possess a very high intrinsic potency against the topo I target enzyme. However, the compound is largely water-insoluble which has made clinical use quite difficult [12]. DB-67 has yet to be implemented into any clinical therapies due to an inability to be delivered in adequate quantities to impact tumor growth and disease progression.

Polyurethanes are a special class of synthetic materials that are widely used in many modern industrial applications as insulations, sealants, coatings, and foams [105]. Many have gained FDA approval and currently find a place in numerous medical technologies due to their unique chemical and physical properties [106-110]. Polyurethanes are easily synthesized from diisocyanate and polyalcohol precursors via a condensation reaction that can be controlled by various urethane formation catalysts. The catalytic mechanisms and their effects on the resultant polymer architecture are well understood and can be tailored to specific material applications.

Polyurethane catalysts for the most part are classified into two simple, distinct categories: organometallic and amine [18, 20]. The reactions they catalyze can be broken down into three categories: blowing, gelling, and cross-linking. The blowing reaction involves the reaction of isocyanate and water and generates a carbamic acid intermediate. As carbamic acid readily decomposes into an amine and CO₂, the polyurethane expands into foam. The gelling reactions simply refer to urethane or urea formation. The crosslinking reactions are generally quite limited

and refer to the reaction of isocyanate with itself, urethanes or ureas. Organometallic catalysts are often tin-based and tend to be more selective for gelling reactions, catalyzing urethane and urea formation. Amine catalysts are chiefly tertiary amines and they catalyze both gelling and blowing reactions. In this study, we focus primarily on the tertiary amine catalysts 1,4-diazobicyclo[2.2.2]-octane (DABCO) and 4,4'-(oxydi-2,1-ethane-diyl)bismorpholine, also known as dimorpholino-diethyl ether (DMDEE). DABCO is rather non-selective in nature and known to catalyze both gelling and blowing reactions, while DMDEE is specific for the blowing reaction.

The stability and degradative characteristics of polyurethane materials are ideal for the construction of controlled-release systems. However, the use of polyurethanes in the arena of drug delivery remains largely unexplored, although studies do exist that support their use [111-114]. Our laboratory has developed a new generation of biocompatible, biodegradable polyurethane constructed from lysine diisocyanate (LDI) and glycerol that degrade predictably via a hydrolytic mechanism into non-toxic components – lysine, glycerol and CO₂ [87, 88]. These materials possess the same versatility as widely used commercial polyurethanes, easily being processed into forms with unique physical properties. We have previously synthesized LDI-glycerol films and demonstrated their use as long-term drug delivery reservoirs. However, we can also fashion these materials into foams possessing different drug-delivery characteristics. We can also attempt to use the catalytic mechanisms to regulate the incorporation of drug and impact the release characteristics of our drug delivery systems. The purpose of this study is to formulate and characterize a drug delivery systems based on hydrolysable polyurethane foams prepared from LDI and glycerol.

3.3 MATERIAL AND METHODS

3.3.1 Materials

Lysine diisocyanate methyl ester (LDI) was purchased from Chemical Division, Kyowa Hakko Kogyo Co. Ltd. (Tokyo, Japan). 7-tert-butyldimethylsilyl-10-hydroxycamptothecin (DB-67) was obtained from Dr. Dennis Curran at the University of Pittsburgh, Chemistry Dept. (Pittsburgh,

PA). The human malignant glioma cell lines U87 and T98G were obtained from the American Type Tissue Culture Collection. LN229 was kindly provided by Dr. Nicolas de Tribolet (Lausanne, Switzerland). The SG388 cell line was established at Children's Hospital of Pittsburgh from a tumor specimen identified by a neuropathologist. MTS reagents were obtained from Promega. Bismuth 2-ethylhexanoate was obtained from Alfa Aesar (Ward Hill, MA). All other chemicals were obtained from Sigma–Aldrich (Milwaukee, WI) and were of reagent grade unless otherwise specified.

3.3.2 Urethane Catalyst Toxicity

T98G cells were plated in MEM media at a density of 100 cells/well in 96-well plates. The plates were incubated for 24 hours to allow for cell adhesion, and the media was changed prior to any treatment. Solutions of bismuth 2-ethylhexanoate (MW 639), tin(II) 2-ethylhexanoate (MW 405), dibutyltin dilaurate (MW 632), DABCO (MW 112) and DMDEE (MW 244) were prepared in DMSO; the final concentration of each solution was 10 mM. The catalyst solutions were mixed thoroughly, and 1.0 ml of each was diluted with 4.0 ml of growth media to arrive at 2 mM solutions. Serial dilutions of the catalyst/media solutions were performed across two 96-well plates, halving the concentration with each dilution. After a 5 day incubation period, the number of viable T98G cells were determined by measuring the bio-reduction of the tetrazolium compound MTS by intracellular hydrolases in the presence of the electron coupling reagent PMS as previously described [96].

The study was then repeated with DABCO (MW 112, 1.122g, 10 mmol) and DMDEE (MW 244, 2.443g, 10 mmol), adding each to 5.0 ml of MEM media. The resulting 2.0 M catalyst/media solutions were mixed until all of the catalyst had dissolved. The solutions were then diluted as before across three 96-well plates, and T98G proliferation was quantified after 5 days via MTS. LD₅₀ values were taken as the lowest catalyst concentration at which the MTS signal registered < 50% of the control value.

3.3.3 Reaction of LDI with DB-67: DMDEE vs. DABCO

DB-67 (MW 479, 32.0 mg, 0.07 mmol) was dissolved in 1.07 ml dry DMSO to yield a 30 mg/ml solution. Two small reaction flasks were each loaded with LDI (MW 212, 5.3 mg, 0.3 mmol) and 400 μ L of the DB-67 solution. DABCO (MW 112, 1.3 mg, 0.01 mmol) was added to one flask, and DMDEE (MW 244, 3.4 mg, 0.01 mmol) was added to the other. Both flasks were briefly mixed and IR spectra immediately taken. The flasks were flushed with nitrogen, sealed, and left to mix in the dark at room temperature; IR spectra were taken again in 4 hours. IR scans were taken at 0 and 4 hours to minimize the occurrence of urethane side-reactions.

3.3.4 Synthesis of LDI-glycerol polyurethane foams

Two small, dry reactions flasks were prepared, each containing glycerol (MW 92, 1.13 g, 12.3 mmol), LDI (MW 212, 3.93 g, 18.52 mmol), DB-67 (MW 479, 10 mg) and dry acetone (2.5 ml). DMDEE (MW 244, 20 mg, 0.08 mmol) was added to one flask, and DABCO (112 MW, 5 mg, 0.04 mmol) was added to the other. Each flask was then flushed with nitrogen, sealed and stirred in the dark at room temperature. During this time, the mixture changed from opaque to translucent and its viscosity increased.

The viscous pre-polymer was transferred to an 80 mm PTFE dish when the viscosity of the mixture measured $>3.0 \times 10^4$ cP (TA Instruments AR2000). Then 200 μ L of distilled, deionized H₂O was added to the pre-polymer and vigorously mixed in – initiating the foaming reaction. The samples were thoroughly mixed 3 times at 2-minute intervals to ensure the H₂O was fully incorporated. The samples were left open to the atmosphere yet covered to protect from light while the curing. The resulting polymer foams were then dried overnight in a vacuum oven at room temperature and placed into storage in the dark at 4 °C for further analysis. Control foams were prepared similarly, except DB-67 was not added to the initial reaction mixture. The foams were then assessed for sol content as previously described by Huang [115].

3.3.5 Distribution of DB-67 within the polyurethane foams

Foam samples were sliced to a thickness of roughly 500 μm and mounted on a glass slide. Fluorescent and non-fluorescent images were taken at 100X filter in order to assess the distribution of DB-67 throughout the DABCO and DMDEE polyurethane foams (Zeiss AX10 Imager.A1). A FITC filter was used to visualize the DB-67 compound within the sample (Chroma).

3.3.6 Release of DB-67 from LDI-glycerol Foams

LDI-glycerol polyurethane foam samples containing DB-67 were incubated at 10 mg/ml in PBS (pH 7.4) on rocking plates in temperature-controlled rooms at 4, 22, 37 and 70 $^{\circ}\text{C}$ for 7-weeks. Sample chambers were protected from light during this time. Every 7 days, 3.0 ml of PBS was retrieved from each sample; during the first week, PBS was also collected on day 3. The amount of DB-67 released from the polymer was detected using fluorescence spectroscopy with 430 nm and 550 nm for the excitation and emission wavelengths, respectively. The total amount of DB-67 collected was calculated as follows:

$$\text{mol}\% = \frac{1}{MW_{DB-67}} \left[3 \sum \left(\frac{m}{V} \right)_i + \left(\frac{m}{V} \right)_j (V_T - 3j) \right]$$

where $(m/V)_i$ represents the concentration of each collected sample and V_T the total volume (where each time point is designated “i” and “j” represents the last). Lysine and glycerol released from the polymer were not assessed at this time. At the end of the 11-week release study, the samples were dialyzed, dried and the mass recorded.

3.3.7 Effect of Polyurethane Foams on Cellular Proliferation

A panel of human malignant glioma cell lines (U87, T98G, and SG388, LN229) was used for the cytotoxicity analysis of our drug releasing polymer foams. For these studies, 1.0×10^2 cells were

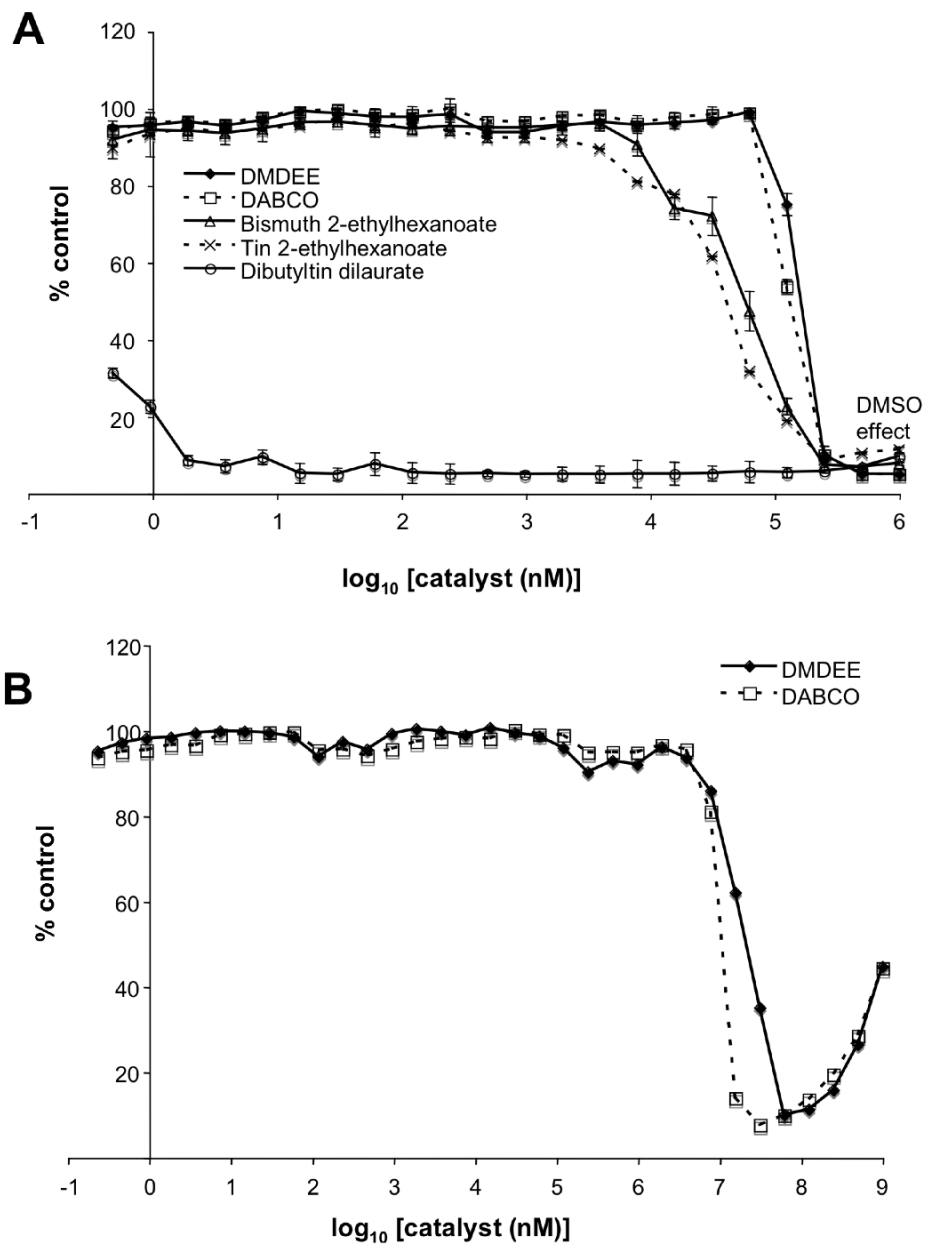
plated and incubated for 24 hr in 100 μ l growth media. Media was replaced and then LDI-glycerol foam samples approximately 5 mg in size were then added to the cells, and they were incubated for treatment periods 3 or 5 days. Positive and negative controls received a stock solution of DB-67 (100 nM final concentration) or media alone, respectively. In all cases, final concentrations of DMSO were $\leq 0.1\%$, well below the concentrations that interfere with the proliferation in the above cell lines. After the incubation period, the number of viable cells was determined by measuring the bio-reduction by intracellular hydrolases of the tetrazolium compound MTS in the presence of the electron coupling reagent PMS as previously described [96]. All samples were analyzed in twelve separate wells and an averaged. A two-tailed, two-sample unequal variance Student's t-test statistic was used to analyze the results.

Prior to beginning the anti-proliferative analysis described, varying numbers of cells from each of the four malignant gliomal cell lines were plated and the MTS signal was measured at 24-hour intervals over a 5 day period (data not shown). From these preliminary studies, it was found that plating 1.0×10^2 cells/well gave a linear MTS signal over a 5-day incubation period.

3.4 RESULTS

3.4.1 Urethane Catalyst Toxicity

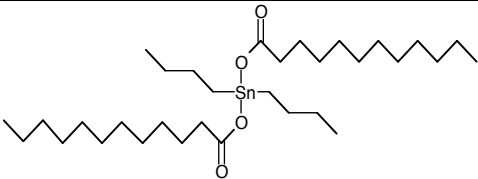
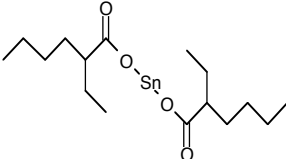
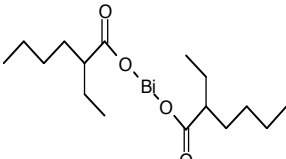
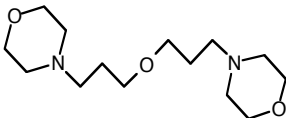
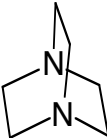
Dose-response profiles were generated for a few common urethane catalysts (Figure 14A). In general, the tertiary amine catalysts were tolerated at much higher concentrations by the T98G cells than the organometallic catalysts. The concentration of DMSO present in the first few lanes of the 96-well plate was calculated to be high enough to interfere with the results for DABCO and DMDEE. As a result, the study was repeated with much higher concentrations of those catalysts in media alone (Figure 14B).



**Figure 14 - Dose-response profiles for various organometallic and tertiary amine urethane catalysts:
 (A) baseline studies (B) extended profile for DABCO and DMDEE**

Table 4 summarizes the urethane catalysts used for this analysis and the corresponding cytotoxic concentrations reported as LD₅₀ values.

Table 4 - Polyurethane catalyst structures and toxicities

<u>Catalyst</u>	<u>Structure</u>	<u>Class</u>	<u>LD₅₀</u>
Dibutyltin dilaurate		organometallic	0 μ M
Tin(II) 2-ethylhexanoate		organometallic	62.5 μ M
Bismuth 2-ethylhexanoate		organometallic	62.5 μ M
Dimorpholino-diethylether (DMDEE)		3° amine	31.3 mM
1,4-Diazobicyclo[2.2.2]octane (DABCO)		3° amine	15.6 mM

3.4.2 Reactivity of DB-67 and LDI with DMDEE or DABCO

DB-67 and LDI were reacted together at a 1:1 molar ratio in the presence of either DABCO or DMDEE. Infrared (IR) spectroscopy was used to monitor the progress of the reaction through signals in the isocyanate ($2400\text{-}2160\text{ cm}^{-1}$) and carbonyl ($1850\text{-}1580\text{ cm}^{-1}$) regions of the spectra. Peak integrations in those regions of the spectra were also calculated at the start of the reactions and at 4 hours. The spectra from the reaction of DB-67/LDI with DMDEE indicate that the isocyanate signal persists at 2265 cm^{-1} over the 4-hour reaction period (Figure 15A). Concerning the signal integrations, the NCO/C=O ratio initially measured 0.66 and remained 0.64 after 4

hours. These findings indicate that DB-67 did not form any urethane bonds with LDI when DMDEE was used as a catalyst. On the other hand, the spectra from the reaction of DB-67/LDI with DABCO reveal a disappearance of the isocyanate signal after the 4-hour reaction period (Figure 15B). Once again using the signal integrations, the NCO/C=O ratio initially measures 0.66 and decreases to 0.20 after 4 hours. These findings indicate that in the presence of DABCO, urethane bonds are formed between DB-67 and LDI.

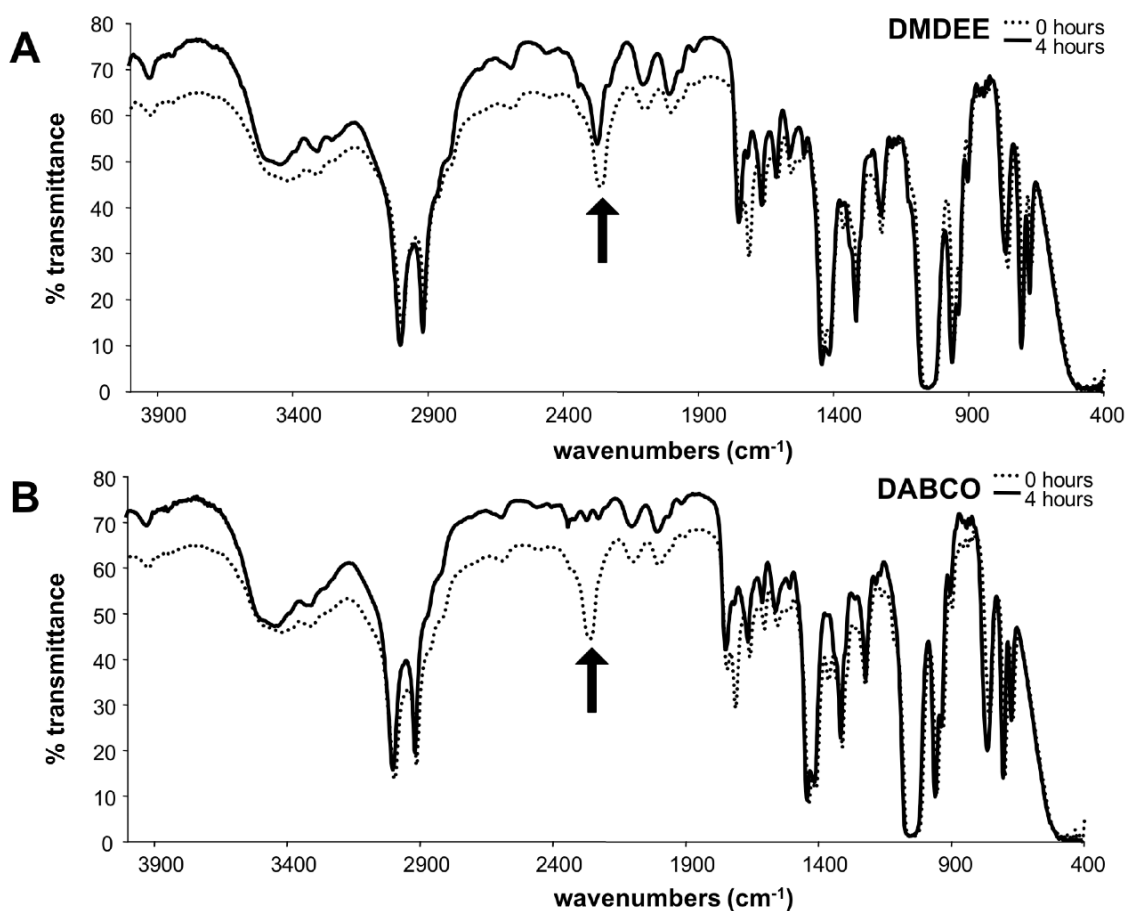


Figure 15 - FT-IR data assessing the reactivity of DB-67 with LDI in the presence of (A) DMDEE and (B) DABCO

3.4.3 Characterization of LDI-Glycerol Foams

It is important that the polyurethane pre-polymer be sufficiently viscous prior to initiation of the blowing reaction so that the rising foam does not collapse on itself prior curing. The viscosity of the pre-polymer was measured when the reaction could no longer be mixed atop a magnetic stirrer, first measuring at a shear stress of 5.0 Pa then again at 50.0 Pa with a 5-minute interval between measurements (Figure 16). It was determined that a value of at least 3.0×10^3 cP must be attained for proper foam formation.

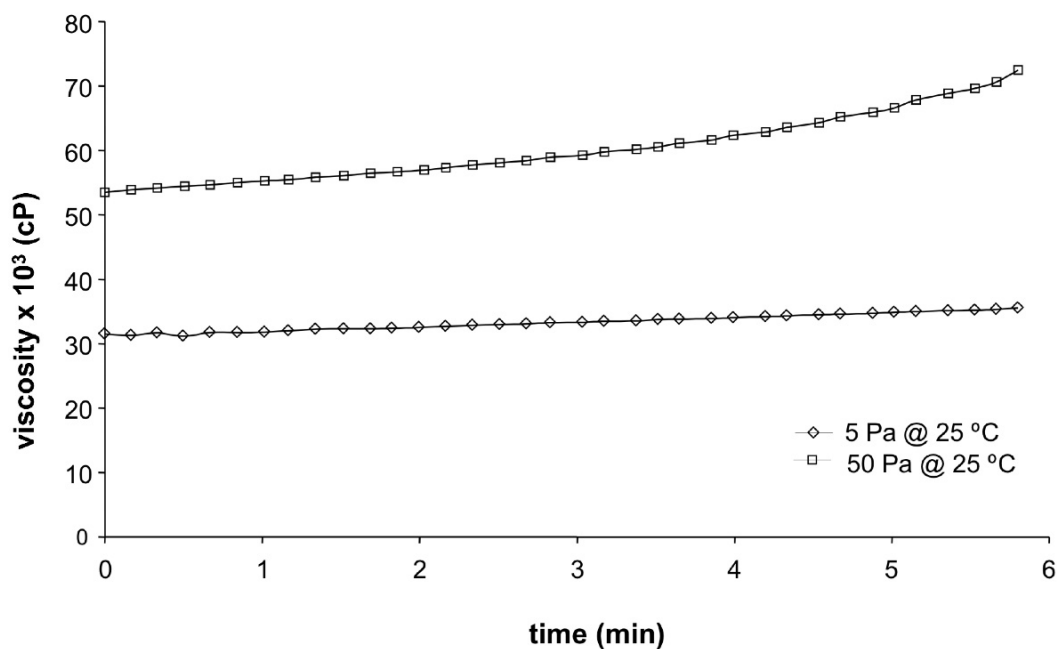


Figure 16 - Viscosity data for LDI-glycerol pre-polymer prior to initiation of the blowing reaction:
(A) 1st run at 5.0 Pa shear stress and (B) 2nd run at 50.0 Pa shear stress

Scanning electron micrograph images were obtained of the LDI-glycerol polyurethane foams made with DABCO and DMDEE. Low-magnification images (25X) reveal the DABCO foam cavitations are elliptical in nature, of similar size, and appear to have a preferred orientation of their long axis as indicated by the arrow (Figure 17A). In contrast, the DMDEE foam cavitations appear randomly distributed in terms of size and shape and have no apparent

directionality (Figure 17B). High magnification images (10,000X) of the LDI-glycerol foams demonstrate “micro-channels” which are apparent on the surface of the materials. The DABCO foam appears to have numerous, fine channels that are similar in size and oriented as indicated by the white arrow (Figure 17C). The DMDEE material exhibits channels that vary in terms of size and orientation and are far less numerous (Figure 17D).

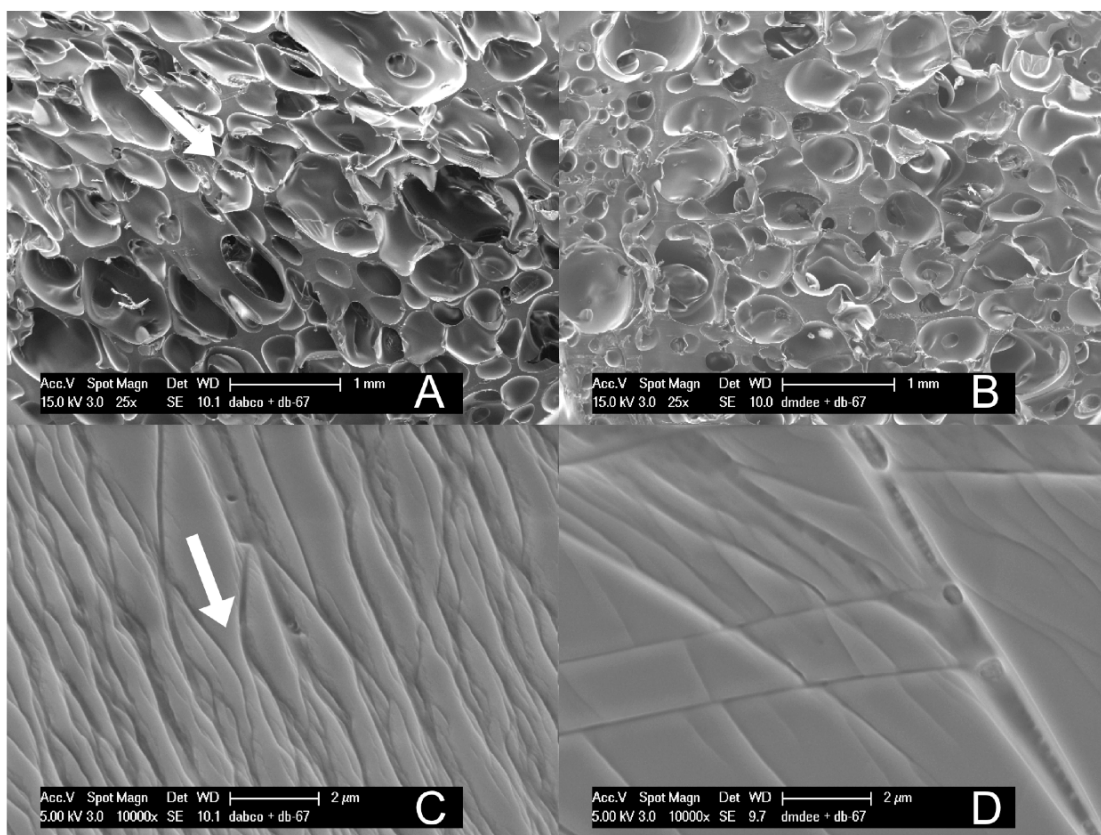


Figure 17 - Scanning electron micrographs of the LDI-glycerol polyurethane foams: (A) DABCO foam @ 25X (B) DMDEE foam @ 25X (C) DABCO foam @ 10,000X (D) DMDEE foam @ 10,000X

Fluorescent and non-fluorescent images were taken in order to assess the distribution of DB-67 throughout the DABCO and DMDEE polyurethane foams (Figure 18). Bright field images show that the DMDEE material possesses a highly ordered foam structure, while that of the DABCO material appears more random in nature. Fluorescent images suggest that DB-67 is uniformly distributed throughout the DABCO sample. However, in the DABCO sample DB-67

appears to reside in much higher concentrations clustered around the cavitations in the foam. Overlaid bright field and FITC images were constructed, and they corroborate these findings.

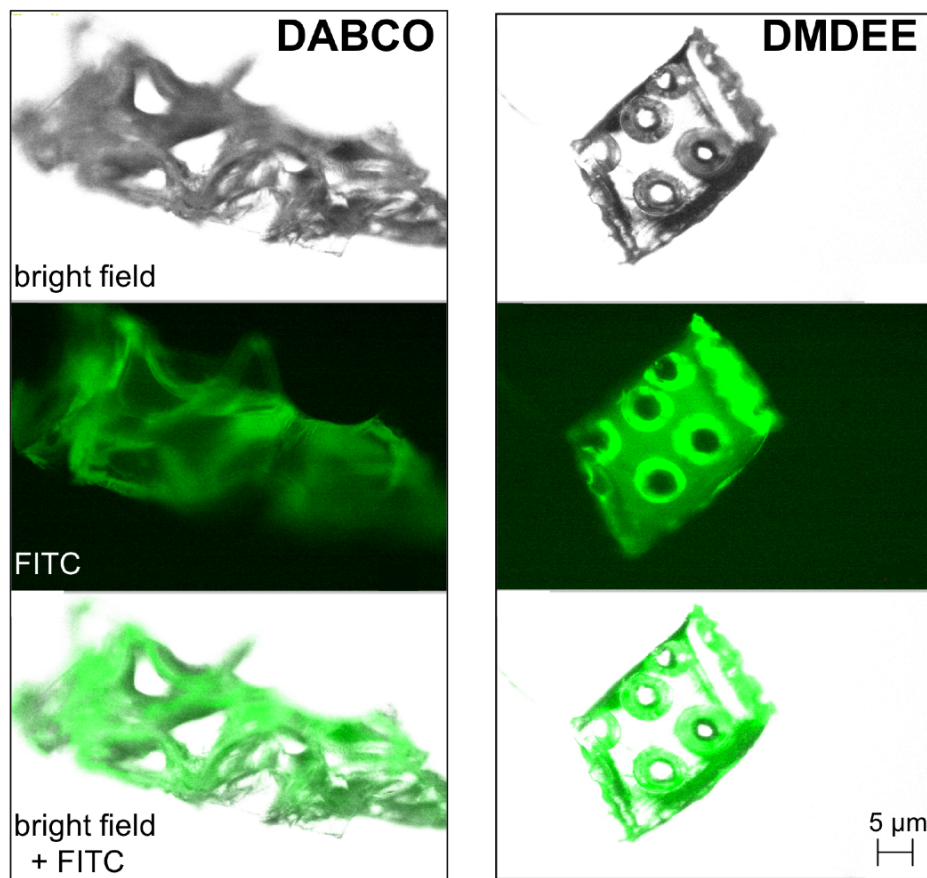


Figure 18 - Fluorescent and non-fluorescent images of the LDI-glycerol polyurethane foams

3.4.4 DB-67 Release from Polyurethane Foams

DB-67 release profiles were obtained for both DABCO and DMDEE polyurethane foams over a 49-day period (Figure 19). Drug release was non-linear and varied in a temperature dependent fashion; the highest drug concentrations were achieved at 70 °C. Significant material degradation was evident in both DMDEE and DABCO samples at 70 °C. At all temperatures except for 4 °C, both foams exhibit an initial burst release of DB-67. Shortly thereafter concentrations slowly

decline in a temperature dependent fashion and were shown to recover at higher temperatures. Maximum concentrations were observed early on for samples incubated at 22 and 37 °C, while those incubated at 4 and 37 °C occur at day-49.

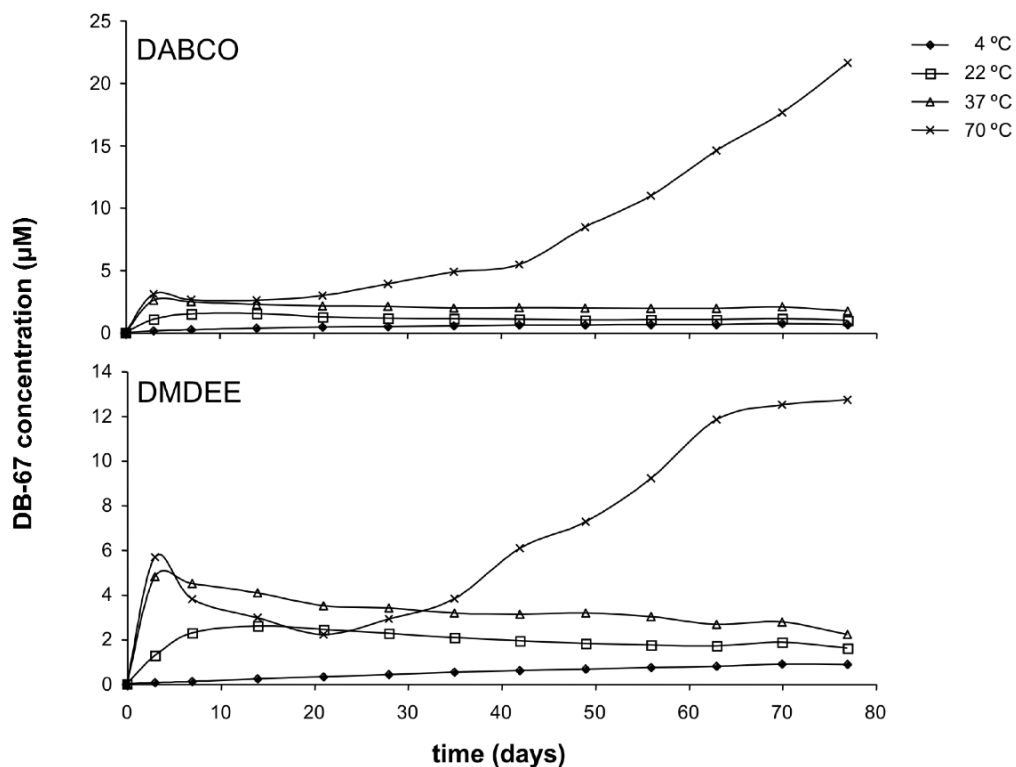


Figure 19 - Temperature dependent DB-67 release profiles for the LDI-glycerol foams

LDI-glycerol foams synthesized using either DABCO or DMDEE exhibit differences in their release profiles. A comparison at 37 °C reveals that greater amounts of DB-67 are released by the DMDEE foam over the 77-day test period (Figure 20). Concentrations in solution are observed to decrease over time for both the DMDEE and DABCO foams. The concentration of DB-67 released from the DMDEE foam remained consistently elevated over that of the DABCO foam. A comparison at 70 °C shows that although higher amounts of DB-67 are initially released from the DMDEE foam, eventually higher concentrations are obtained from the DABCO foam by day-77 (Figure 21).

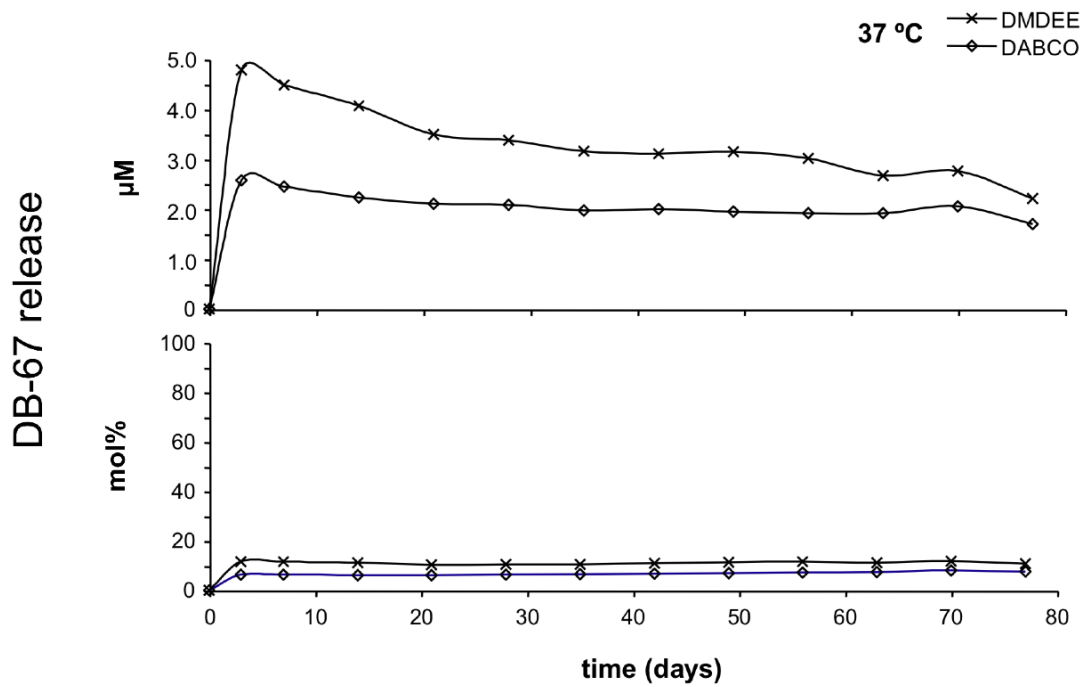


Figure 20 - Comparison of DB-67 release by DABCO and DMDEE foams at 37 °C

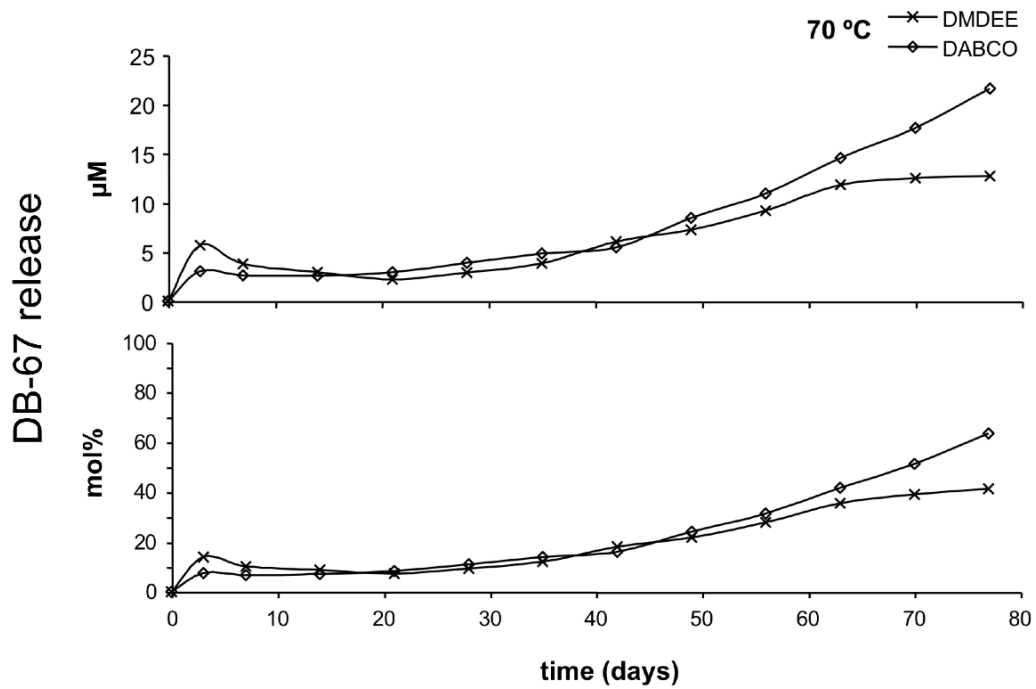


Figure 21 - Comparison of DB-67 Release by DABCO and DMDEE foams at 70 °C

At day-77, concentrations of DB-67 in solution are 21.6 μM and 12.7 μM for the DABCO and DMDEE foams, respectively. At that time, 63.4 and 41.4% of the total DB-67 had been released for from the DABCO and DMDEE foams, respectively. At day-63, the release of DB-67 from the DMDEE foam is noted to decline, while the DABCO foam continues releasing drug into solution. Release characteristics of the DABCO and DMDEE foams have been summarized in Table 5.

Table 5 - Release characteristics of the LDI-glycerol polyurethane foams

Catalyst	sol content (%)	Temperature ($^{\circ}\text{C}$)	DB-67 (mol%) ^a	Mass loss (%) ^a	Maximum concentrations (μM)	day	Initial concentrations (μM) ^b	Max/initial ratio
DABCO	7.0	4	2.2	7.8	0.7	70	0.1	7.0
		22	4.2	8.1	1.5	14	1.1	1.4
		37	7.5	9.7	2.6	3	2.6	1.0
		70	63.4	78.1	21.6	77	3.1	7.1
DMDEE	7.2	4	2.9	6.6	0.9	77	0.1	9.0
		22	7.1	7.3	2.6	14	1.3	2.00
		37	10.8	8.8	4.8	3	4.8	1.00
		70	41.4	62.8	12.7	77	5.7	2.2

a = at day-77, b = at day-3

3.4.5 Polyurethane Foam Cytotoxicity

The cytotoxicity of DABCO and DMDEE LDI-glycerol polyurethane foams was assessed in a panel of human malignant glioma cell lines (SG388, T98G, U87, LN229) via the MTS bio-reduction assay (Figure 22).

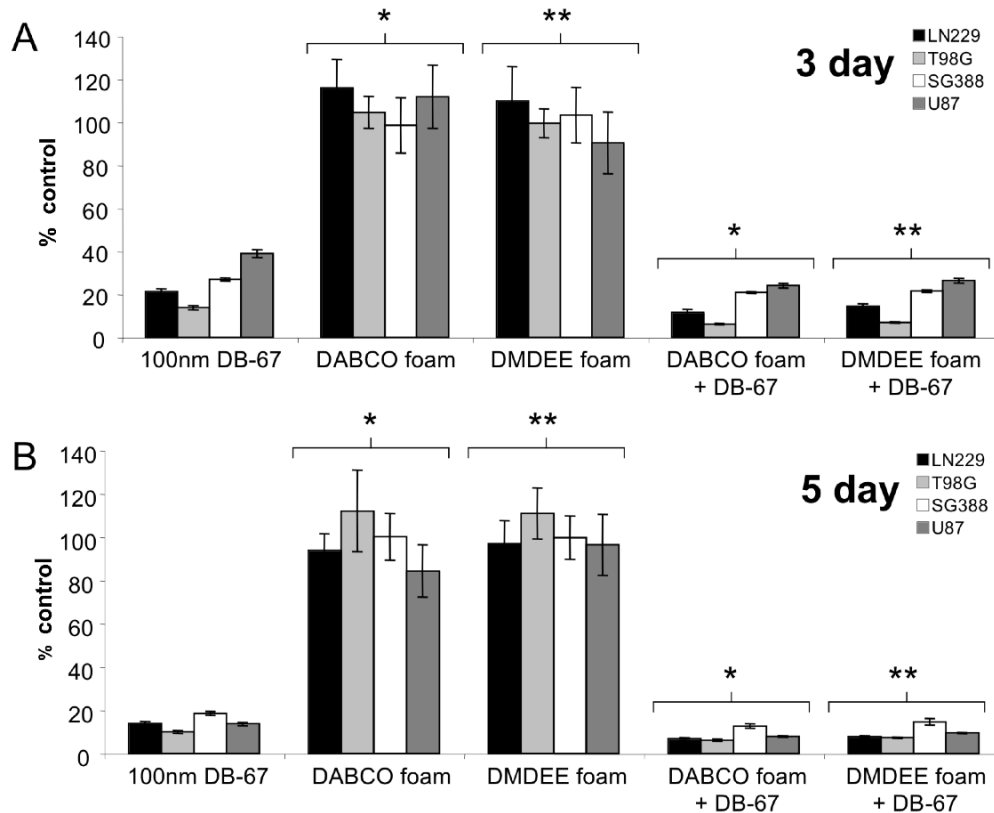


Figure 22 - In vitro cytotoxicity results of (A) 3-day and (B) 5-day treatments on malignant gliomal cell lines. Error bars represent one standard deviation from the mean

In every malignant glioma cell line tested, a statistically significant difference in cellular proliferation was seen for both catalysts between empty and DB-67 loaded foams ($p < 1.0 \times 10^{-8}$). There was also no significant difference in cytotoxicity detected between the drug-loaded DABCO and DMDEE foams ($p < 0.001$) except in the SG388 3-day treatment group ($p > 0.25$). The MTS signals from cells grown with empty DABCO and DMDEE polymer foams were found to not differ significantly from those of cells grown in media alone ($p < 0.05$) in 11 out of 16 treatment groups. Finally, in every malignant glioma cell line tested, a significant difference existed between the 100nM DB-67 solution and either the DABCO or DMDEE drug-loaded foam ($p < 1.0 \times 10^{-6}$). Note that without exception the MTS signal was always greater for the 100 nM DB-67 solution. The MTS data has been summarized for the reader in Table 6.

Table 6 - *In vitro* cytotoxicity of DB-67 loaded LDI-glycerol polyurethane foams

<i>Cell line</i>	3-Day Treatment MTS^a Signals					
	<u>+/- Controls</u>		<u>Empty Foams</u>		<u>DB-67 Foams</u>	
	Media (+)	100 nM DB-67 (-)	<u>DABCO</u>	<u>DMDEE</u>	<u>DABCO</u>	<u>DMDEE</u>
T98G	2.355 ± 0.080	0.324 ± 0.024	2.460 ± 0.175	2.342 ± 0.158	0.145 ± 0.007	0.162 ± 0.007
LN229	1.207 ± 0.088	0.257 ± 0.015	1.400 ± 0.158	1.325 ± 0.194	0.140 ± 0.016	0.173 ± 0.016
SG388	0.933 ± 0.047	0.250 ± 0.007	0.920 ± 0.120	0.964 ± 0.120	0.194 ± 0.005	0.201 ± 0.005
U87	0.602 ± 0.051	0.234 ± 0.011	0.673 ± 0.089	0.544 ± 0.087	0.144 ± 0.007	0.159 ± 0.007

<i>Cell line</i>	5-Day Treatment MTS^a Signals					
	<u>+/- Controls</u>		<u>Empty Foams</u>		<u>DB-67 Foams</u>	
	Media (+)	100 nM DB-67 (-)	<u>DABCO</u>	<u>DMDEE</u>	<u>DABCO</u>	<u>DMDEE</u>
T98G	1.967 ± 0.092	0.197 ± 0.013	2.201 ± 0.371	2.179 ± 0.230	0.122 ± 0.008	0.144 ± 0.005
LN229	1.985 ± 0.222	0.277 ± 0.016	1.861 ± 0.151	1.922 ± 0.213	0.135 ± 0.013	0.154 ± 0.011
SG388	1.288 ± 0.171	0.240 ± 0.011	1.289 ± 0.139	1.284 ± 0.128	0.164 ± 0.012	0.189 ± 0.020
U87	1.569 ± 0.193	0.214 ± 0.012	1.323 ± 0.191	1.512 ± 0.220	0.124 ± 0.006	0.149 ± 0.006

^a MTS = absorbance at 490 nm

3.5 DISCUSSION

Many commercial urethane catalysts are known to exhibit moderate to severe toxic side effects [116, 117]. Therefore, it is important to attempt to minimize any toxicity associated with our polyurethane materials via proper catalyst selection. To this end, dose-response profiles were generated for a series of commonly used organometallic and tertiary amine urethane catalysts. From the data, it is clear that tertiary amine catalysts are better tolerated than the organometallic catalysts. Consequently, one would expect LDI-glycerol foams prepared with either DABCO or DMDEE to be less cytotoxic than our LDI-glycerol discs previously fashioned with tin(II) 2-ethylhexanoate.

Central to our newly developed delivery technology is the ability of a therapeutic compound to incorporate into a polyurethane network. Drug incorporation provides the opportunity for long-term controlled release through passive hydrolysis of urethane bonds. We have previously shown that DB-67 will react with LDI in the presence of an organometallic catalyst, but it was uncertain if the same would be true of the tertiary amine catalysts. Via infrared spectroscopy, it has been concluded that DB-67 reactivity with LDI is indeed catalyst dependent. The non-selectivity of DABCO and the specificity of DMDEE can be utilized to manipulate the incorporation of DB-67 into LDI-glycerol polyurethane foams. These differences likely account for some of the differences observed in the drug release profiles of the foams.

It is essential that drug delivery systems be able to be reliably reproduced in the amounts and under the conditions required for clinical use [4]. When fashioning polyurethane foams, the pre-polymer viscosity is quite important. This value must be sufficiently large to prevent foam collapse, but not so large as to inhibit the foam expansion [118, 119]. For our LDI-glycerol polyurethane foams, this value was found to be 3.0×10^3 cP. An inspection of the viscous curves reveals that the viscosity of the pre-polymer slowly increased over each measurement period and jumps significantly from one measurement to the next. This is certainly due to initiation of the blowing reaction by atmospheric moisture content.

Scanning electron images reveal differences in the structure of the polyurethane foams, while fluorescent images indicate important differences in the distribution of DB-67. SEM shows DABCO foams possessing a more ordered structure at both high and low magnification in terms of the cavitations (i.e. - size, shape, and orientation) and micro-channels (i.e. – number and orientation). Conversely, SEM shows the DMDEE foams appearing more random in terms of the cavitations and micro-channel distribution. Bright field images further confirm these structure-catalyst correlations. Fluorescent images indicate DB-67 is present in higher concentrations around the cavitations in the DMDEE foam. In the DABCO foam, DB-67 appears to be much more uniformly distributed. Images lack focus in certain regions of the images due to sample thickness being greater than the focal plane of the microscope.

When interpreting the DB-67 release profiles, one must realize that we are merely taking snapshots in time of the concentration profiles, and we may indeed be missing the true concentration peaks due to the sampling intervals chosen. This arises due to the lack of stability of DB-67 fluorescence signal in aqueous solution that has previously been described [97].

However, “structure-catalyst” and “distribution-catalyst” correlations can be used to elucidate some of the differences observed in the DB-67 release profiles of the foams. First, the initial burst release is always seen to be greater in the DMDEE foams regardless of temperature. The concentration of DB-67 around the cavitations and the lack of DB-67 incorporation in the DMDEE foam can account for this observation. Secondly, the maximum DB-67 concentrations and mol% observed are always higher for the DMDEE foams except at 70 °C. Significant material degradation at 70 °C and subsequent release of entrapped DB-67 from the DABCO foam can explain the observed difference. It is likely at lower temperatures that diffusive rather than degradative processes are accounting for the majority of DB-67 release. As such, the DMDEE foam will generally have released more DB-67 on any given day. Finally, the max-to-initial ratio listed in Table 5 is generally equal to one in every case except for the 70 °C samples. Here the DABCO ratio is significantly greater than the DMDEE, again suggesting the fact that material degradation accounts for significant DB-67 release.

DB-67 release from the foams was shown to be sufficient to inhibit the proliferation of malignant glioma cells. The empty DABCO and DMDEE LDI-glycerol polyurethane foams were found to be well tolerated by all of the malignant glioma cell lines assessed. The MTS signals from cells grown with empty DABCO and DMDEE polymer foams were found to not differ significantly from those of cells grown in media alone in 11 out of 16 treatment groups. Surprisingly when the difference was significant, the cells grown with the empty catalyst foam displayed the higher MTS signal more than half the time. In every malignant glioma cell line tested, a significant difference existed between the 100nM DB-67 solution and either the DABCO or DMDEE drug-loaded foam; without exception the MTS signal was always greater for the 100 nM DB-67 solution.

3.6 CONCLUSIONS

In this study, we present a novel approach to the controlled, long-term delivery of the CPT analog DB-67 employing biocompatible, biodegradable polyurethane foams constructed from LDI and glycerol. We have demonstrated the importance of proper catalyst selection in maintaining the biocompatibility of medical-grade polyurethanes. It was also shown that DB-67

reactivity and incorporation could be controlled through appropriate selection of a tertiary amine urethane catalyst. Structure-catalyst and distribution-catalyst correlations were seen to dictate drug release via diffusion and slow, passive hydrolysis of urethane bonds. Release of DB-67 from LDI-glycerol polyurethane foams was shown to steadily occur over a prolonged periods suitable for medical implants. Therapeutic concentrations of a potent anticancer compound were attained over a 49-day test period with the potential to continue for much longer periods. Cellular proliferation assays conclude that only LDI-glycerol foams loaded with DB-67 exhibited a potent cytotoxic effect on human malignant glioma cell lines. Catalyst choice did not appear to affect the cytotoxicity of the delivery system. These results from clearly demonstrate that catalyst-dependent controlled drug release can be achieved from degradation of LDI-glycerol polyurethane foams.

4.0 CHEMICAL STRUCTURE AND FUNCTIONALITY OF A DRUG DICTATES ITS CONTROLLED-RELEASE PROFILE FROM DEGRADABLE LDI-GLYCEROL POLYURETHANE FOAMS: A STUDY ON NAPHTHALENE AND RELATED COMPOUNDS

4.1 ABSTRACT

The purpose of the present study was to determine how the chemical structure of a drug could be used in the development of controlled release systems. To this end, a series of naphthalene analogs with differing hydroxyl and amine functionality were incorporated into degradable polyurethane foams based on lysine and glycerol. The excitation and emission spectra of the various naphthalene analogs in aqueous solution were examined to ensure they were capable of being quantitatively detected at low concentrations. Then the fluorescence stability of the compounds was assessed over a 2-week period at 70 °C, and the analogs were found to exhibit significant fluorescent signal decay. The polyurethane materials containing the various analogs were then examined via scanning electron microscopy, and the incorporation of small naphthalene ligands did not alter the gross morphology of the foams. The distribution of the analogs was then assessed with fluorescence microscopy using a DAP filter, and they appeared to be evenly distributed throughout the material. Polyurethane foam samples containing various analogs were then incubated at 10.0 mg/ml in PBS buffer solution (pH 7.4) at 4, 22, 37, and 70 °C. Release rates of the naphthalene analogs and mass loss from the polyurethane foam were found to be temperature dependent. The release rates were also found to be highly dependent upon the functional groups present on the naphthalene analog. These results clearly demonstrate that the chemical structure of a drug can be used to control its release from degradable drug delivery systems.

Keywords: drug delivery, controlled release, naphthalene, polyurethane

4.2 INTRODUCTION

Naphthalene is a volatile, white, crystalline, polycyclic aromatic hydrocarbon that exhibits fluorescence near the ultraviolet region of the spectrum [120]. Naphthalene is a natural product, being produced in trace amounts by magnolias and specific types of deer [121-123]. It has also been found in the termite *Coptotermes formosanus*, possibly used as a repellent against ants, poisonous fungi and nematodes [124]. It is commonly used as both an antiseptic and insecticide, being best known as the primary ingredient in mothballs. Naphthalene is manufactured from coal tar, a by-product of the coking process, and is routinely converted to phthalic anhydride, a compound vital to the manufacture of many commercial solvents and plastics [125-128]. Naphthalene is easily modified via electrophilic aromatic substitution reactions; analogs that are substituted with combinations of strongly electron-donating functional groups, such as alcohols and amines, are intermediates in the preparation of many synthetic dyes [129].

The term “polyurethane” refers to any polymer consisting of a chain of organic units joined by urethane bonds. However, the term is often used to broadly classify materials possessing both urethane and urea linkages. A urethane bond is produced via the exothermic condensation of an alcohol and an isocyanate, while an analogous reaction between an amine and an isocyanate generates a urea bond [19]. These reactions are generally referred to as “gelling” reactions, contributing to the overall molecular weight increases observed during polymerization. Polyurethane materials also undergo “blowing” reactions in which an isocyanate reacts with H₂O to form a carbamate intermediate [18]. The carbamate readily decomposes into an amine and CO₂, expanding the polyurethane into foam. The generated amine then reacts with any free isocyanate remaining in the reaction volume, curing the expanded foam.

Hydrolysis is one of the dominant mechanisms for polyurethane degradation in aqueous environments [100]. Thermoplastic polyurethanes exhibit the highest degree of hydrolytic instability due to the presence of ester linkages found within their soft-segments [130]. The urethane and urea linkages found in the hard-segments tend to be less susceptible to hydrolysis [131]. Polyurethane films, thermosets, and highly cross-linked networks lacking a true soft-segment are generally viewed as stable entities in aqueous environments; yet, they remain susceptible to hydrolysis. Urethane and/or urea degradation in these materials proceeds at an incredibly slow rate due to the hydrophobic shielding of the urethane bond. However, their

degradation rates can be altered by concomitant increases and decreases in the aliphatic and aromatic character of the polyols, polyamines and isocyanates used to fashion them [132]. Urethanes and ureas are also known to be sensitive to ion concentrations, redox environments, enzymes, and cellular degradation – exhibiting elevated decomposition *in vivo* [133, 134].

Our laboratory has developed a new generation of biocompatible, biodegradable polyurethanes constructed from lysine diisocyanate (LDI) and glycerol that degrade hydrolytically into non-toxic components – lysine, glycerol and CO₂ [87, 88]. These materials possess the same versatility as widely used commercial polyurethanes, easily being processed into forms with unique morphology and physical properties. We have previously synthesized LDI-glycerol films and foams, demonstrating long-term delivery of DB-67 via hydrolytic release and shown *in vitro* cytotoxicity against malignant glioma cell lines. We propose that urethane hydrolysis can be further utilized in the design of controlled-release drug delivery systems. In this study, naphthalene and some of its functionalized derivatives were chosen as model drug compounds, and they were used to elucidate the connection between urethane hydrolysis and the functionality of the incorporated drug. The various functional groups present on the model drugs will provide urethane and urea bonds with subtle differences in chemical character. The various functional groups present on the naphthalene compounds will in turn determine the nature of the resulting urethane bonds, which ultimately impacts their stability, rate of hydrolysis, and subsequent release of the compounds from the polyurethane foam.

4.3 MATERIALS AND METHODS

4.3.1 Materials

Lysine diisocyanate methyl ester (LDI) was purchased from Chemical Division, Kyowa Hakko Kogyo Co. Ltd. (Tokyo, Japan). All other chemicals were obtained from Sigma–Aldrich Chemical Co. and were of reagent grade unless otherwise specified (Milwaukee, WI).

4.3.2 Excitation-emission spectra of naphthalene compounds

A 1.0 mg/ml stock solution of each naphthalene compound was prepared in DMSO, and each sample was sonicated for 5 min at 25 °C to ensure complete dissolution. Then 3.0 µL of each solution was diluted into 3 ml of PBS (pH 7.4) to arrive at 1.0 µg/ml standard solutions. Each 10.0 µg/ml solution was then iteratively scanned over ranges of excitation and emission wavelengths, finding the maximal fluorescent spectra for each naphthalene compound.

4.3.3 Naphthalene fluorescence stability

Stock solutions of naphthalene and all derivative compounds were prepared in DMSO at a concentration of 1.0 mg/ml. Samples were sonicated until all of the material had dissolved and mixed thoroughly. They were then diluted to a concentration of 1.0 µg/ml by taking 50 µL of DMSO stock and adding it to 50 ml PBS (pH 7.4). The resulting solutions were mixed thoroughly, and a 3 ml sample was immediately collected and a baseline fluorescence signal was determined for each compound. All samples were then incubated at 70 °C and protected from ambient light. Three-milliliter samples were withdrawn every 24 hours for 2-weeks, and the fluorescent signal was measured within 1-hour of the sample being collected. Fluorescent decay curves were then constructed from the data.

4.3.4 Synthesis of Naphthalene Foams

Glycerol (MW 92.01, 1.15 g, 12.5 mmol), DABCO (MW 112.18, 6.0 mg, 0.053 mmol), and dry DMSO (2.5 ml) were added to a small, dry 20 ml reaction flask. Eight such samples were prepared and 0.04 mmol of each naphthalene compound was added to a different flask. The flasks were sonicated until the all the reactants had dissolved in the DMSO. Then LDI (MW 212.20, 4.00 g, 18.9 mmol) was added, and the flasks were flushed with nitrogen prior to being sealed. The reaction was allowed to stir atop a magnetic stir plate in the dark at room temperature until the viscosity had attained a value of at least 3.0×10^4 cP. At that time the viscous pre-polymer was transferred to a 100 mm PTFE dish and 100 µL distilled, deionized H₂O was

added. The pre-polymers were thoroughly mixed 3 times at 2-minute intervals to ensure the H₂O was fully incorporated. The rising foams were left open to the atmosphere yet covered to protect from light while the curing. The resulting polymer foams were then placed into a vacuum oven overnight at 25 °C. The foams were then placed into storage in the dark at 4 °C for further analysis. Sol content was also obtained for each foam sample and was calculated as previously described by Huang [115].

4.3.5 Evaluation of foam architecture by SEM

Polyurethane foams containing the various naphthalene compounds were cut into small 5 mm x 5mm x 1mm sections, dried thoroughly, and mounted on sample holders. Samples were observed at 25X magnification to ensure there were no gross irregularities. Then 10 images were collected at 75X from various regions of each foam sample. Metamorph image analysis software (Molecular Devices) was then used to differentiate pores from polymer through a threshold algorithm. The threshold images were then used to estimate the % porosity of each polyurethane foam.

4.3.6 Distribution of naphthalene compounds within polyurethane

Foam samples were sliced to a thickness of roughly 500 μm and mounted on a glass slide. Fluorescent and non-fluorescent images were taken at 100X filter in order to assess the distribution of DB-67 throughout the DABCO and DMDEE polyurethane foams (Zeiss AX10 Imager.A1). A 4',6-diamidino-2-phenylindole (DAPI) filter was used to visualize the distributions of 1-naphthalene methylamine, 1-naphthol, 1,5-diaminonaphthalene, 5-amino-1-naphthol within the sample (Chroma). Naphthalene and the remaining analogs were unable to be visualized due to the location of their emission bands. Empty polymer foam not containing any analog was used as a control.

4.3.7 Naphthalene Release

LDI-glycerol polyurethane foam samples containing the naphthalene compounds were incubated at 10 mg/ml in PBS (pH 7.4) on rocking plates in temperature-controlled rooms at 4, 22, 37 and 70 °C for 11-weeks. Sample chambers were protected from light during this time. Every 7 days, 3.0 ml of PBS was retrieved from each sample; during the first week, PBS was also collected on day 3. The amount of naphthalene compound released from the polymer was detected via fluorescence spectroscopy using the excitation and emission wavelengths particular for each compound. Standard curves were constructed and used to determine the concentration of the various naphthalene species in solution. The total amount collected throughout the study was calculated as follows:

$$mol\% = \frac{1}{MW} \left[3 \sum \left(\frac{m}{V} \right)_i + \left(\frac{m}{V} \right)_j (V_T - 3j) \right]$$

where $(m/V)_i$ represents the concentration of each collected sample and V_T the total volume (where each time point is designated “i” and “j” represents the last). Lysine and glycerol released from the polymer were not assessed at this time.

4.4 RESULTS

4.4.1 Excitation-emission spectra of naphthalene compounds

Naphthalene exhibits a characteristic, intense fluorescent spectrum that has been used in the past under aqueous conditions to examine partitioning kinetics of micellar systems [135, 136]. An investigation of naphthalene and its analogs’ fluorescent behavior was undertaken to ensure each was capable of being sufficiently detected in an aqueous environment. The excitation and emission spectra of naphthalene, 1-naphthol, 1-naphthylamine, 1-naphthalene methanol, 1-

naphthalene methylamine, 1,5-dihydroxynaphthalene, 1,5-diaminonaphthalene, and 5-amino-1-naphthol in PBS (pH 7.4) were obtained in PBS buffer (pH 7.4) (Figure 23).

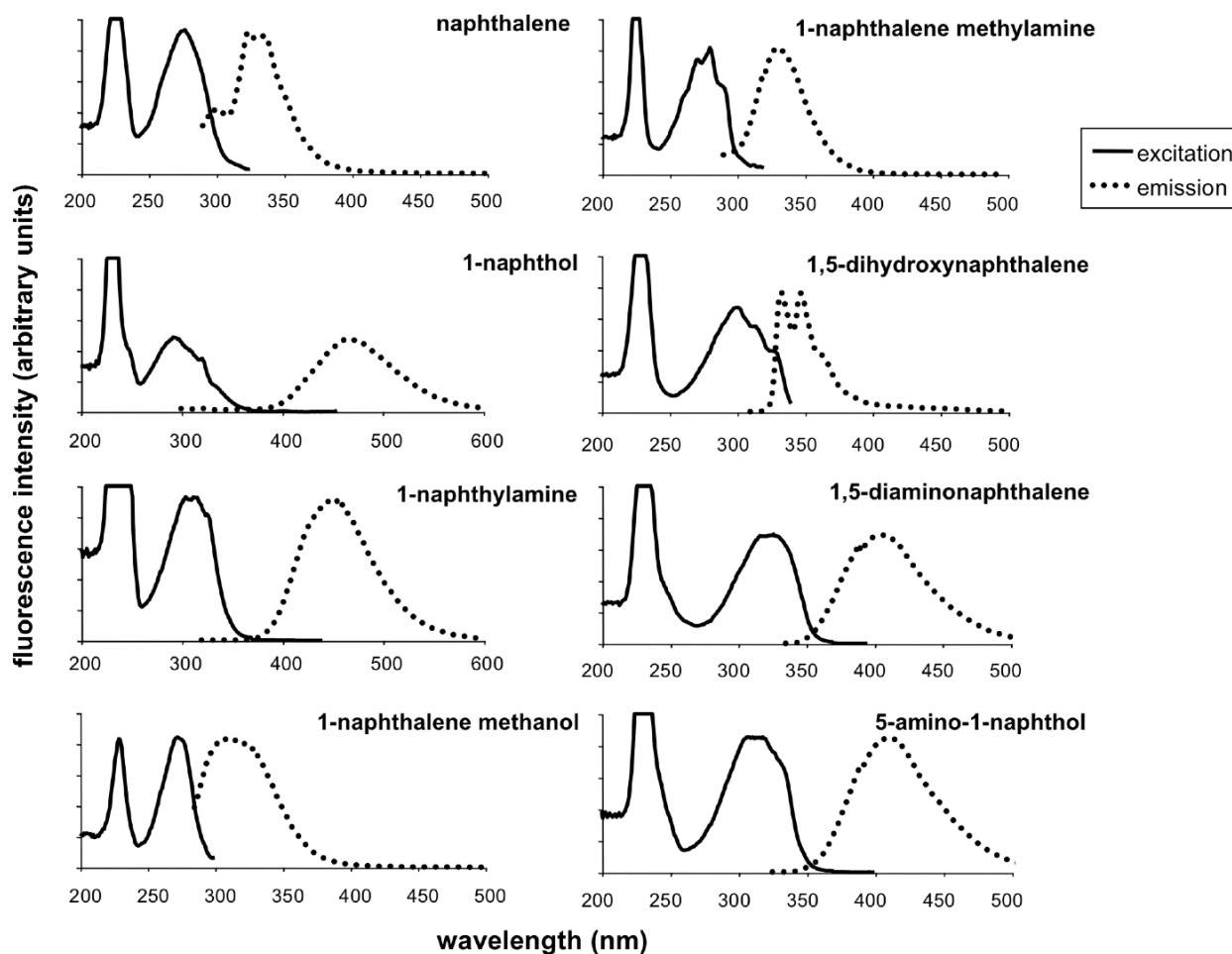
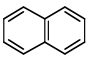
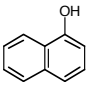
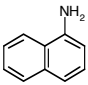
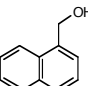
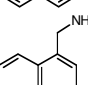
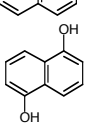
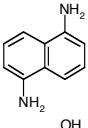
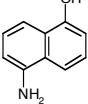


Figure 23 - Fluorescence excitation and emission spectra for naphthalene compounds in aqueous media

The fluorescence spectrophotometer was adjusted so that the excitation and emission signals registered in the maximum range of the detector. All the naphthalene compounds exhibited intense excitation bands in the range of 275-325 nm. The emission bands were equally intense yet scattered, ranging from 330-470 nm. The excitation and emission peaks were well delineated and free from background interference of the PBS buffer (data not shown). Standard concentration curves from 1.0 – 1000.0 ng/ml were constructed for each compound, and found to be linear (data not shown); 5-amino-1-naphthol exhibited the lowest R^2 value (0.9791). The

excitation and emission wavelengths for each naphthalene compound are listed along with their chemical structure and functionality in (Table 7).

Table 7 - Naphthalene compounds – structure, functionality and fluorescent wavelengths

Compound	Structure	Functionality	Fluorescence (nm)	
			Excitation	Emission
Naphthalene		----	275	330
1-naphthol		Aromatic hydroxyl	290	470
1-naphthylamine		Aromatic amine	315	450
1-naphthalene-methanol		Primary hydroxyl	280	335
1-naphthalene-methylamine		Primary amine	280	330
1,5-dihydroxy-naphthalene		Dual aromatic hydroxyl	300	345
1,5-diamino-naphthalene		Dual aromatic amine	325	405
5-amino-1-naphthol		Aromatic hydroxyl, aromatic amine	320	410

4.4.2 Naphthalene fluorescence stability

Naphthalene has been found to be susceptible to photochemical degradation in aqueous and oxidative environments [137-140]. Although much harsher conditions than we propose were used in these studies, an assessment of the stability of the naphthalene compounds in PBS (pH 7.4) buffer was needed. The naphthalene analogs were found to lose their fluorescence signal over a 2-week test period to varying degrees (Figure 24).

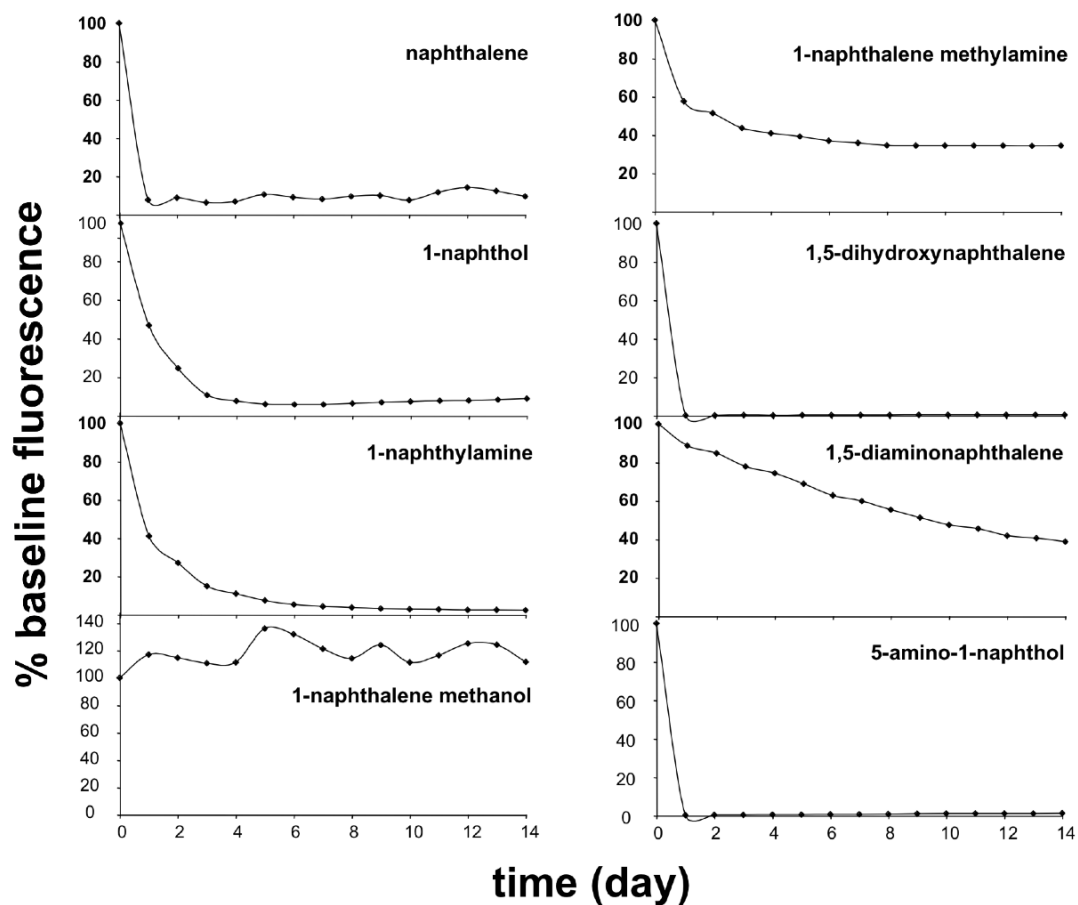


Figure 24 - Fluorescence decay profiles for the naphthalene analogs in PBS buffer (pH 7.4) solution

Fluorescent signal decay of naphthalene, 1-naphthol, 1-naphthylamine, 1,5-dihydroxynaphthalene, 5-amino-1-naphthol and to a much lesser extent 1-naphthalene methylamine and 1,5-diaminonaphthalen was observed. The fluorescent signal of 1-naphthalene methanol was the only one that remained near its baseline level throughout the 2-week test period.

4.4.3 Polyurethane foams: SEM Analysis and Distribution

Low-magnification scanning electron micrographs (25X) were taken in order to assess the morphology of the polyurethane foam samples (Figure 25).

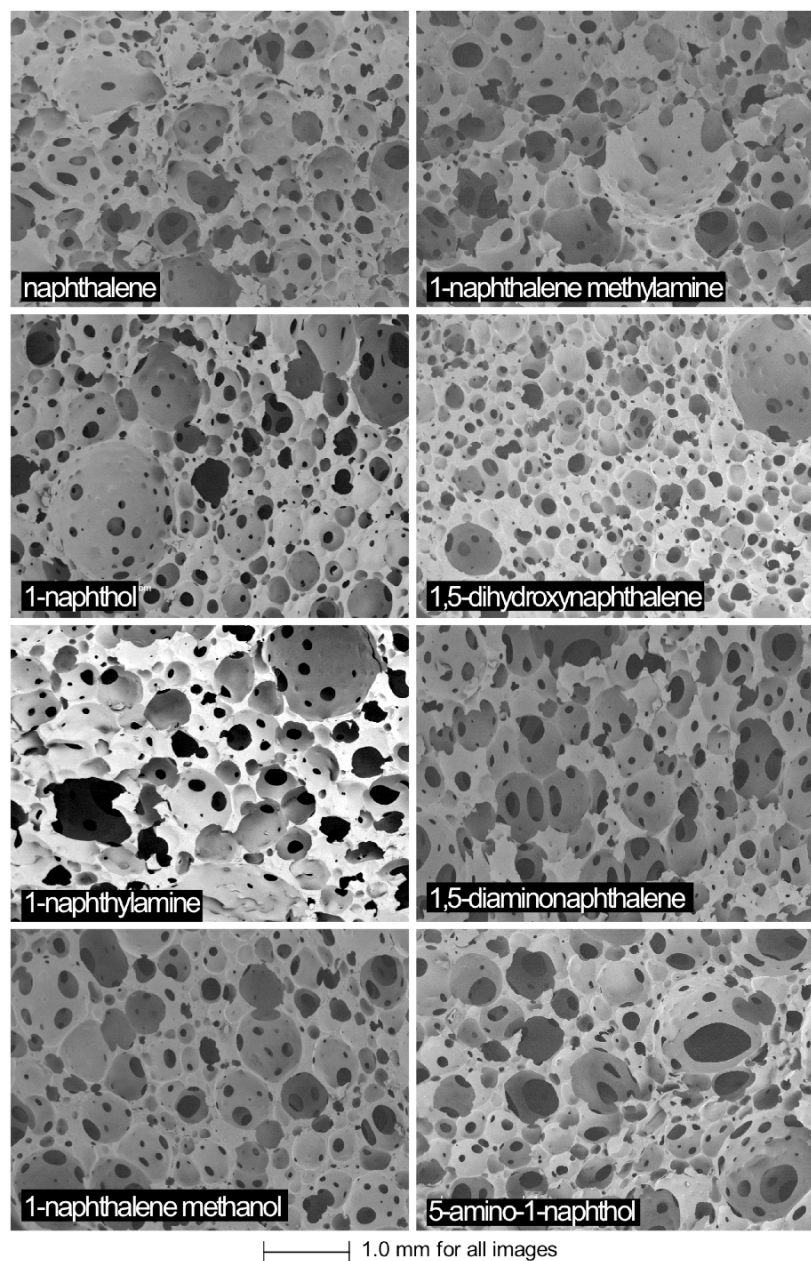


Figure 25 - Low-magnification scanning electron micrographs (25X) of the LDI-glycerol polyurethane foams containing the various naphthalene analogs

These images reveal the foams largely similar in terms of pore size, shape and distribution. Some variation in the foam morphology is to be expected, resulting from the processing methods used to fabricate each sample. Higher magnification images (75X) taken from regions of the foam

specimens, and the porosity was estimated using a threshold imaging technique. Metamorph imaging software was able to clearly delineate between the polymer and pore regions of the images (Figure 26). The average porosity of each foam sample can be found in Table 9, listed along with the degradation characteristics.

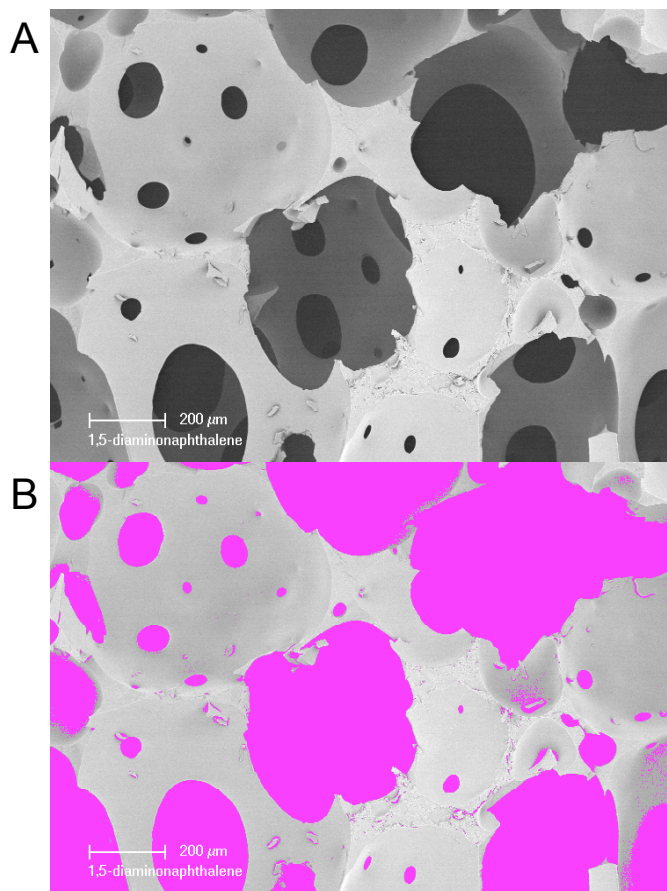


Figure 26 - High-magnification SEM image of 1,5-diaminonaphthalene: (A) before and (B) after a threshold was applied to determine the porosity of the foam

DAPI is a fluorescent stain that binds strongly to DNA; it is used extensively in fluorescence microscopy. When bound to double-stranded DNA its absorption maximum lies in the near-UV at 358 nm and its emission maximum is at 461 nm. The emission band is broad and appears blue. The emission wavelength of DAPI closely approximates the fluorescent bands of some of the naphthalene analogs. Therefore, a DAPI filter was used to visualize polyurethane

foam samples containing either 1-naphthol, naphthalene methylamine, 1,5-diaminonaphthalene, or 5-amino-1-naphthol in order to determine the distribution of these analogs throughout the material (Figure 27).

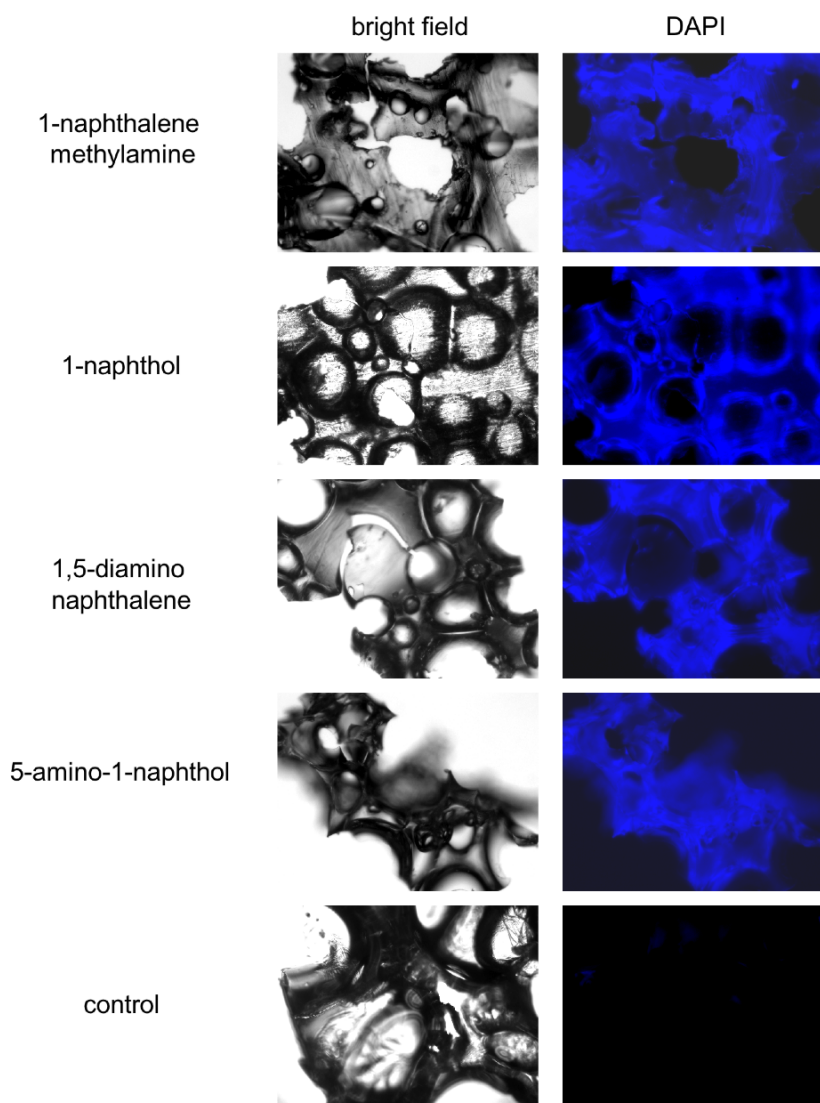


Figure 27 - Fluorescent images depicting the distribution of select naphthalene analogs in the LDI-glycerol polyurethane foam

The naphthalene analogs were evenly dispersed throughout the polyurethane samples except in the case of 1-naphthol, which showed a slight preferential accumulation around the pore surface.

Variations in the intensity of the fluorescent signal can largely be attributed to differences in sample thickness. There was no appreciable signal arising from the control sample.

4.4.4 Naphthalene release

The release of naphthalene analogs from the LDI-glycerol polyurethane foams was assessed at 4, 22, 37 and 70 °C over a 77-day period (Figure 28).

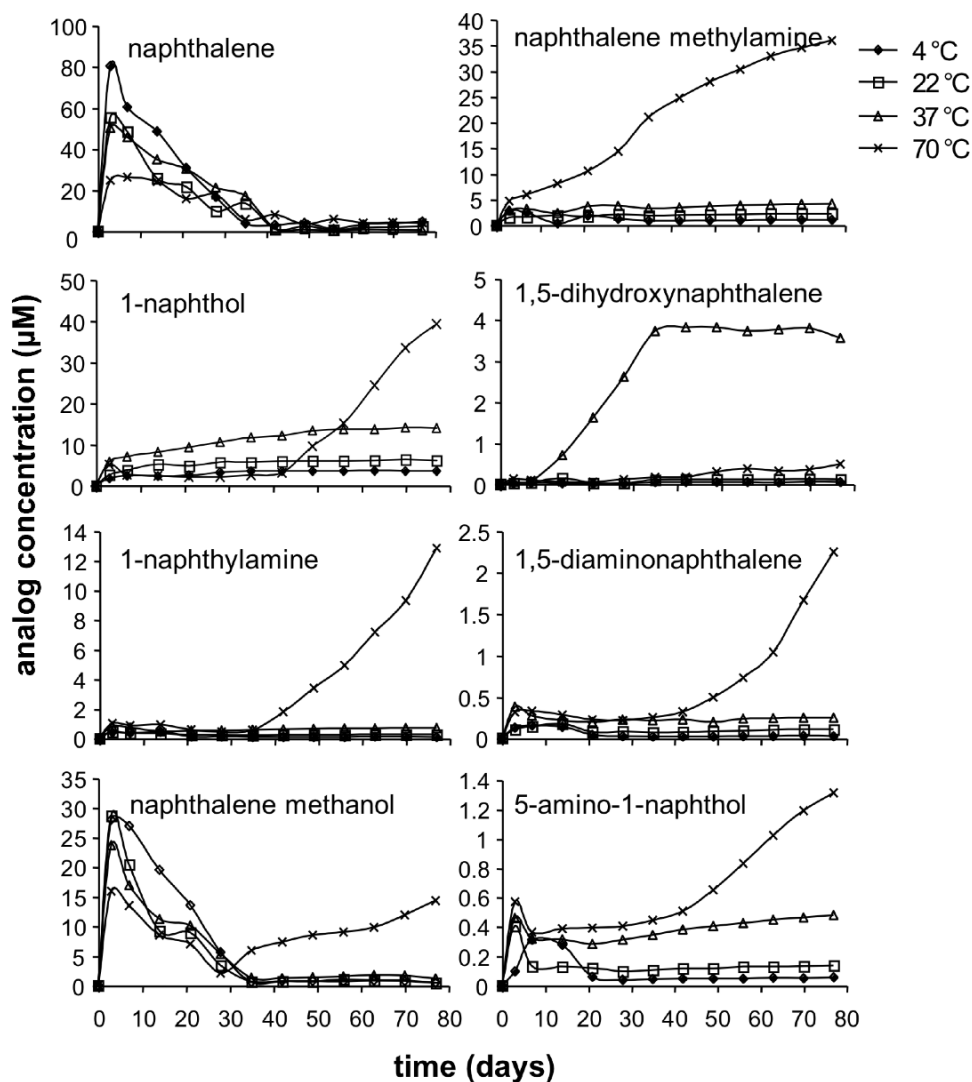


Figure 28 - Concentration profiles depicting the release of the naphthalene analogs from the LDI-glycerol polyurethane foams

The total amount of analog released and previously collected was also calculated as a percent of the total amount used in the synthetic reaction and reported as mol% (Figure 29).

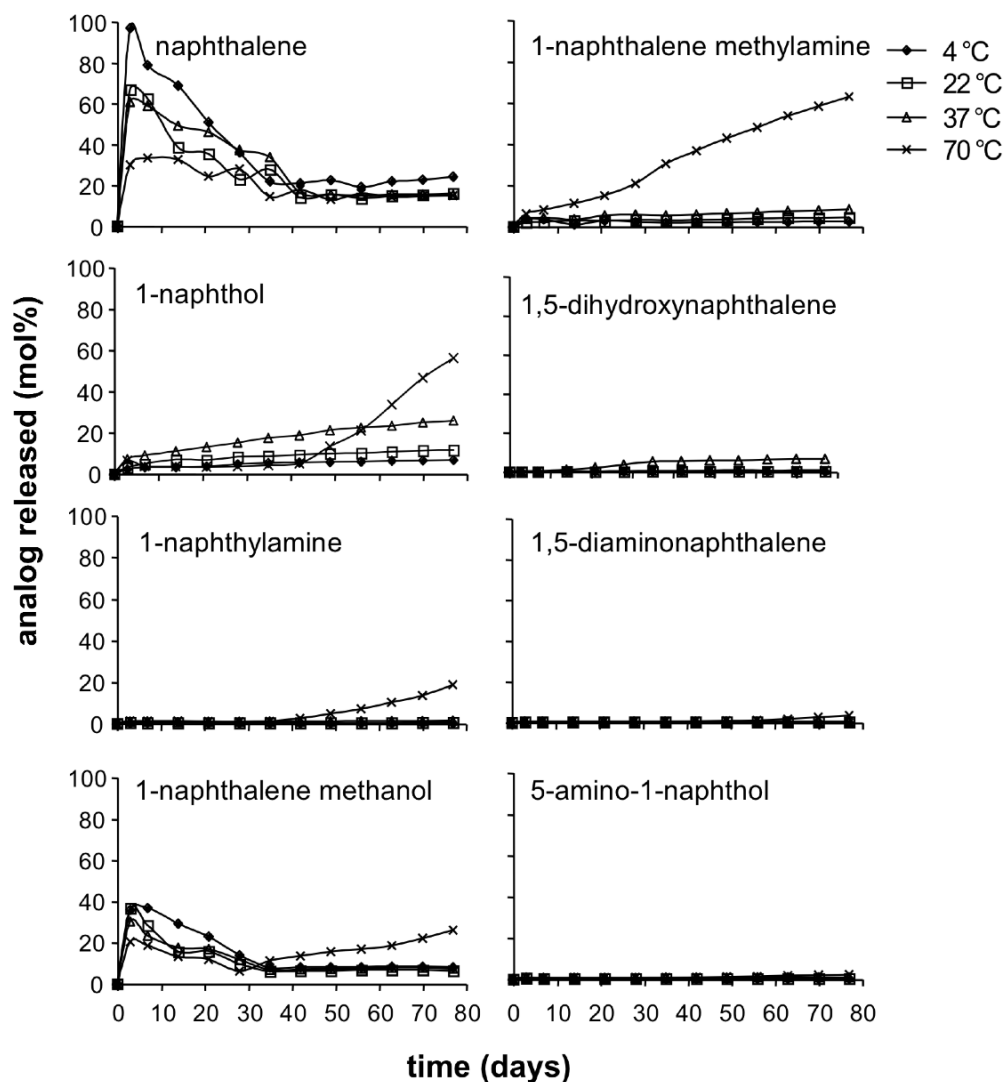


Figure 29 - Profiles depicting the mol% of the naphthalene analogs released from the LDI-glycerol polyurethane foams

In general, the compounds were found to be eluted in a temperature dependent fashion, with the highest concentrations and mol% being found at 70 °C. Significant material erosion was observed by day-49 in all of the 70 °C samples. As a result, the samples tend to display

significant changes in release kinetics around this time. Mass loss for the samples was also seen to vary with temperature, with the highest percentages being lost at 70 °C for each sample. Sol content of each foam sample was determined and noted to be similar for each of the polyurethane samples. Day-3 to day-77 concentration ratios provide insight into the release mechanisms – less than one indicates bursting, while greater than one indicates delayed release. The release data for each of the compounds has been summarized in Table 8.

Table 8 – Release characteristics naphthalene compounds from LDI-glycerol polyurethane foams

Compound	porosity (%)	sol content (%)	Temperature (°C)	mol% ^a	mass loss ^b (%)	day-77 concentration (µM)	day-3 concentration (µM)	day-77/day-3 ratio
Naphthalene	42.2 ± 7.2	32.2	4	24.0	34.3	4.6	80.4	0.06
			22	16.0	35.5	2.3	55.3	0.04
			37	15.3	36.3	0.5	50.3	0.01
			70	14.8	85.4	4.0	24.7	0.2
1-naphthol	47.7 ± 7.0	27.1	4	6.6	35.1	3.5	1.8	1.9
			22	11.6	36.1	6.1	2.6	2.3
			37	25.7	37.7	14.0	5.8	2.4
			70	56.1	83.7	39.4	5.1	7.7
1-naphthylamine	32.9 ± 9.3	29.6	4	0.3	34.5	0.1	0.4	0.3
			22	0.5	35.9	0.3	0.5	0.6
			37	1.4	36.6	0.7	0.8	0.9
			70	18.6	82.7	12.8	1.0	12.8
1-naphthalene-methanol	46.3 ± 9.4	30.2	4	7.9	36.1	0.4	28.0	0.01
			22	6.2	37.5	0.5	28.7	0.02
			37	7.3	38.2	1.2	23.7	0.05
			70	18.5	95.2	8.7	15.9	0.5
1-naphthalene-methylamine	45.2 ± 11.0	30.7	4	2.3	36.1	1.0	2.7	0.4
			22	4.4	37.5	2.3	1.5	1.5
			37	8.1	38.2	4.2	2.9	1.4
			70	62.3	89.9	36.0	4.7	7.7
1,5-dihydroxy-naphthalene	33.0 ± 9.4	32.9	4	0.8	32.3	0.05	0.03	1.7
			22	2.0	33.5	0.1	0.03	3.3
			37	6.4	34.3	3.6	0.1	36.0
			70	0.3	68.3	0.2	0.1	2.0
1,5-diamino-naphthalene	43.4 ± 8.7	31.3	4	0.1	34.7	0.03	0.1	0.3
			22	0.2	36.8	0.1	0.1	1.0
			37	0.5	39.7	0.2	0.4	0.5
			70	3.3	65.9	2.2	0.3	7.3
5-amino-1-naphthol	32.8 ± 9.7	27.5	4	0.1	34.9	0.05	0.1	0.5
			22	0.3	35.6	0.1	0.4	0.3
			37	1.0	36.6	0.5	0.5	1.0
			70	2.1	67.5	1.3	0.6	2.2

a: at day-77, b: mass loss = (initial mass - final mass)/(initial mass) x 100%

Naphthalene was released from the polyurethane foam in a burst fashion. Its concentration profiles peaked for each of the temperatures at day 3, and slowly decayed thereafter. The aromatic analogs 1-naphthol and 1-naphthylamine were found to differ significantly from naphthalene in their release kinetics. Naphthol exhibited an early release profile with elevated concentrations detectable in solution by day 3. The concentrations in solution were sustained at 4 and 22 °C and observed to rise at 37 °C. Subtle burst release was seen early on in the 70 °C profile followed by rapid decay, with release once again becoming apparent at day 49. Naphthylamine exhibited a delayed release profile, with the only apparent concentration change occurring at day 42 in the 70 °C sample. Furthermore, the primary functional groups demonstrated extreme differences in their release profiles. Naphthalene methanol was found to exhibit early burst release followed by steady concentration decay. Only after day 28 in the 70 °C sample was significant release once again observed. Naphthalene methylamine did not exhibit any early burst release regardless of temperature. Interestingly, at 70 °C linear release kinetics were observed for the mono-functional primary amine.

The dual aromatic analogs demonstrated release behavior distinct from those already observed in the aromatic and primary functional groups. Small concentrations of 1,5-dihydroxy-naphthalene, 1,5-diamino-naphthalene, and 5-amino-1-naphthol were detected in solution, suggesting that the materials are tightly bound within the polyurethane network. Elevation in the concentration of 1,5-dihydroxy-naphthalene was observed to occur at day 14 for the 37 °C sample. Elevated concentrations of 1,5-diaminonaphthalene were only observed after day 42 in the 70 °C sample. Finally, 5-amino-1-naphthol displayed small changes in concentration, further demonstrating that compounds with two functional groups elute from the polymer at slow rates. The observed changes in concentration are small for the dual functional aromatics relative to the total amount of analog used, but still were well within the detectable range of our assay.

4.5 DISCUSSION

We have chosen to pursue a strategy for the long-term controlled release of drugs from polyurethane materials constructed from lysine and glycerol. The unique feature of our drug delivery technology relies on the drug's incorporation into the polymer through pendent

functional groups. We have previously described this strategy for the controlled release of DB-67, a potent anti-cancer compound, from polyurethane foams and films. Through those studies, we demonstrated that material morphology and even the urethane catalyst used play a significant role in release behavior. This study provides some insight into the relationship that exists between the release of compounds and the functional groups present on them.

Naphthalene was chosen as our model drug for its fluorescent properties, simple chemical structure, and availability of a wide variety of functionalized derivatives. The characteristic, intense fluorescent spectra of naphthalene and its analogs provide an easy method for quantitative detection in solution following release from our polyurethane materials. It was unfortunate that many of the naphthalene compounds were subject to significant photo bleaching when exposed to aqueous media at 70 °C. Over the 2-week period, all of the naphthalene analogs except for 1-naphthalene methanol were shown to lose their fluorescence signals to varying degrees. While this fact prohibited us from closing the mass balance of our systems, it did have some benefit. Once administered, drugs find themselves subject to a myriad of physiologic mechanisms that act to deplete their concentration and limit their performance. We can think of the fluorescence decay as clearance or inactivation rate. The results we obtained in light of the fluorescence decay suggest that the LDI-glycerol polyurethane is able to provide a protective, stabilizing environment for the analogs. This may prove useful in the future, as many promising drug candidates are unable to be used due to inactivation via oxidative, acid-base, or conformational changes. The signal decay allowed us to note the precise moment at which release rates became significant to overcome the decay process. Lastly, an examination of the release profiles suggests that the decay is highly temperature dependent allowing for detection of some species at temperatures below 70 °C.

The LDI-glycerol polyurethane foams were found to be quite similar to one another in terms of their morphology. The incorporation of small amounts of naphthalene analog did not appear to grossly affect the bulk material. All of the foams were supple and pliable, and could easily be cut to specification. While there was some variability in the porosity of the foams, it was not statistically significant. Variability in the foam porosity can be expected due to the processing methods we used to fabricate the foam systems, and it does not appear to impact the various release profiles. The foams were also remarkable similar in terms of their sol content. The distribution of the naphthalene analogs in the foam samples could not be assessed in full due

to the location of many of the fluorescent excitation and emission bands. However, a DAPI filter did provide an opportunity to visualize four of the eight analogs. The distribution was largely similar, and the number or type of functional group did not appear to impact the distribution.

The degradation and release studies did define a number of structure-release relationships existing among the analogs. First, the results suggest the aromatic urea to be much more resistant to hydrolysis than the aromatic urethane. This is evident from a comparison of the release profiles of 1-naphthol and 1-naphthylamine. Steady release of naphthol was observed to occur at 4, 22, and 37 °C, while significant release of naphthylamine was observed to occur only at 70 °C following that of naphthol. The greater stability of the urea over the urethane is again confirmed by examining the bi-functional aromatic analogs, 1,5-dihydroxynaphthalene and 1,5-diaminonaphthalene. The release of 5-amino-1-naphthol more closely resembles that of 1,5-diaminonaphthalene than 1,5-dihydroxynaphthalene, suggesting that the aromatic urea dictates its release.

A similar rationale can be used to suggest the primary urethane is more stable than the primary urea. An examination of the release profile of 1-naphthalene methanol shows an initial burst release, later followed by steady release. Incomplete reaction of the primary hydroxyl in naphthalene methanol, can account for the initial rise in concentration. This can be attributed to the differences in the relative reactivity of primary amines and hydroxyls with isocyanate [141-145]. However, the release profile of 1-naphthalene methylamine demonstrates slow, steady release throughout the duration of the experiment. Since there is no initial burst release, this can be attributed to primary urea degradation.

The aforementioned structure-release trends can be seen in plots of the mol% release and the release normalized to the maximum mol% of each species (Figure 30).

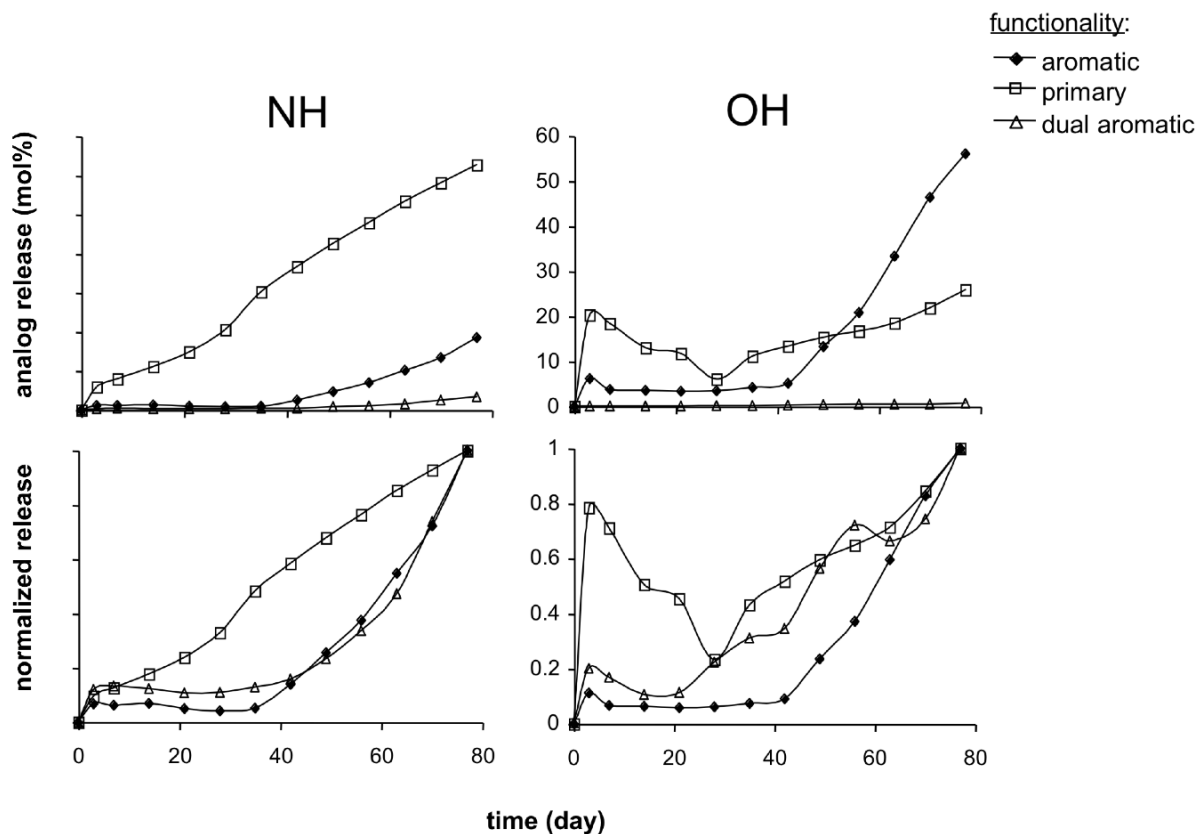


Figure 30 - Functional group comparison of the mol% and normalized release of naphthalene analogs from the LDI-glycerol foams

Examination of the mol% release amongst the amine species shows that primary amines are released first, then single aromatic amines, and then the bi-functional aromatic amines. Surprisingly, when the mol% is normalized, the aromatic amines display strikingly similar release profiles. The hydroxyl release is complicated by variations in the relative reactivity of the hydroxyl species. Primary hydroxyl groups are still seen to release from the polyurethane before the aromatics. However, the aromatic trend is reversed in the normalized plot. This is likely due to the extremely low concentration of 1,5-dihydroxynaphthalene detected in solution due to the rapid fluorescence decay of this species, and the trend is greatly influenced by signal noise.

4.6 CONCLUSIONS

In this study, we have demonstrated that the pendant functional groups present in the chemical structure of a drug dictate how it is released from degradable polyurethane foam. We used a series of naphthalene analogs possessing different chemical functionality in terms of the type and number of amine or hydroxyl groups. The urethane and urea bond formed from the reaction of the functional groups with isocyanate exist in differing chemical environments and result in different hydrolytic rates. The hydrolytic rates then determine how and when the structure is eluted from the polyurethane foam into the surrounding media. The polyurethane also served to protect the naphthalene analogs from fluorescent signal decay until they were released. The results of this study clearly demonstrate that release from degradable LDI-glycerol polyurethane foams is highly dependent upon the chemical structure of a drug.

5.0 RELEASE OF DB-67, DOXORUBICIN AND PACLITAXOL OCCURS SIMULTANEOUSLY AT DIFFERING RATES FROM SINGLE-PHASE LDI-GLYCEROL POLYURETHANE FOAMS

5.1 ABSTRACT

In the present study, we present a novel approach to the controlled release of multiple chemotherapeutic agents from single-phase polyurethane foams constructed from lysine diisocyanate (LDI) and glycerol. DB-67, doxorubicin, and taxol were incorporated into the polyurethane foam network via labile urethane and urea linkages. The reactions of DB-67 and doxorubicin with LDI were monitored over a 4-hour period via infrared spectroscopy; each compound was found to react to differing degrees with LDI. Doxorubicin, DB-67 and taxol were then incorporated alone and in combination into a series of polyurethane foams. The sol content, porosity, and drug distribution of each foam sample was measured and found to be similar amongst the samples. The fluorescent spectra of DB-67 and doxorubicin were then measured in PBS buffer solution (pH 7.4), and the stability of each compound's fluorescent signal was assessed over a 2-week period at 70 °C. Release rates of DB-67 and doxorubicin from the foams were assessed over a 10-week period at 4, 22, 37, and 70 °C via fluorescence spectroscopy. The rates were found to vary with temperature and were dependent upon the chemical structure of the incorporated drug. This study demonstrates the controlled release of multiple agents from single-phase LDI-glycerol polyurethane foams occurs at differing rates dependent upon the chemical structure of the incorporated drug.

Keywords: polyurethane, drug delivery, doxorubicin, DB-67, lysine diisocyanate

5.2 INTRODUCTION

DB-67 (7-t-butyl dimethylsilyl-10-hydroxycamptothecin), doxorubicin (Adriamycin), and Taxol (paclitaxol) are all potent anti-cancer compounds, each exerting their cytotoxic effects by interrupting processes essential to cellular growth and proliferation. DB-67 functions by inhibiting the enzyme topoisomerase I, a member of a nuclear enzyme family responsible for repairing DNA during replication [80, 81, 146, 147]. Doxorubicin functions via two mechanisms: first, intercalating DNA and inhibiting transcription, and then by inhibiting the enzyme topoisomerase II [148-151]. Finally, taxol exerts its effects via stabilizing polymerized microtubules; it is able to halt cell division as well as other vital processes relying on the rearrangement of the cytoskeleton [152, 153]. However, when using any of these compounds to combat malignancies in the body, it is impossible to avoid exposing normal functioning cells to their deleterious effects. The toxic side effects of these compounds ultimately are responsible for limiting their efficacy [5, 154-157].

Many strategies have evolved in an attempt to selectively deliver chemotherapeutics to localized, regions of malignant tissue within the body [4, 41]. One such strategy that has proven effective is implantation of degradable polymeric devices at the tumor site loaded with select chemotherapeutic agents [158, 159]. Instead of administering a drug to the entire body, these strategies serve to limit the exposure of the therapeutic to only a single body compartment or even a select region of that compartment. This strategy has proven efficacious and has resulted in several patented devices approved by the FDA for the treatment of solid tumors [48, 49, 82, 160, 161]. Most often, these systems focus on the delivery of a single therapeutic, relying solely on diffusion as the primary release strategy. In these systems, the drug load will often be exhausted prior to the degradation and absorption of the polymeric material.

Systems for the simultaneous delivery of multiple therapeutic compounds have also been proposed [162-166]. Polymeric systems for the delivery of multiple agents generally consist of multiple, distinctly defined phases each capable of delivering a separate compound [167, 168]. Typically, each phase possesses different diffusive properties that govern the liberation of the impregnated compound. Some of these systems even use multiple synthetic layers to achieve staggered rates of delivery [169]. However, the synthesis of such systems is often complex, costly, and time-consuming – ultimately preventing their commercialization and application in a

clinical setting. A single-phase polymer capable of simultaneous release of multiple therapeutic compounds at differing rates would offer an advantage over these systems in terms of cost and ease of fabrication.

Our laboratory has developed polyurethane materials based on lysine and glycerol that degrade hydrolytically into non-toxic components – lysine, glycerol and CO₂ [87, 170]. These polymers can easily be fashioned into differing morphologies using standard urethane processing techniques. The degradation characteristics of LDI-glycerol polyurethanes have proven useful in design of novel drug delivery systems. The present study is an expansion upon previous work, seeking to determine if the release of multiple chemotherapeutic agents at differing rates can be achieved from a single-phase polymer system. The delivery strategy is centered on the incorporation of drugs into the polymer backbone, being released via passive hydrolysis of urethane and urea bonds. The chemical structures of taxol, DB-67, and doxorubicin contain different functional groups, and we propose that they can be used to form urethane and urea linkages with differing degrees of hydrolytic susceptibility. Due to different rates of hydrolysis, each drug should elute from the polyurethane material in a different fashion.

5.3 MATERIALS AND METHODS

5.3.1 Materials

Lysine diisocyanate methyl ester (LDI) was purchased from Chemical Division, Kyowa Hakko Kogyo Co. Ltd. (Tokyo, Japan). All other chemicals were obtained from Sigma–Aldrich Chemical Co. and were of reagent grade unless otherwise specified (Milwaukee, WI).

5.3.2 Synthesis of drug-loaded polyurethane foams

Glycerol (MW 92.01, 0.600 g, 6.5 mmol), LDI (MW 212.20, 2.00 g, 9.5 mmol), DABCO (MW 112.18, 3.0 mg, 0.027 mmol), and dry DMSO (1.25 ml) were added to a small, dry 20 ml reaction flask; four such samples were prepared. Taxol (MW 853.9, 5.0 mg, 5.9×10^{-3} mmol),

doxorubicin (MW 579.9, 5.0 mg, 8.6×10^{-3} mmol), and DB-67 (MW 478.7, 5.0 mg, 1.0×10^{-2} mmol) were each added to a different flask. To the fourth flask, the same amounts of taxol, doxorubicin, and DB-67 were all added. The flasks were flushed with nitrogen prior to being sealed. The reactions were allowed to stir atop a magnetic stir plate in the dark at room temperature until the viscosity had attained a value of at least 3.0×10^4 cP. At that time the viscous pre-polymer was transferred to a 100 mm PTFE dish and 100 μ L distilled, deionized H₂O was added. The pre-polymers were thoroughly mixed 3 times at 2-minute intervals to ensure the H₂O was fully incorporated. The rising foams were left open to the atmosphere yet covered to protect from light while the curing. The resulting polymer foams were then placed into a vacuum oven overnight at 25 °C. The foams were then placed into storage in the dark at 4 °C for further analysis.

5.3.3 Drug Reactivity with LDI

Solution of doxorubicin and DB-67 were prepared in dry DMSO at concentrations of 30.0 and 10.0 mg/ml, respectively. Two small 5 ml reaction flasks were dried thoroughly and flushed with nitrogen, and DABCO (1.5 mg) was added to each flask. To one flask, 400 μ L of the DB-67 (0.025 mmol) solution and LDI (MW 212, 5.3 mg, 0.025 mmol) were added to give a 1:1 molar ratio of DB-67 to LDI. To the other flask, 200 μ L of the doxorubicin (0.003 mmol) solution and LDI (MW 212, 2.2 mg, 0.009 mmol) were added to give a 1:3 molar ratio of doxorubicin to LDI. In each case, a 1:1 isocyanate to total-amine/hydroxyl ratio was obtained. Infrared spectra were recorded immediately upon addition of the LDI and 4 hours later in order to determine the reactivity of each drug. Taxol reactivity was not assessed at this time due to limited quantities of the drug.

5.3.4 Excitation-emission spectra and fluorescence stability

Stock solutions of DB-67, doxorubicin, and paclitaxol were prepared in DMSO at a concentration of 1.0 mg/ml. Each sample was sonicated for 5 min at 25 °C to ensure complete dissolution. Then 3.0 μ L of each solution was diluted into 3 ml of PBS (pH 7.4) to arrive at 1.0 μ g/ml standard solutions. Each 1.0 μ g/ml solution was then scanned over a range of excitation

and emission wavelengths to elucidate the maximum fluorescent spectra for each compound (Cary Eclipse).

Stock solutions of DB-67 and doxorubicin in DMSO at a concentration of 1.0 mg/ml were diluted to a concentration of 1000 ng/ml by taking 50 μ L of DMSO stock and adding it to 50 ml PBS (pH 7.4). The resulting solutions were mixed thoroughly, and a 3 ml sample was immediately collected and analyzed for content via fluorescence spectroscopy. The samples were then incubated at 70 °C and protected from ambient light. Three-milliliter samples were withdrawn every 24 hours, and the fluorescent signal was measured within 1-hour of the sample being collected. Fluorescent decay curves were then constructed from the data collected.

5.3.5 Evaluation of foam architecture by SEM

Polyurethane foams containing either DB-67, doxorubicin, taxol, or all three were cut into small 5 mm x 5mm x 1mm sections, dried thoroughly, and mounted on sample holders. Samples were observed at 25X magnification to ensure there were no gross irregularities. Then 10 images were collected at 75X from various regions of each sample. Metamorph image analysis software (Molecular Devices) was then used to differentiate pores from polymer via a threshold algorithm. Threshold images were then used to estimate the % porosity of each polyurethane foam.

5.3.6 Distribution of DB-67 and doxorubicin within polyurethane

Foam samples were sliced by hand to a thickness of roughly 500 μ m and mounted on a glass slide. Fluorescent and non-fluorescent images were taken at 100X in order to assess the distribution of drug throughout the polyurethane foams (Zeiss AX10 Imager.A1). Alexafluor 647 and FITC filters were used to visualize the doxorubicin and DB-67, respectively (Chroma).

5.3.7 DB-67 and doxorubicin release

LDI-glycerol polyurethane foam samples each containing either DB-67, doxorubicin, or taxol and one containing all three were incubated at 10 mg/ml in PBS (pH 7.4) on rocking plates in

temperature-controlled rooms at 4, 22, 37 and 70 °C for 10-weeks. Sample chambers were protected from light during this time. Every 7 days, 3.0 ml of PBS was retrieved from each sample; during the first week, PBS was also collected on day 3. The amount of drug released from the polymer was detected via fluorescence spectroscopy using the excitation and emission wavelengths particular for each compound. The amount of drug collected was expressed as a percent of the total used in the synthetic reaction, being calculated as follows:

$$mol\% = \frac{1}{MW} \left[3 \sum \left(\frac{m}{V} \right)_i + \left(\frac{m}{V} \right)_j (V_T - 3j) \right]$$

where $(m/V)_i$ represents the concentration of each collected sample and V_T the total volume (where each time point is designated “i” and “j” represents the last). Lysine and glycerol released from the polymer were not assessed at this time.

5.4 RESULTS

5.4.1 DB-67 and Doxorubicin Reactivity with LDI

The reactivity of DB-67 and doxorubicin with LDI in the presence of DABCO was determined via infrared spectroscopy (Figure 31). Infrared scans of a 1:1 molar reaction between DB-67 and LDI show disappearance of the isocyanate (NCO) signal at 2265 cm^{-1} over the 4-hour reaction period. The ratio between the peak integrations of the NCO and carbonyl (C=O) was used to monitor the extent of the reaction; the ratio decreased from 1.0 to 0.2 over the 4-hour reaction period, representing an 80% decrease. Analogous scans of a 1:3 molar reaction between doxorubicin and LDI also reveal decay of the isocyanate signal. Initially, the NCO:C=O ratio measured 2.8 and decreased to 0.74, representing a 74% decrease of the initial signal.

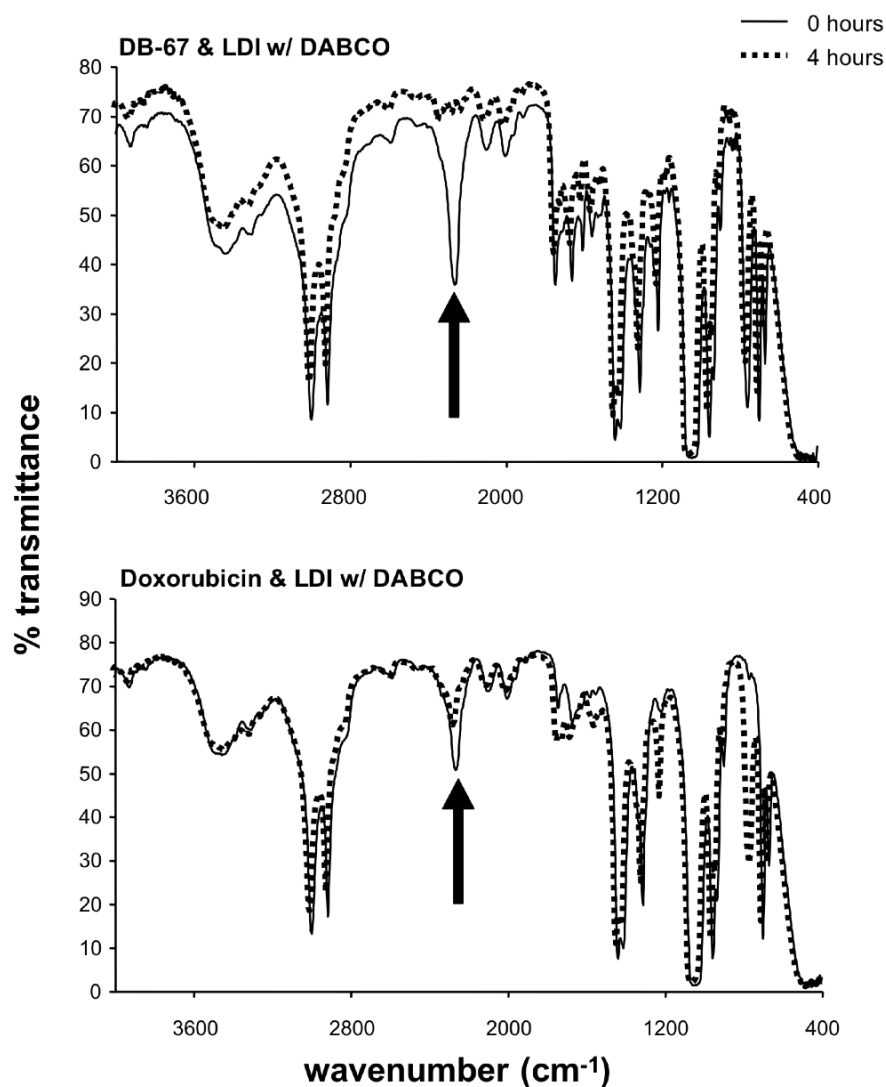


Figure 31 – FT-IR spectra depicting the reactivity of DB-67 and doxorubicin with LID in the presence of a tertiary amine urethane catalyst

5.4.2 Excitation-emission spectra and fluorescent stability

DB-67 and doxorubicin each exhibit characteristic, intense fluorescent spectra that have been utilized to study their membrane partitioning kinetics and intracellular mechanisms of action [80, 81, 171-173]. Taxol also exhibits a fluorescent spectrum, but it is highly dependent upon solvent polarity [174]. Each compound also possesses multiple functional groups that can serve as points

for chemical attachment into our polyurethane network. An investigation of each compound's fluorescent behavior was undertaken to ensure they were capable of being detected over prolonged periods in PBS (pH 7.4) buffer solution. The excitation and emission spectra of DB-67 and doxorubicin were obtained in PBS buffer (pH 7.4) solution (Figure 32).

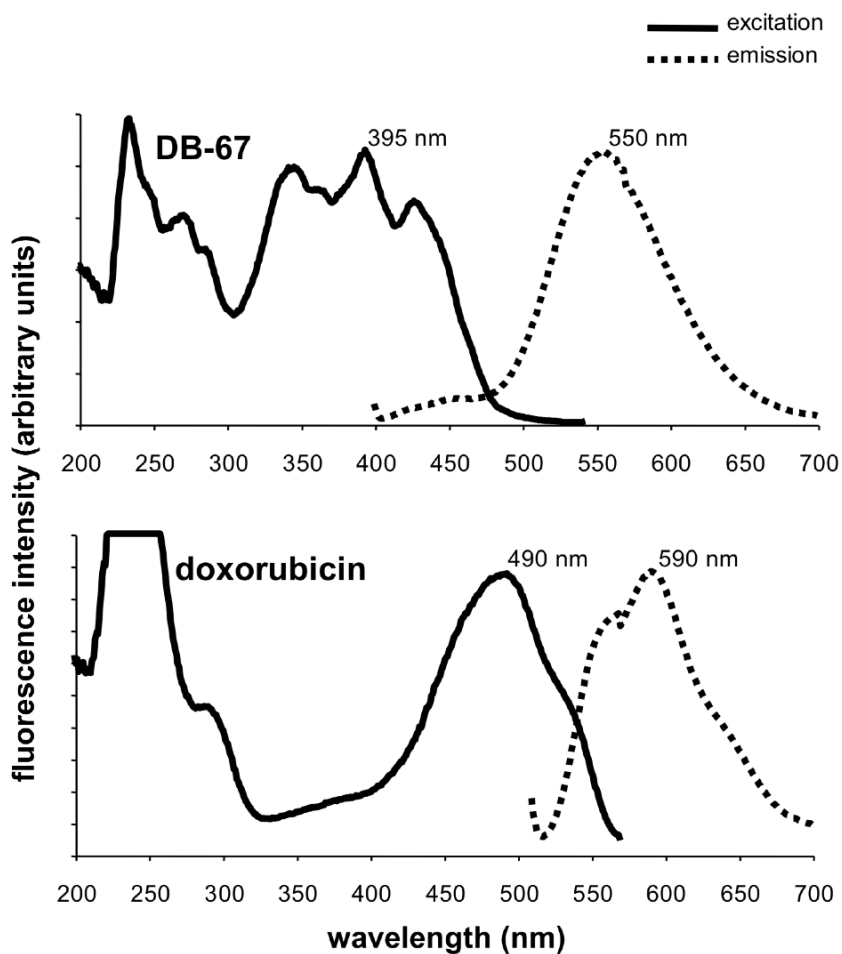
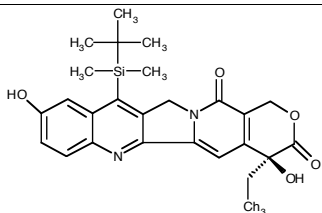
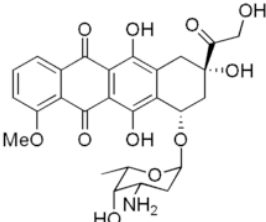
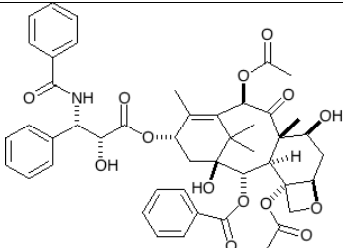


Figure 32 – Fluorescent excitation and emission spectra of DB-67 and doxorubicin

The excitation wavelengths for DB-67 and doxorubicin were found to be 395 and 490 nm, respectively. The emission wavelengths for DB-67 and doxorubicin were 550 and 590 nm, respectively. Unfortunately, the fluorescence of taxol was found to be extremely weak and insufficient for accurate detection in PBS buffer solution (data not shown). The chemical

structures, number of synthetic attachments, and the excitation and emission wavelengths for each compound have been summarized in table 9.

Table 9 – Chemical structure and fluorescent properties of DB-67, doxorubicin, and taxol

Compound	Structure	Attachments	Fluorescence (nm)	
			Excitation	Emission
DB-67		<u>2 total:</u> aromatic OH, tertiary OH	394	553
Doxorubicin		<u>6 total:</u> primary OH, secondary OH, tertiary OH, 2 aromatic OH, primary NH	490	590
Taxol		<u>4 total:</u> 2 secondary OH, 1 tertiary OH, secondary NH	n/a	n/a

The fluorescence spectrophotometer was then tuned so that the excitation and emission signals of DB-67 and doxorubicin registered in the maximum range of the detector. The excitation and emission peaks were well delineated from one another and free from background interference of the PBS buffer (data not shown). Standard curves ranging from 1.0 – 1000.0 ng/ml were constructed for each compound, and found to be linear over those concentrations (data not shown). Out of the three compounds incorporated into our polyurethane drug delivery system, only DB-67 and doxorubicin could be adequately quantified via fluorescence.

DB-67 and doxorubicin have been found to be susceptible to chemical degradation in aqueous and oxidative environments [175-178]. Although much harsher conditions than we

propose were used in these studies, an assessment of the fluorescence stability of the compounds in PBS (pH 7.4) buffer was needed (Figure 33).

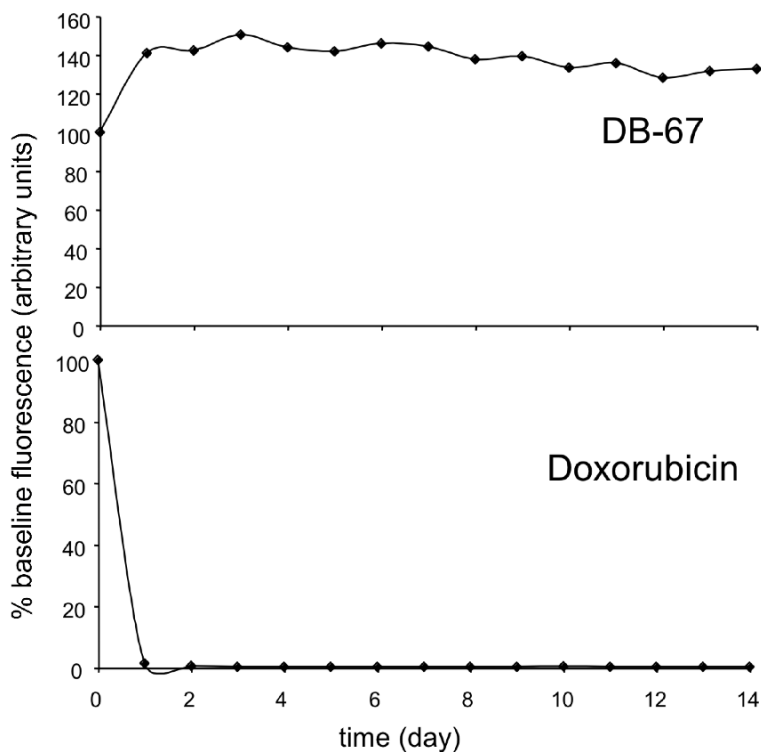


Figure 33 – Fluorescent decay profiles of DB-67 and doxorubicin at 70 °C over a 2-week period

We chose to only evaluate the fluorescence stability at 70 °C. Over a 2-week test period, DB-67's fluorescent signal was found to increase. On day 14 of the study, DB-67 had achieved a 32% increase over its original baseline value. On the other hand, doxorubicin's fluorescent signal was found to decay almost immediately upon exposure to aqueous media at 70 °C. By day-2 of the study only 1.4% of the baseline signal remained, and by day-14 only 0.3% registered.

5.4.3 Polyurethane Foams: SEM analysis and Drug Distribution

Low-magnification scanning electron micrographs (25X) were taken in order to assess the morphology of the polyurethane foam samples (Figure 34).

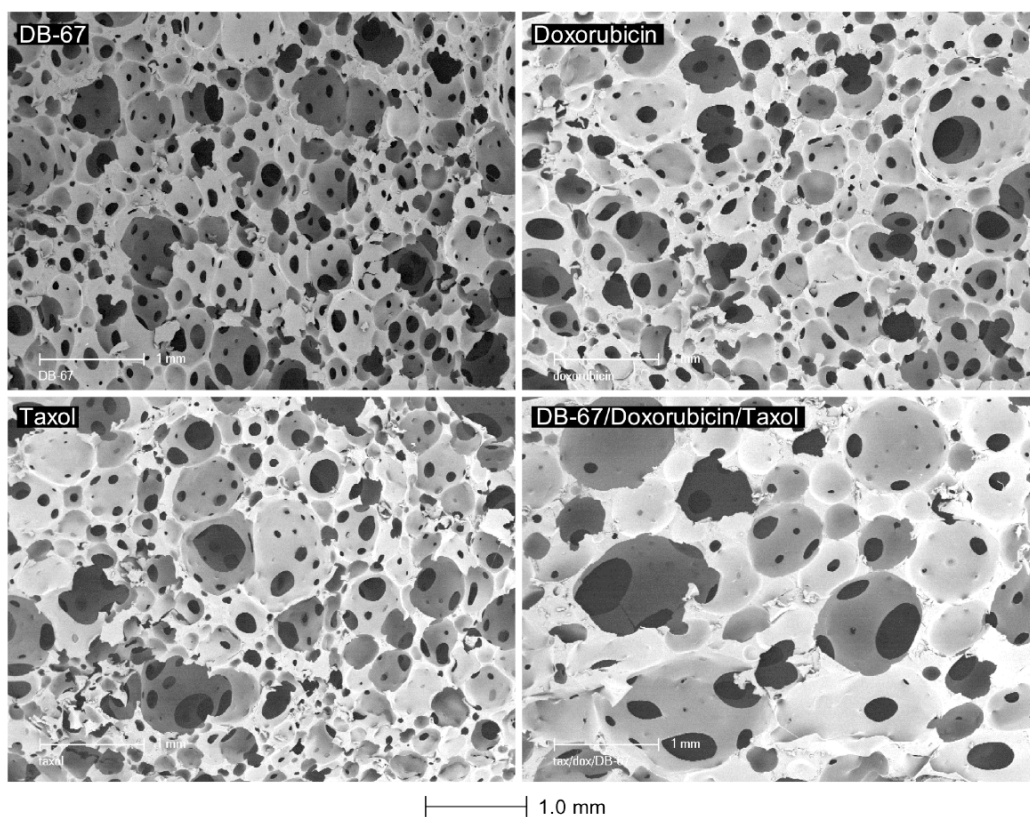


Figure 34 – Scanning electron micrographs demonstrating the morphological features of LDI-glycerol polyurethane drug foams

These images reveal the foams largely similar in terms of pore size, shape and distribution. Some variation in the foam morphology is to be expected, resulting from the processing methods used to fabricate each sample. Higher magnification images (75X) taken from regions of the foam specimens, and the porosity was estimated using a threshold imaging technique. Metamorph imaging software was able to clearly delineate between the polymer and pore regions of the images (data not shown). The average porosity of each foam sample is listed along with the release data found in Table 10.

Fluorescent and non-fluorescent images were obtained in an attempt to qualitatively assess the distribution of DB-67 and doxorubicin throughout the LDI-glycerol polyurethane foams (Figure 35).

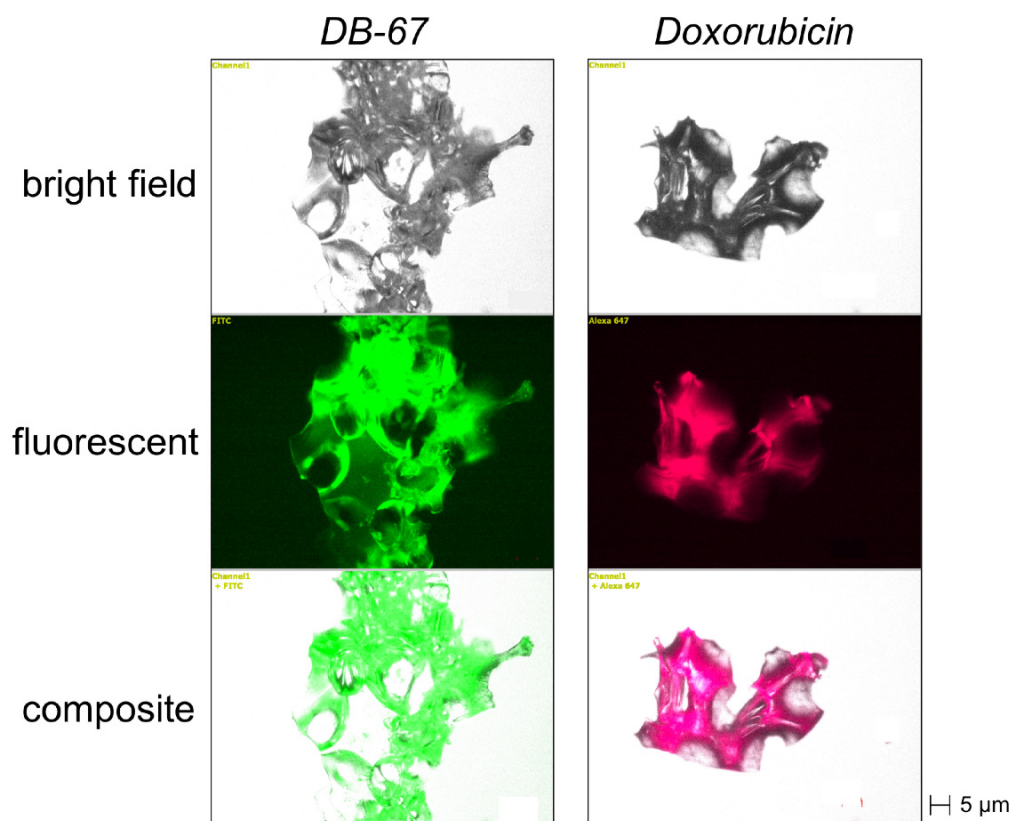


Figure 35 – Fluorescent microscope images showing the distribution of DB-67 and doxorubicin through the LDI-glycerol polyurethane foam

Bright field images of the foams, each loaded with only a single drug species, appear very similar in morphology. Darkened regions of the bright field images are attributable to sample thickness. Fluorescent images reveal uniform drug distributions, with the thicker areas of the foam samples possessing greater fluorescent signal. Overlaid composite images further prove the distribution of both DB-67 and doxorubicin to be uniform throughout the materials.

Fluorescent images were then obtained of a sample containing all three drug compounds, but only the DB-67 and doxorubicin distributions were assessed (Figure 36).

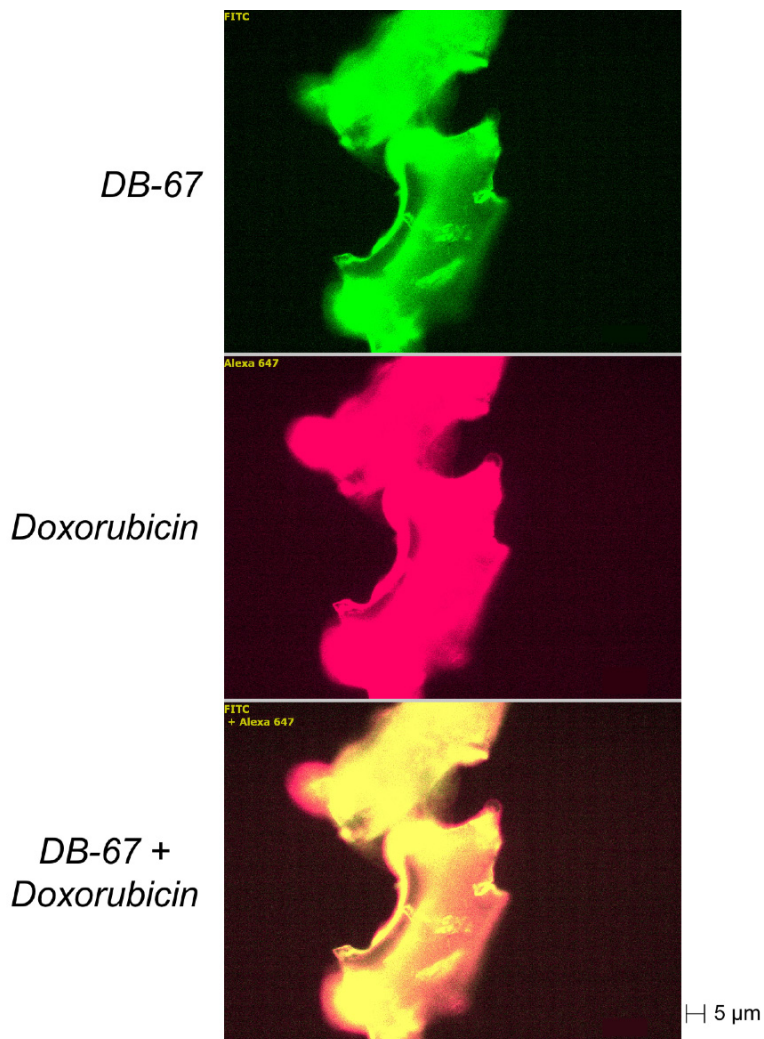


Figure 36 – Fluorescent microscope images showing the distribution of DB-67 and doxorubicin through multi-drug LDI-glycerol polyurethane foams

The fluorescence of the multi-drug foam appears more intense than that of the single-drug foams, but this can be attributed to sample thickness. The images reveal both DB-67 and doxorubicin to be uniformly dispersed throughout the polyurethane, with a composite image further confirming this finding.

5.4.4 Drug release

The release of DB-67 and doxorubicin from the polyurethane foams was monitored over a 10-week period at 4, 22, 37 and 70 °C. The release of each drug species was assessed from multiple samples. Polyurethane foams were synthesized containing only DB-67, Taxol or doxorubicin; another sample was prepared containing all three. For reasons already mentioned, only DB-67 and doxorubicin release could be assessed via fluorescence. DB-67 release from the polyurethane samples was found to occur in a temperature dependent fashion, with similar amounts liberated from both the single and multiple drug foams (Figure 37).

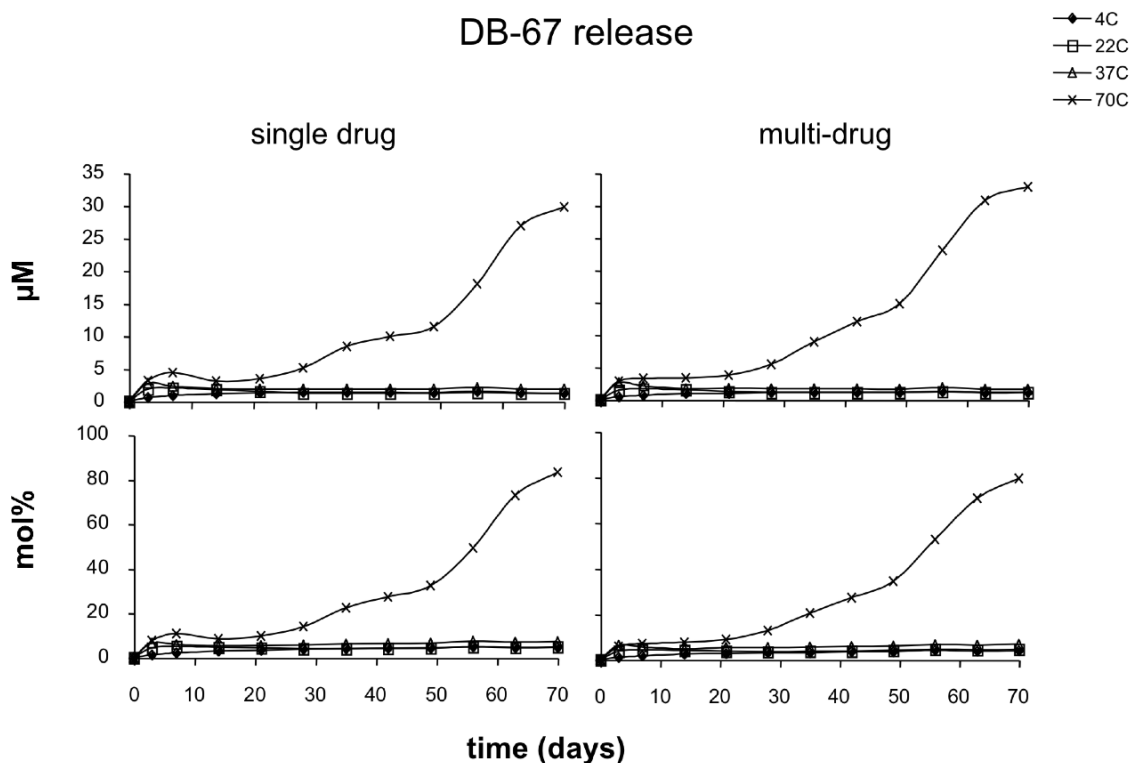


Figure 37 – DB-67 release profiles for single and multi-drug LDI-glycerol polyurethane foams

By day-70 of the degradation studies, 83.9 and 79.4 mol% of the DB-67 had been released from the single and multiple agent foams at 70 °C, respectively. The amounts of DB-67 released from each foam sample at 4, 22, and 37 °C were substantially less, but occurred in similar amounts for

the single and multi-drug foams. Doxorubicin release from the single and multi-drug foams was seen to occur in the same temperature dependent fashion (Figure 38).

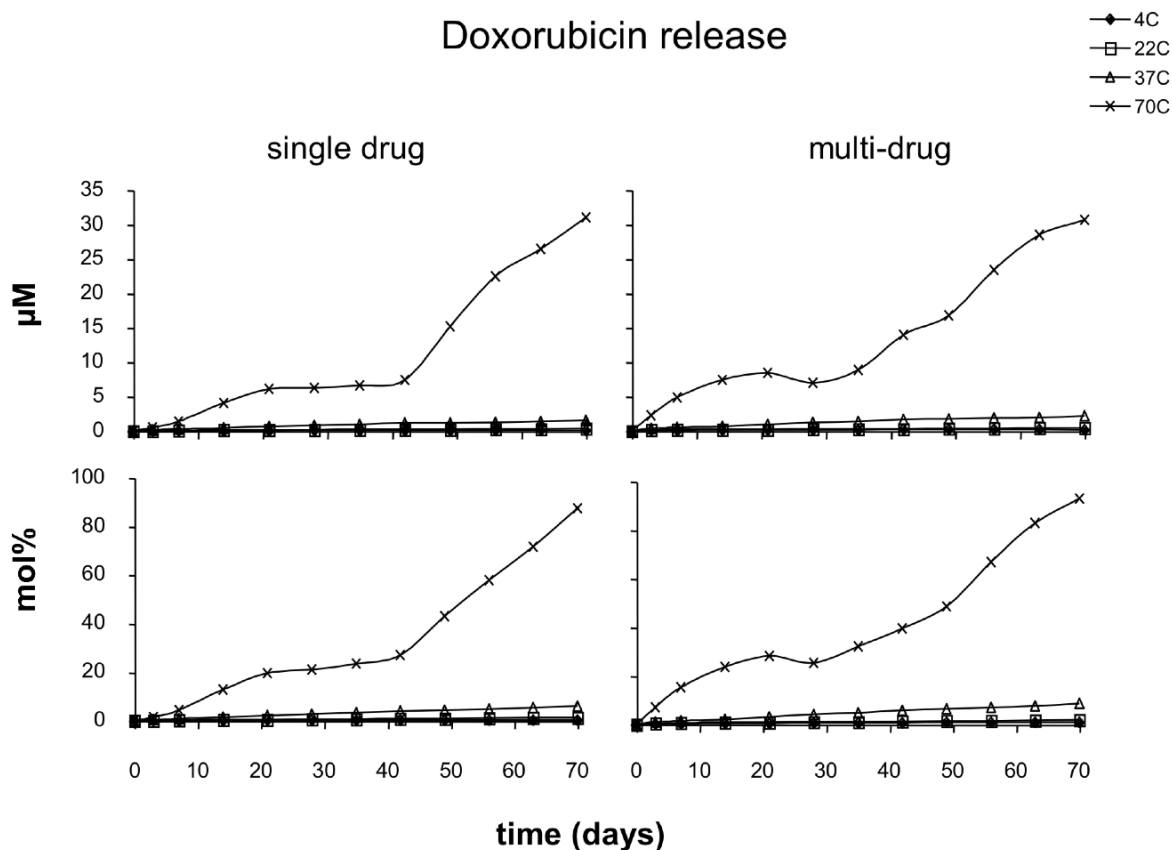


Figure 38 - Doxorubicin release profiles for single and multi-drug LDI-glycerol polyurethane foams

By day-70, 87.5 and 92.3 mol% were released from the single and multiple drug foams at 70 °C, respectively. Again, the amounts released at lower temperatures were substantially less but were comparable between the two samples. The release data for the single and multiple drug polyurethane foams along with has been summarized in table 10.

Table 10 - Release characteristics of DB-67 and Doxorubicin from single and multi-drug LDI-glycerol polyurethane foams

System	Compound	porosity (%)	sol content (%)	Temperature (°C)	mol% ^a	mass loss ^b (%)	day-70 concentration (μM)	day-3 concentration (μM)	day-70/day-3 ratio
Single	DB-67	36.4 ± 7.8	25.0	4	4.58	39.2	1.23	0.57	2.2
				22	4.94	40.1	1.22	1.88	0.6
				37	7.25	39.8	1.84	2.74	0.7
				70	83.30	95.7	29.78	3.20	9.3
	Doxorubicin	24.7 ± 7.0	24.5	4	0.25	37.4	0.06	0.01	6.0
				22	1.31	37.6	0.33	0.03	11.0
				37	6.00	38.6	1.51	0.13	11.6
				70	87.49	92.1	31.03	0.50	62.1
	Taxol	28.6 ± 9.8	27.5	4	-----	38.1	-----	-----	-----
				22	-----	38.8	-----	-----	-----
				37	-----	38.9	-----	-----	-----
				70	-----	98.8	-----	-----	-----
Multiple	DB-67	28.4 ± 11.1	25.1	4	3.99	37.9	1.08	0.43	2.5
				22	4.50	37.1	1.10	1.48	0.7
				37	6.69	40.7	1.63	2.59	0.6
				70	79.37	92.3	32.91	2.86	11.5
	Doxorubicin	same as above	same as above	4	0.79	same as	0.17	0.06	2.8
				22	1.87	above	0.46	0.15	3.1
				37	2.14	above	2.14	0.33	6.6
				70	92.95	above	30.62	2.27	13.5
	Taxol	same as above	same as above	4	-----	same as	-----	-----	-----
				22	-----	above	-----	-----	-----
				37	-----	above	-----	-----	-----
				70	-----	above	-----	-----	-----

a: at day-70, b: mass loss = (initial mass - final mass)/(initial mass) x 100%

The release profiles of the multi-drug polyurethane foams reveal substantial differences to exist between the two drug species at different temperatures (Figure 39). At 37 °C, there is an initial rapid rise of DB-67 that stabilizes at a concentration around 1.6×10^{-6} M (6.7 mol%). The doxorubicin concentration slowly rises in a linear fashion from the onset of the degradation experiment, eventually elevating above the concentration of DB-67 on day-49, reaching a maximum of 2.1×10^{-6} M (8.6 mol%) at day-70. At 70 °C, the concentrations of DB-67 and doxorubicin in solution are seen to rise in parallel with one another. Doxorubicin is slightly higher at the onset and then later surpassed by DB-67 by day-63. However, the relative percentages of the material eluting from the polymer indicate that doxorubicin is eluting more rapidly than is DB-67.

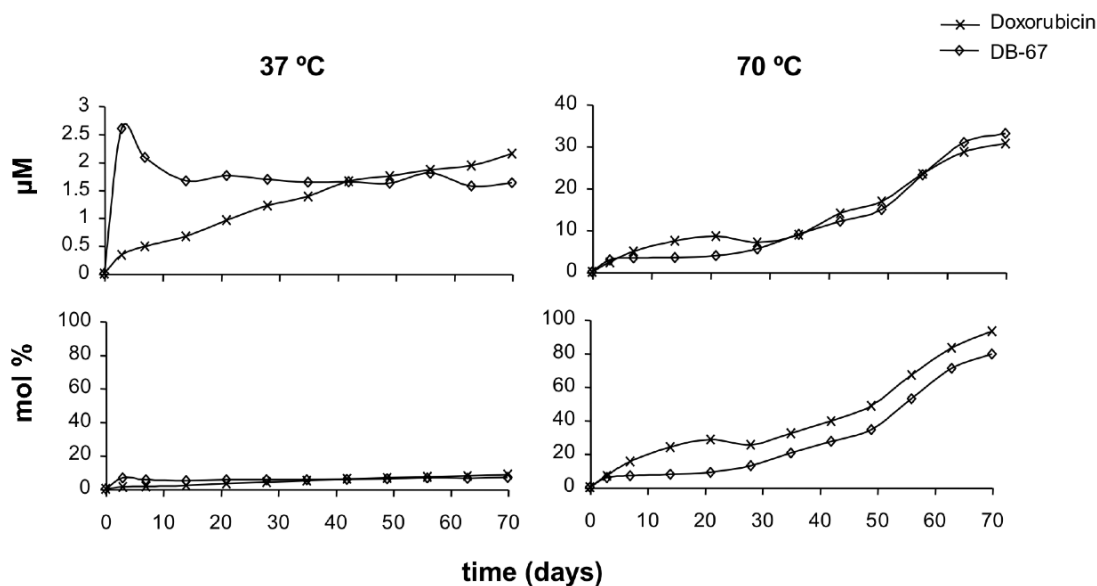


Figure 39 – Comparison of DB-67 and doxorubicin release from multi-drug LDI-glycerol polyurethane foams at 37 and 70 C°

5.5 DISCUSSION

The reactions of DB-67 and doxorubicin with LDI reveal differences in their ability to form urethane bonds. After a 4-hour period, nearly all the isocyanate signal has disappeared from the reaction mixture. The signal registering in the isocyanate region after 4 hours is largely attributed to background noise. Notice that there has also been a concomitant decrease in the signal around the carbonyl region of the spectra around 1700 cm^{-1} . In the reaction of LDI and doxorubicin, we would expect a much larger initial NCO : C=O ratio due to the number of functional groups present on the drug. However, in the reaction between doxorubicin and LDI there appears to be a lower initial isocyanate signal relative to the DB-67 reaction. This apparent discrepancy can be largely attributed to the rapid reaction of the primary hydroxyl and amine groups in doxorubicin's structure with the isocyanate before the initial IR scan could be obtained. There is also an increase in the carbonyl region of the spectra after 4 hours that was used to calculate the NCO:C=O ratio.

The fluorescent spectra of DB-67 and doxorubicin exhibit distinct differences and provide an opportunity to follow the simultaneous release of both species from a single polyurethane foam sample. The doxorubicin excitation band at 490 nm, while somewhat broad, is well delineated from the 395 nm excitation band of doxorubicin. The excitation band of DB-67 at 395 nm does overlap to a small degree with doxorubicin, but if the sample is sufficiently dilute, ensuring all of the DB-67 reaches an excited state, minimal interference at the 550 nm emission should be present. Furthermore, the aqueous fluorescence of taxol was found to be extremely weak, and its inclusion in the polymer sample should not interfere with the detection of DB-67 and doxorubicin. Furthermore, the fluorescent excitation and emission bands of taxol lie closer to the ultra-violet region of the spectra. These bands being well removed from those of DB-67 and doxorubicin should not interfere with their detection.

While the fluorescent intensity of free doxorubicin was found to decay rapidly in PBS at 70 °C, the same was not found to be true when the drug was released from polyurethane foam. The signal of doxorubicin was found to persist throughout the duration of the study allowing us to account for more than 85% of the original content, suggesting that the reaction of the drug with LDI retarded its fluorescent decay. The ability of the polyurethane foam to stabilize the fluorescence of doxorubicin is a striking feature of our delivery system. We have noted similar effects related to the release of fluorescent naphthalene analogs from our delivery system in the past. Many promising drug candidates have failed to provide any clinical benefit due to premature inactivation in the body before interaction with a target site; DB-67 is one such candidate. It is our hope that incorporation of a drug into our polyurethane delivery vehicle will prove useful in counteracting these limitations imposed by the body's unique chemical and metabolic environment.

The synthetic conditions and processing methods used in this study resulted in remarkable consistent polyurethane foams. The sol% amongst each sample was found to be remarkably similar and the porosity was well conserved. The mass losses measured after the degradation experiments demonstrated temperature dependence, and the mol% of drug released was similar between multi and single drug systems. The distribution of the drugs also appears to be uniform when assessed with fluorescent microscopy. It is interesting to consider the ratio of drug concentration at day-70 to the initial concentration measured on day-3. A ratio less than one can be considered to represent a "burst" release pattern, while a ratio greater than one indicates a

“delayed” release pattern. Under this classification, doxorubicin is always released in a delayed fashion regardless of temperature. In contrast, DB-67 is released in a burst fashion at 4 and 70 °C, while delayed release is observed at 22 and 37 °C. The contrasting release features at different temperatures can account for the initial burst release of DB-67 followed by the delayed release of doxorubicin at 37 °C in the multiple drug system.

5.6 CONCLUSIONS

In the present study, we have described the synthesis and performance of novel drug-eluting polyurethane foams synthesized from LDI and glycerol capable of releasing multiple drugs at different rates. This is achievable due to the incorporation of the drug moieties into the backbone of the polyurethane network, utilizing each drug’s pendant functional groups to achieve differing rates of hydrolysis. The staggered release of multiple drugs from a single-phase material represents an improvement over current controlled-release technology. The improvements are manifest in the simplified processing techniques required to achieve staggered-release. This research opens new avenues of exploration in dosing strategies limited to select regions of tissue accessible to the implanted devices. Also, combining the synergistic actions DB-67 and doxorubicin on the topoisomerase enzyme target would certainly prove useful in halting tumor progression. It is our hope that this release technology will enable the further development of drug candidates previously considered inadequate for clinical use.

6.0 INCORPORATION OF INCORPORATION OF CATIONIC AND ANIONIC CONSTITUENTS ACCELERATES THE RELEASE OF DB-67 FROM LDI-GLYCEROL POLYURETHANE IMPLANTS

6.1 ABSTRACT

This study seeks to determine the effect of ionic ligands on the drug delivery characteristics of biodegradable polyurethane materials synthesized from lysine diisocyanate (LDI) and glycerol. Two naturally occurring ionic ligands, choline chloride (CC) and isethionic acid (ISE), and DB-67, a potent anti-cancer compound, were covalently incorporated into LDI-glycerol polyurethane films and foams using a tertiary amine catalyst. It was shown that the sulfonate group on ISE does not react to a significant degree with LDI. The morphological characteristics of the polyurethane films and foams were then assessed via SEM, and significant differences related to the ionic ligands were found to exist. Differences in the distribution of DB-67 throughout the films and foams were assessed via fluorescence microscopy. The materials were then evaluated for their drug delivery characteristics in vitro. The results of this study clearly indicate that the incorporation of ionic ligands into LDI-glycerol polyurethanes has significant effects on the morphology and drug distribution characteristics, ultimately affecting the drug delivery profiles of these materials.

Keywords: choline chloride, isethionic acid, polyurethane, drug-delivery, camptothecin

6.2 INTRODUCTION

Ionic species are prevalent in biology and are intricately involved in many of the essential physiologic processes required to maintain homeostasis. Choline chloride (CC) is a naturally occurring amine salt that is found in the lipids that make up cell membranes and in the neurotransmitter acetylcholine [179]. It has been classified as an essential nutrient by the Food and Nutrition Board of the National Institute of Medicine, usually grouped within the Vitamin B complex. Isethionic acid (ISE) is a short chain alkane sulfonate containing hydroxyl group that is a water soluble liquid used in the manufacture of mild, biodegradable and high foaming anionic surfactants [180]. It is also naturally occurring and studies suggest that cardiac myocytes are capable of converting taurine to isethionic acid [181, 182]. The carbon analogue of choline, 3,3-dimethyl-butanol (DMB), while not naturally occurring, has been used in the past to probe the physiology of cholinergic transmission [183, 184]. These three structures, while each serving separate and vastly different physiologic roles, do share a unique relationship.

These three compounds are all similar in terms of their chemical structures, each possessing a primary alcohol and an organic functional group separated by an ethyl chain (Figure 37). The various organic functional groups – quaternary amine for CC, sulfonate for ISE, and t-butyl for DMB – impart a specific ionic character to the molecule: CC is cationic, ISE is anionic, and DMB can be considered a neutral species. These three compounds with similar organic structures provide a starting point to begin exploring the effect of ionic additives in erosive drug delivery implants.

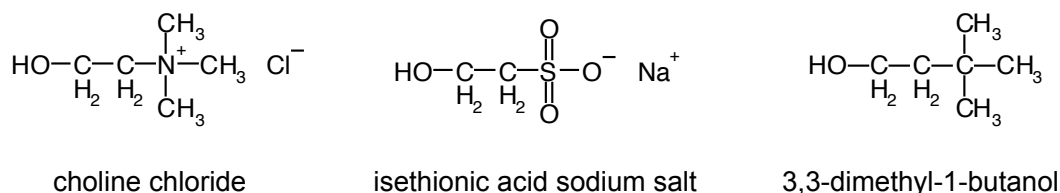


Figure 40 – Structure of CC, ISE and DMB

Hydrolysis is one of the dominant mechanisms for polyurethane degradation, and its rate is highly dependent upon material composition [185]. Hydrolysis can essentially be considered as a “reversal of condensation”. Most degradable polyurethanes are thermoplastic elastomers copolymers that are heterogeneous in nature, being composed of both hard and soft segments. The hard segment is typically comprised of high glass transition temperature (T_g), semi-crystalline aromatic diisocyanate with a low molecular weight chain extender; the soft segment is typically low T_g polyester with high molecular weight. Degradation in these materials occurs quite quickly via ester hydrolysis, while the urethane bond is more resistant to cleavage [131]. However, urethane hydrolysis does occur, albeit at a much slower rate that is largely dependent upon the hydrophobic character of the diisocyanate used to fashion the polyurethane [186].

Our laboratory has synthesized a new class of polyurethane materials based on lysine and glycerol that degrade hydrolytically into non-toxic components – lysine, glycerol and CO_2 [87]. Lysine diisocyanate (LDI) and glycerol readily react to form dense polyurethane networks suitable for a variety of biomaterial applications [88, 170, 187]. These materials hydrolyze on a much longer time scale than the typical degradable polyurethane, and we have previously fashioned hydrolysable drug delivery systems from these materials intended for the long-term controlled release of therapeutic compounds within the body. Our delivery technology relies on the chemical incorporation of therapeutic compounds into a polyurethane network via pendant hydroxyl and amine functional groups present within a drug’s chemical structure. Drug release occurs in a slow, predictable fashion as the polyurethane erodes.

In an attempt to alter the degradation rates and hence the release characteristics of our delivery systems, we propose the incorporation of ionic species into LDI-glycerol polyurethanes. Urethane degradation alters in response to local ion concentrations [188], and it is our hope that inclusion of biocompatible ionic species into the polymer will provide a similar effect. This study should provide yet another means to the alter degradation rates of our LDI-glycerol polyurethanes and control the release profiles of drug delivery systems fashioned from them.

6.3 MATERIALS AND METHODS

6.3.1 Materials

Lysine diisocyanate methyl ester (LDI) was purchased from Chemical Division, Kyowa Hakko Kogyo Co. Ltd. (Tokyo, Japan). 7-tert-butyldimethylsilyl-10-hydroxycamptothecin (DB-67) was obtained from Dr. Dennis Curran at the University of Pittsburgh, Chemistry Dept. (Pittsburgh, PA). Bismuth 2-ethylhexanoate was obtained from Alfa Aesar (Ward Hill, MA). All other chemicals were obtained from Sigma–Aldrich Chemical Co. and were of reagent grade unless otherwise specified (Milwaukee, WI).

6.3.2 Synthesis of Ionic Films and Foams

Polyurethane films were fashioned by taking glycerol (MW 92.01, 1.00g, 10.9 mmol), Bismuth 2-ethylhexanoate (MW 638.61, 5 mg, 7.8×10^{-3} mmol), DB-67 (MW 478.70, 10 mg, 2.1×10^{-3} mmol), and dry DMSO (2.5 ml) and adding them to a small, dry 20 ml reaction flask. The requisite amount of isethionic acid (ISE) (MW 148.1, 370 mg, 2.5 mmol) choline chloride (CC) (MW 139.6, 349 mg, 2.5 mmol) or 3,3-dimethyl-butanol (DMB) (MW 102.2, 255 mg, 2.5 mmol) to arrive at 6.0 mol% was added to the flask. Mol% was calculated as the number of mols of additive over the total mols of reactant, expressed as a percent. The contents were mixed at room temperature until thoroughly dissolved. The reaction flask was then transferred to an ice bath atop a magnetic stir plate and allowed to chill for 15 min. LDI (MW 212.20, 6.00 g, 28.3 mmol) was then added and the vial was flushed with nitrogen prior to being sealed. The flask was placed back in the ice bath and mixed for 1 hr. The reaction flask was removed from the ice bath and stirred at room temperature until the viscosity sufficiently increased such that it could no longer be mixed atop the magnetic stir plate; its viscosity was approximately 3.0×10^4 cP at this time. The viscous pre-polymer was then transferred to a 65 mm PTFE dish submerged in an ethyl acetate (EtAc) bath. The polymer was allowed to cure for 48 hours in the EtAc bath. The PTFE dish was then removed from the bath and placed into a vacuum oven at 25 °C for 24 hours. The polymer films were then stored in the dark at 4 °C for further processing and analysis.

The same procedure and amounts of reactants were used in fashioning the polyurethane foams, except this time 1,4-diazobicyclo[2.2.2]-octane (DABCO) (MW 112.2, 8.0 mg, 7.0×10^{-2} mmol) was used as a urethane catalyst. After sufficient viscosity had been attained, the viscous pre-polymer was transferred to a 100 mm PTFE dish and 100 μ L distilled, deionized H₂O was added. The pre-polymers were thoroughly mixed 3 times at 2-minute intervals to ensure the H₂O was fully incorporated. The rising foams were left open to the atmosphere yet covered to protect from light while the curing. The resulting polymer foams were then placed into a vacuum oven overnight at 25 °C. The foams were then placed into storage in the dark at 4 °C for further analysis. The average hydroxyl functionality (F_{avg}) was calculated for each of the materials according to the following equation:

$$F_{avg} = \frac{\sum n_i x_i}{\sum x_i}$$

where n_i is the number of hydroxyl functional groups on a molecule and x_i is the number of moles of that molecule.

6.3.3 ISE Reactivity with LDI

In order to determine if the sulfonate group of ISE reacts with isocyanate (NCO), LDI (89mg), ISE (125 mg), and 2.0 ml dry, DMSO were added to a small dry reaction flask to achieve a 1:1 OH to NCO ratio. Another vial was prepared with the same amount of DMSO and ISE, but LDI (178 mg) was used to provide a 1:1 ratio of LDI to ISE. Infrared spectra of each reaction were obtained immediately after the addition of LDI. No urethane catalyst was used to facilitate the reactions. The flasks were mixed atop a magnetic stir plate for 6 days, and infrared spectra were recorded again. Peak integrations for the NCO and carbonyl (C=O) peaks were obtained and used to track the progress of the reactions over the 6-day period.

6.3.4 Swelling studies

Polyurethane foams and films containing either 6 mol% CC, ISE or DMB and corresponding control materials containing 0 mol% ionic constituent were prepared as previously described. Small samples on the order of 50.0 mg was obtained from each of the polyurethane foams, and a 30.0 mg discs was cut from each film with a 4 mm tissue biopsy punch (Sklar Instruments). The samples were weighed and then placed in 40.0 ml distilled, deionized water atop a magnetic stir plate and slowly agitated. Their weights were recorded over time in the following manner: every minute for the first 10 minutes, every 2 min for the next ten minutes, every five minutes for the rest of the first hour, every 10 minutes during the second hour, every 20 minutes during the third hour, and then every 30 minutes for the remaining 2 hours. The samples were weighed again after 24 hours. The amount of water taken up by the foam and film samples was expressed as a percent increase over the original weight. The samples were then dried to constant weight, and the sol content of each sample was determined as previously described by Huang [115].

6.3.5 SEM Evaluation of Polymer Architecture

Polyurethane foams and films containing either choline chloride, isethionic acid, taxol, or all three were cut into small 5 mm x 5mm x 1mm sections, dried thoroughly, and mounted on sample holders. The foam materials were sliced through on horizontal and vertical cross-sections in various places about the samples. A 4 mm tissue biopsy probe was used to remove discs from several regions of the film, and those discs were sliced through on horizontal and vertical cross-sections. Samples were observed at 25X magnification to ensure there were no gross irregularities. A series of images were taken of each specimen. For foams, images were taken at 25X, 100X, and 2000X of the sample top, bottom, and cross-section. For films, images were taken at 100X, 200X, and 2000X of the sample top, bottom, and cross-section. Images were then compared to one another in order to elucidate the morphological changes imparted by the ionic constituents.

6.3.6 DB-67 Distribution throughout the Polyurethanes

Film and foam samples were dried thoroughly and then sliced to a thickness of approximately 500 μm and mounted on a glass slide. Fluorescent and non-fluorescent images were taken at 100X filter in order to assess the distribution of DB-67 throughout the ionic and control film and foam polyurethane materials (Zeiss AX10 Imager.A1). A FITC filter was used to visualize the DB-67 compound within the sample (Chroma).

6.3.7 Drug Release

LDI-glycerol polyurethane foam samples containing DB-67 and 6 mol% of CC, ISE, or DMB were incubated at 10 mg/ml in PBS (pH 7.4) on rocking plates in temperature-controlled rooms at 4, 22, 37 and 70 $^{\circ}\text{C}$ for 10-weeks. A sample containing only DB-67 and no ionic constituent was incubated at 10 mg/ml as well. Sample chambers were protected from light during this time. Every 7 days, 3.0 ml of PBS was retrieved from each sample; during the first week, PBS was also collected on day 3. The amount of DB-67 released from each polymer sample was detected via fluorescence spectroscopy using the excitation and emission wavelengths particular for DB-67. The total amount of drug collected was calculated as follows:

$$\text{mol}\% = \frac{1}{MW_{DB-67}} \left[3 \sum \left(\frac{m}{V} \right)_i + \left(\frac{m}{V} \right)_j (V_T - 3j) \right]$$

where $(m/V)_i$ represents the concentration of each collected sample and V_T the total volume (where each time point is designated “i” and “j” represents the last). Lysine and glycerol released from the polymer were not assessed at this time.

6.4 RESULTS

6.4.1 ISE Reactivity with LDI

It is well known that primary hydroxyl groups readily react with isocyanate to form urethane bonds with or without the addition of a urethane catalyst. It is easily concluded that both CC and DMB will readily incorporate into LDI-glycerol polyurethane materials in a predictable fashion. However, it is difficult to predict how the presence of a sulfonate group in ISE will affect the synthetic reaction. Therefore, it was of interest to determine the reactivity of ISE with LDI, and this was monitored via infrared spectroscopy (Figure 41).

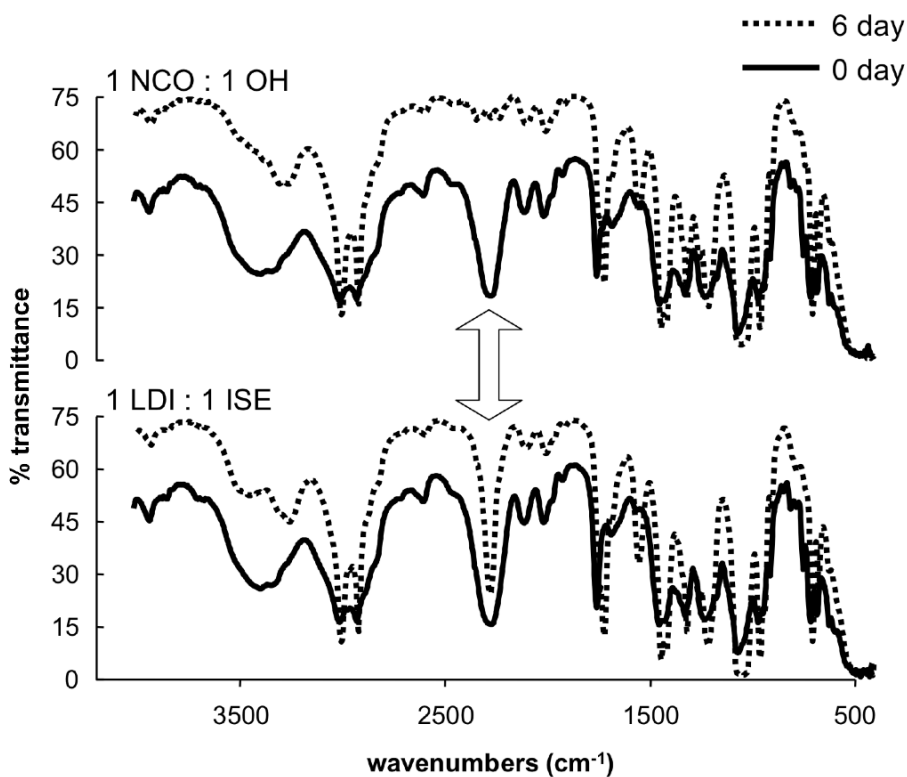


Figure 41 - FT-IR data depicting the reaction of LDI with ISE at 1 NCO : 1OH and 1LDI : 1 ISE molar ratios

In the 1:1 NCO to OH reaction, complete disappearance of the NCO signal is realized by day-6. The ratio of the NCO to carbonyl (C=O) peak integrations progresses from 1.9 at day-0 to 0.3 at

day-6, indicating that all of the NCO has reacted with the primary OH. In a 1:1 LDI to ISE reaction, significant NCO signal is observed to persist at day-6. The NCO/C=O peak ratio changes from 2.1 at day-0 to 1.0 at day-6, indicating that half of the isocyanate has reacted.

6.4.2 Swelling Studies

Polyurethane foam and film samples loaded with 6 mol% ISE, CC, or DMB and corresponding control materials containing no ionic additives were assessed for their ability to take up water in an aqueous environment incrementally over a 5 hour period (Figure 42).

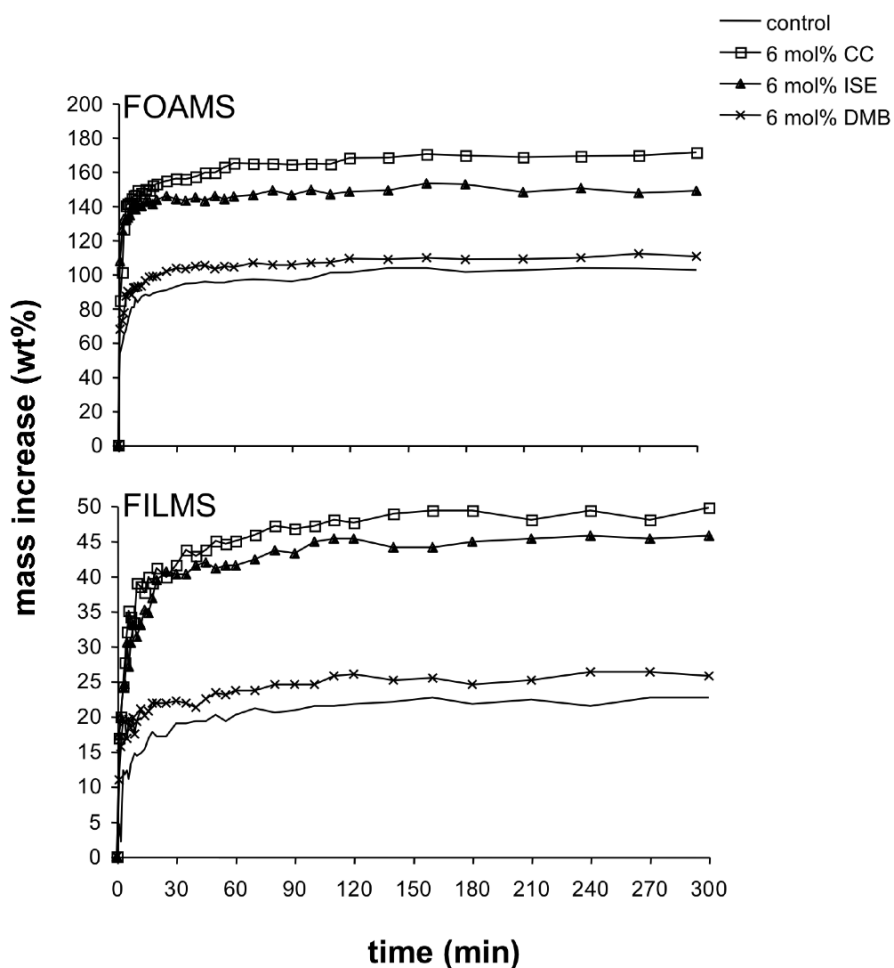


Figure 42 - Swelling studies for the 6 mol% CC, ISE, DMB, and control foam and film LDI-glycerol polyurethanes loaded with DB-67

Foam samples were observed to take up approximately 3 to 4 times more water than their corresponding films. Over a 24-hour period, the control foam and film samples were observed to absorb an additional 103% and 23%, respectively. The non-ionic DMB species were observed to absorb slightly greater amounts of water, with the foam and film species each absorbing an additional 110% and 26%, respectively. The amounts of water absorbed by the ionic foams and films were significantly greater than those observed for either of the controls. The ISE foam and film samples absorbed 149% and 46%, while the CC foams and films absorbed an additional 171% and 50%, respectively. The general trend amongst the foam and film samples regarding water uptake was as follows: CC > ISE > DMB > control. The samples were left to soak for a full 24-hours, and the mass was recorded again. The trend was still observed with each material taking up slightly more mass over the 19-hour interval, except for the ISE and CC foams which had begun to deteriorate.

6.4.3 SEM analysis and DB-67 distribution

Scanning electron micrographs of the LDI-glycerol polyurethane materials demonstrate that some significant changes in morphology occur with the addition of ionic constituents. All internal surfaces of the sample obtained via horizontal and vertical cross sectioning were similar in appearance. The top surfaces of the foams and films both appeared smooth in nature. The tops of the film samples were free of pores, while the top surface of the foam samples had a reduced number and size of pores. The bottom surfaces of the film samples appeared similar in nature to the top, and the bottom surfaces of the foams appeared similar to the cross sections. Only vertical cross-sectional images are shown to illustrate the material morphology. Low and high magnification images demonstrate the differences that exist between the film samples (Figure 43).

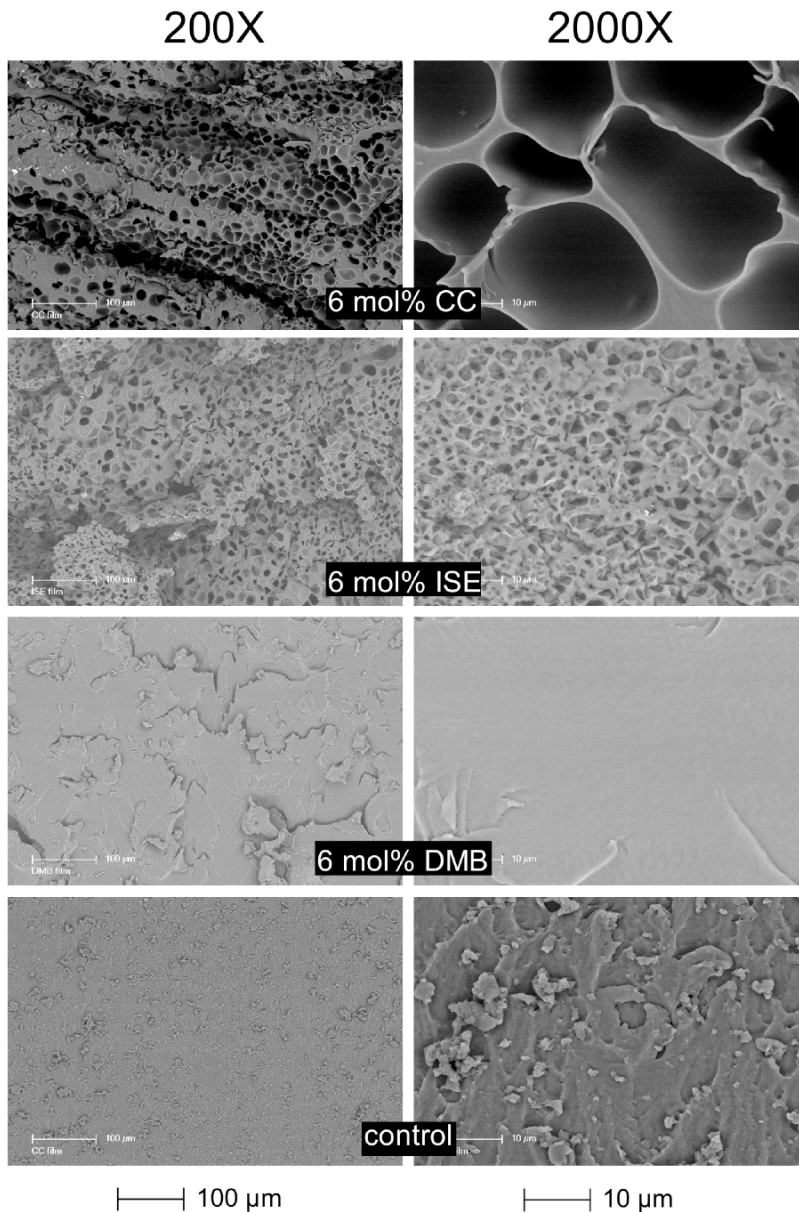


Figure 43 - SEM images of the 6 mol% CC, ISE, DMB, and control LDI-glycerol polyurethane films loaded with DB-67

The images indicate that the ionic samples, CC and ISE, both possess cavitations throughout the materials. The cavitations in the CC sample appear much more ordered and larger at higher magnification than those in the ISE material. There are no cavitations present in either the DMB or 0 mol% control foams, although there are some distinct surface irregularities. The

irregularities are much more prevalent at high magnification on the surface of the 0 mol% control film than on the DMB film. Low and high magnification SEM images of the LDI-glycerol polyurethane foam materials reveal the materials to be much more similar to one another than previously observed amongst the film samples (Figure 44).

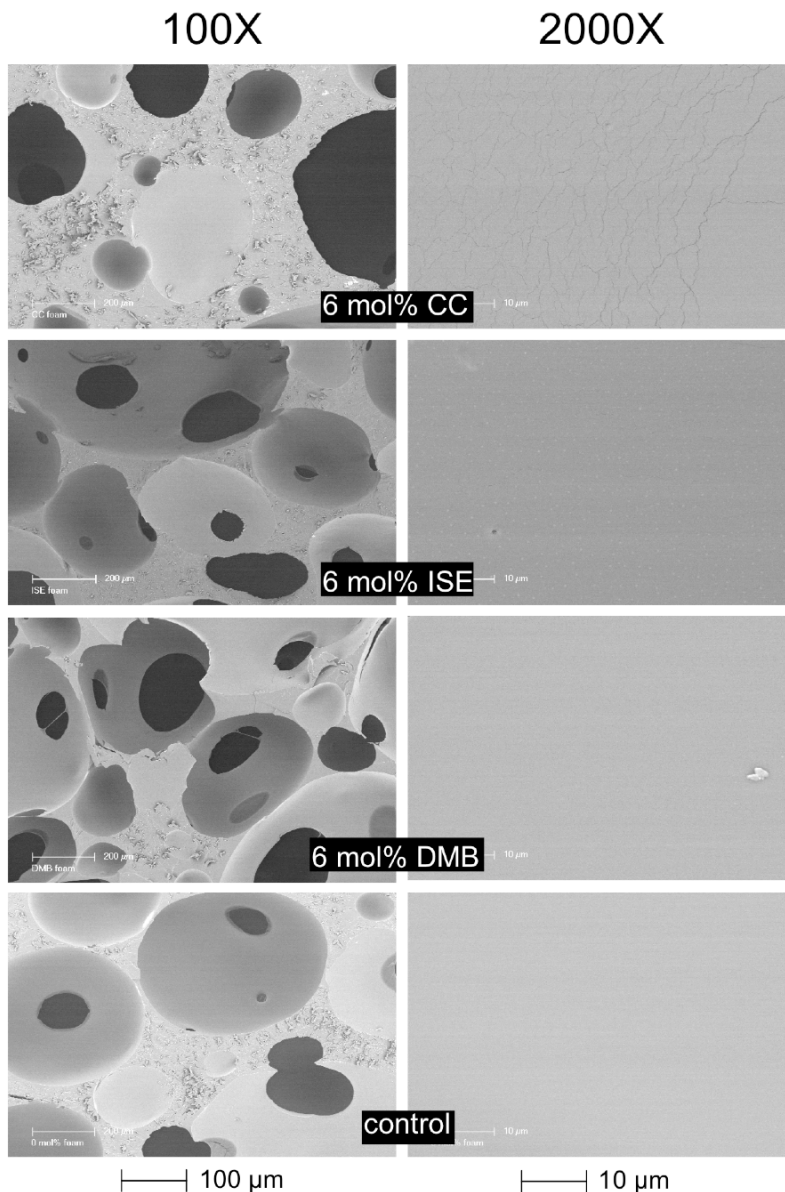


Figure 44 - SEM images of the 6 mol% CC, ISE, DMB, and 0 control LDI-glycerol polyurethane foams loaded with DB-67

There are slight variations amongst the foam morphologies in terms of the number and size of the pores. However, high magnification images show that the surfaces of the materials are all very similar in nature. The surface irregularities are much less drastic in nature than the film samples. The surface of the CC foam exhibits small cracks across its surface, while the other samples are quite smooth and uniform.

DB-67 possesses an intense, characteristic fluorescent profile, making an ideal candidate for assessing the controlled-release characteristics of our polyurethane materials [81, 177]. The emission band of the DB-67 moiety corresponds closely with that of FITC, a fluorescent probe commonly used in many biological assays. As such, we were able to visualize the distribution of DB-67 throughout thin sections of the various polyurethane materials using fluorescence microscopy. The distribution of DB-67 throughout the polyurethane films was observed to vary to a considerable degree (Figure 45).

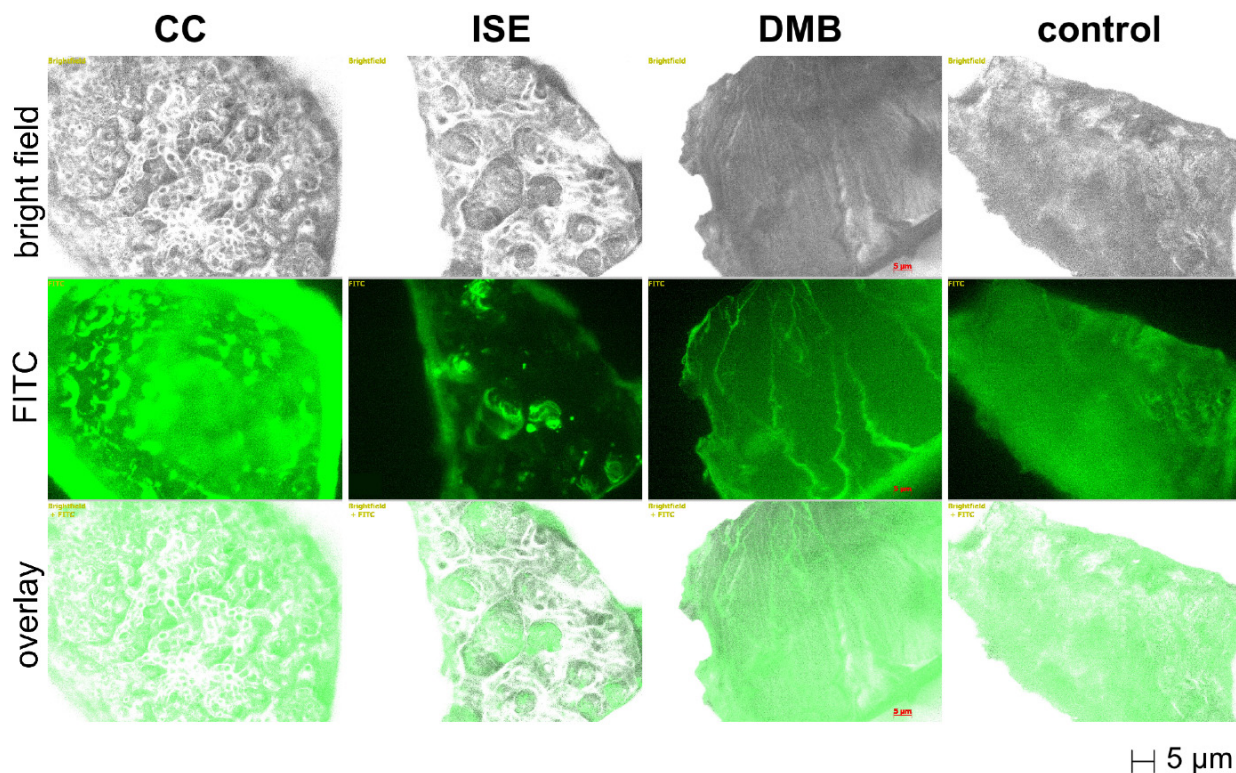


Figure 45 - Fluorescent microscope images demonstrating DB-67 distribution through the CC, ISE, DMB and control LDI-glycerol polyurethane film samples

Bright field images reveal the ionic film samples to each possess a unique material morphology, each differing in appearance quite considerably from either of the control species. Fluorescent images of the ionic films demonstrate the DB-67 distribution closely following the material morphology, with intense pockets of signal scattered throughout. The DMB sample exhibits a relatively disperse distribution of drug, but does possess intense bands coursing throughout the film. The control film possesses a uniform distribution of DB-67, similar to what was observed in the polyurethane foam materials. The distribution of DB-67 throughout the polyurethane foam materials was observed to be uniform relative to the film materials (Figure 46).

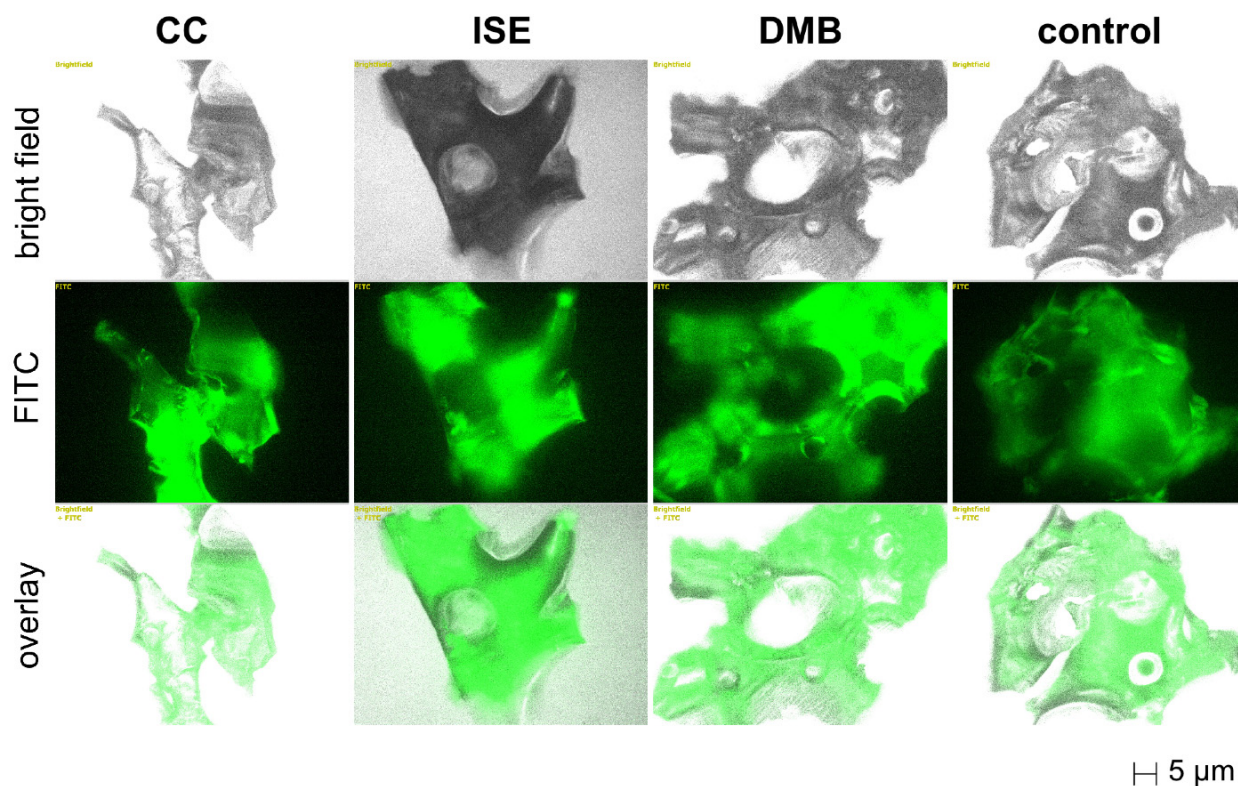


Figure 46 - Fluorescent microscope images demonstrating DB-67 distribution through the CC, ISE, DMB and control LDI-glycerol polyurethane foam samples

Bright field images demonstrate variations in pore size and shape to exist, and some slight variation can be expected after considering the material processing methods used to fashion the

foams. The fluorescent images reveal that the DB-67 distribution to be relatively and uniform, with signal intensity closely following foam thickness and morphology.

6.4.4 Drug release

Incorporation of ionic ligands has already proved to alter the swelling characteristics of the ionic foams relative to the DMB and control materials. As a result, we can anticipate distinct differences to occur amongst the materials with regard to their release of incorporated DB-67. The release of DB-67 and from the polyurethane films and foams was monitored over a 6-week period at 4, 22, 37 and 70 °C. The release of each drug species was assessed from multiple samples. The concentration profiles of DB-67 obtained in solution for the LDI-glycerol polyurethane films and foams were found to be temperature dependent and revealed some interesting differences (Figure 47).

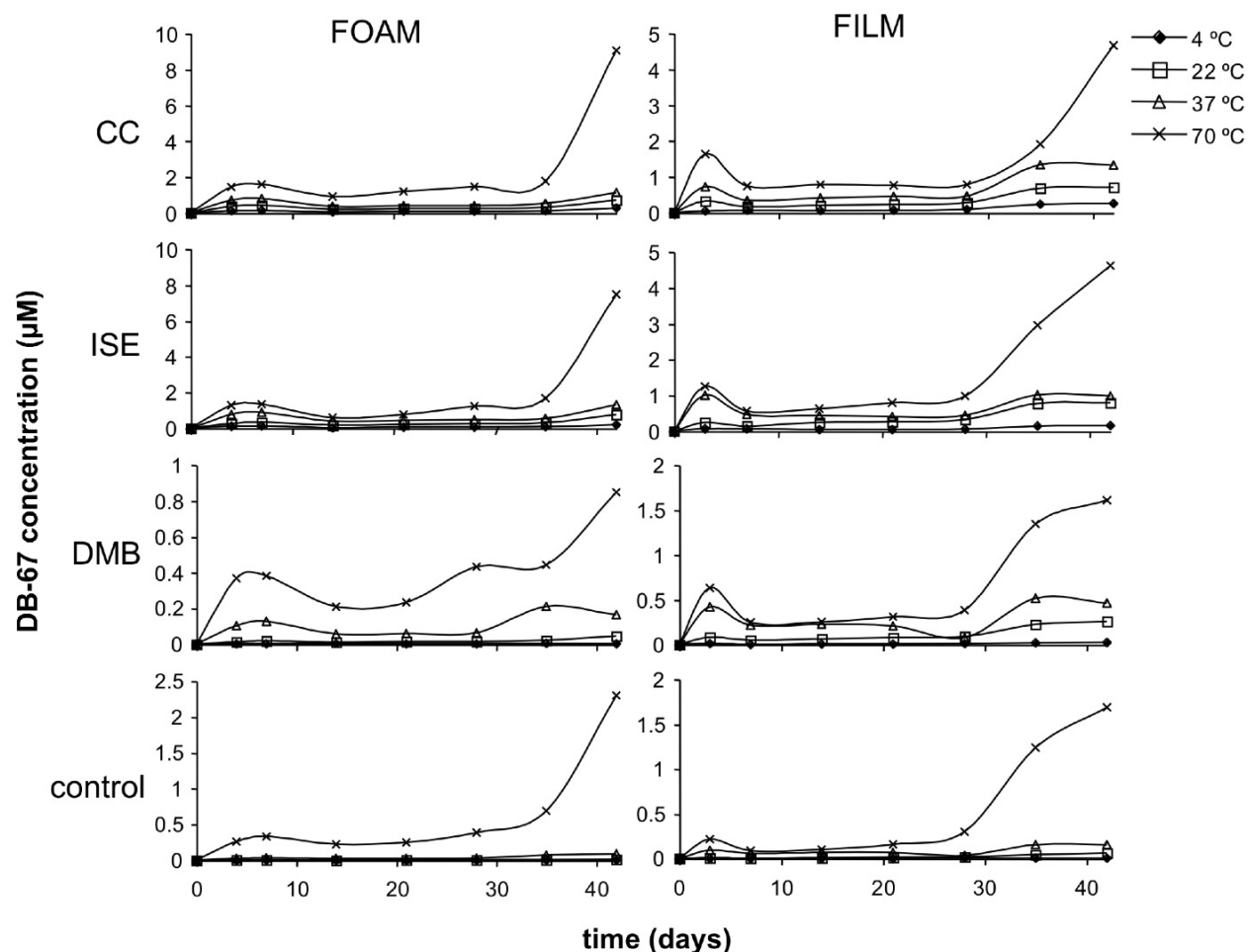


Figure 47 - Concentration profiles for the release of DB-67 from the CC, ISE, DMB, and control LDI-glycerol polyurethane films and foams

Initially, all of the materials exhibit a burst release of drug with subsequent decay. The day-3 concentrations of DB-67 in solution can be ordered with regard to ionic constituent and follow the trend $CC > ISE > DMB > control$. Concentrations of DB-67 obtained from the ionic CC and ISE foams were approximately twice those contained from the corresponding films. Surprisingly, more DB-67 was released from the DMB film than from the corresponding foam. Similar concentrations of DB-67 were obtained from each of the control materials.

In addition, the relative amount of DB-67 liberated from each film and foam system was recorded, eliciting some key differences between the various materials (Figure 48).

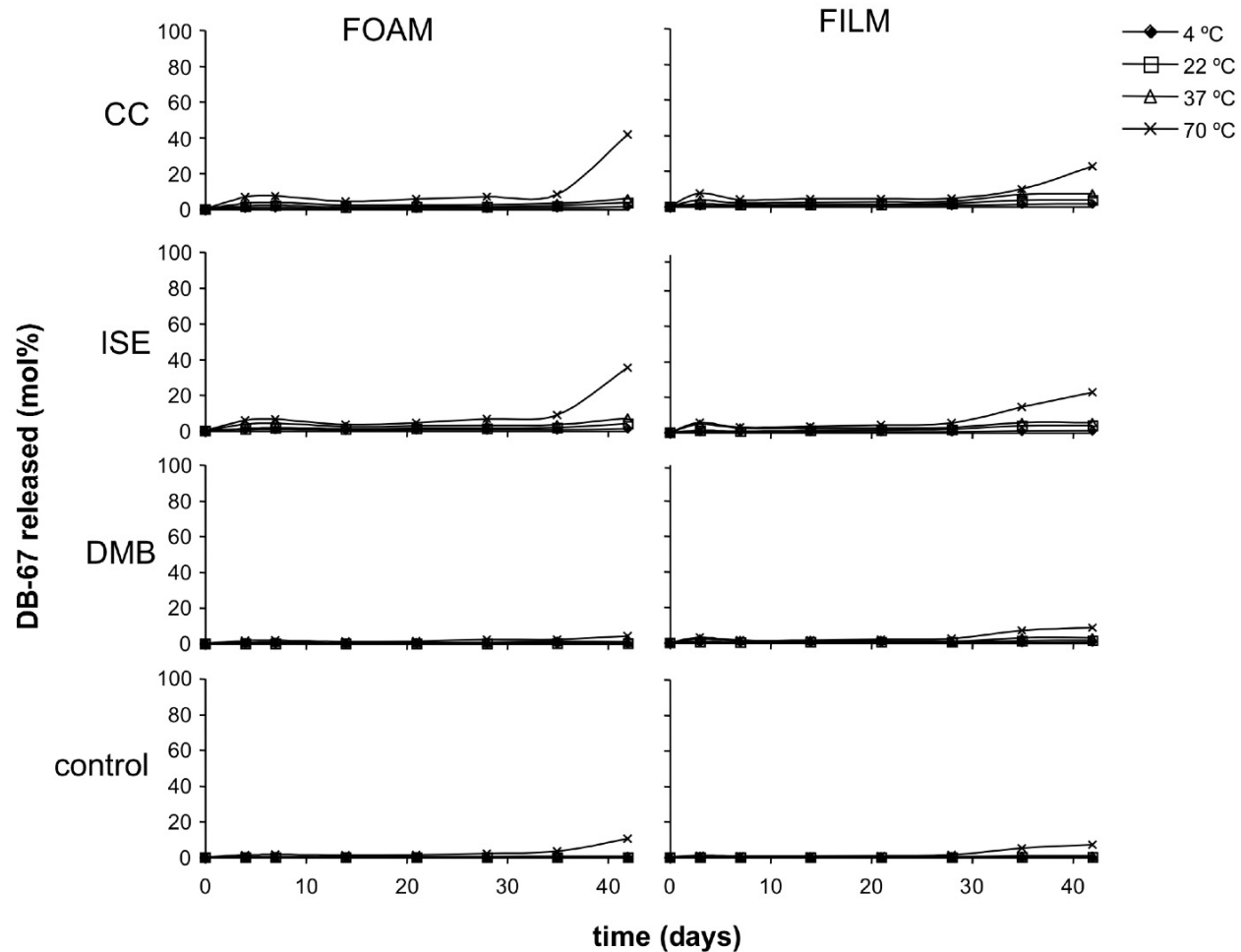


Figure 48 - Release profiles showing the mol% of DB-67 retrieved from the CC, ISE, DMB, and control LDI-glycerol polyurethane films and foams

The burst release observed in the concentration profiles for the films and foams is observed to be quite small relative to the total DB-67 content of the materials. At the end of the 6-week period, the ionic films had released a greater percentage of their total drug load into solution than the corresponding foams. The CC and ISE foams released 42.0% and 35.0% of their DB-67 content, respectively, while each of the ionic films each released 22.4%. The DMB and control materials each released significantly less DB-67 than the materials containing any ionic ligands. The drug release characteristics have been summarized in Table 11.

Table 11 - Release characteristics of DB-67 from ionic and control LDI-glycerol polyurethane films and foams

System	Compound	F _{avg}	sol content (%)	Temperature (°C)	mol% ^a	day-42 concentration (μM)	day-3 concentration (μM)	day-42/day-3 ratio
Film	choline chloride	2.6	20.3	4	1.3	0.25	0.05	5.0
				22	3.5	0.71	0.32	2.2
				37	6.9	1.33	0.71	1.9
				70	22.3	4.67	1.64	2.8
	isethionic acid	2.6	28.3	4	0.8	0.16	0.06	2.7
				22	4.0	0.79	0.24	3.3
				37	5.4	0.98	1.00	1.0
				70	22.4	4.61	1.24	3.7
	3,3-dimethyl-butanol	2.6	23.4	4	0.02	0.12	0.01	12.0
				22	1.4	0.26	0.08	3.3
				37	2.5	0.46	0.42	1.1
				70	8.3	1.61	0.63	2.6
none	3.0	19.9	4	0.03	0.01	0.00	-----	
			22	0.3	0.06	0.01	6.0	
			37	0.7	0.15	0.09	1.7	
			70	6.9	1.69	0.22	7.7	
Foam	choline chloride	2.6	28.1	4	1.4	0.28	0.10	2.8
				22	3.8	0.73	0.35	2.1
				37	6.2	1.15	0.70	1.6
				70	58.0	12.66	1.42	8.9
	isethionic acid	2.6	26.5	4	1.1	0.21	0.12	1.8
				22	4.4	0.85	0.27	3.1
				37	7.4	1.34	0.77	1.7
				70	46.3	9.54	1.28	7.5
	3,3-dimethyl-butanol	2.6	25.9	4	0.06	0.01	0.00	-----
				22	0.4	0.09	0.01	9.0
				37	0.9	0.17	0.10	1.7
				70	6.9	1.5	0.37	4.1
none	3.0	24.3	4	0.04	0.01	0.00	-----	
			22	0.09	0.02	0.00	-----	
			37	0.6	0.11	0.02	5.5	
			70	14.2	3.07	0.26	11.8	

a: at day-42

6.5 DISCUSSION

Infrared spectroscopy was used to monitor the reaction of ISE with LDI to determine how the presence of the sulfonate group would affect the urethane chemistry. The reactions were carried out in the absence of any urethane catalyst in order to avoid many of the common side reactions associated with their use [19, 20, 144]. It was determined that all of the available NCO was consumed in a 1:1 NCO to OH reaction, and that only half of the NCO was consumed in a 1:1 LDI to ISE reaction. These findings indicate that the NCO did not react to a significant degree

with the sulfonate group present on ISE. Its presence in the reaction should not interfere with the synthetic chemistry used to synthesis the polyurethane materials.

Swelling studies reveal significant differences to exist amongst the polyurethane foam and film materials in terms of their water uptake over a 24-hour period. The incorporation of ionic ligands can be expected to have two effects on the polymer's water uptake. First, cations and anions are known to hydrate to differing degrees, so the cationic and anionic polymers may follow similar trends [189]. Second, the monofunctional additives interrupt the network architecture, serving as a site of chain termination since each ionic species is mono-functional. In order to control for this, DMB was chosen as a non-ionic control so that the uptake due to alterations in the network could be examined separate from the ionic species. As expected, the DMB foams and films did absorb more mass than the corresponding control, indicating F_{avg} has an effect on swelling. However, the difference between the ionic and non-ionic species was substantially larger than the difference between the DMB and control species.

SEM images indicate that the material morphology is vastly different between the film and foam samples. The film samples demonstrate a unique characteristic morphology for each of the CC and ISE ionic samples. Each one demonstrates distinct pores to be present throughout the bulk of the material. The film samples also reveal surface irregularities that are strikingly different from one another, but it may be that these irregularities are artifacts of the cross-sectioning process. A razor blade was used to slice the materials so that the internal surfaces could be visualized. However, the irregularities are sufficiently different from one another to suggest that they are likely related to the material structure. The foam samples for the most part appear quite similar under low and high magnifications.

The vast differences between the film and foam morphology can easily be correlated to the processing techniques used to prepare them. A non-solvent casting technique was used to prepare the film samples, which provided the materials significant time to cure. The extended curing time allowed the pre-polymer to reorient itself prior to the formation of covalent urethane bonds. However, the foam process is relatively rapid, and occurs over a much shorter time interval. This interval is likely insufficient to allow for material rearrangement. As a result, the materials appear quite similar under the electron microscope.

Fluorescence microscopy was able to clearly demonstrate the distribution of DB-67 throughout each polyurethane material. Signal intensity is not necessarily representative of the

amount of DB-67 from one image to the next due to variations in sample thickness and microscope settings, but we do obtain a clear distribution pattern. There was a considerable difference observed between the foam and film samples with respect to drug distribution. Each of the polyurethane foams exhibited a relatively uniform distribution, while the film materials samples each possessed a rather unique distribution characteristic of the material morphology. These apparent differences are believed to be by-products of the processing techniques used to fashion the foams and films. The foam curing process was rapid, occurring over a period of hours. The film curing process was slow, occurring over a period of days. The extended duration of film curing process allows the material to segregate, a process that appears to be dictated by the ionic species incorporated into the sample. As a result, the DB-67 distribution in the ionic materials can be expected to be quite different from that observed in the foam materials. Differential release of DB-67 occurred from the ionic film and foam materials in a temperature dependent manner. A comparison of the concentration profiles from the materials at 37 °C demonstrates reveals some interesting trends that can be correlated to ionic character (Figure 49).

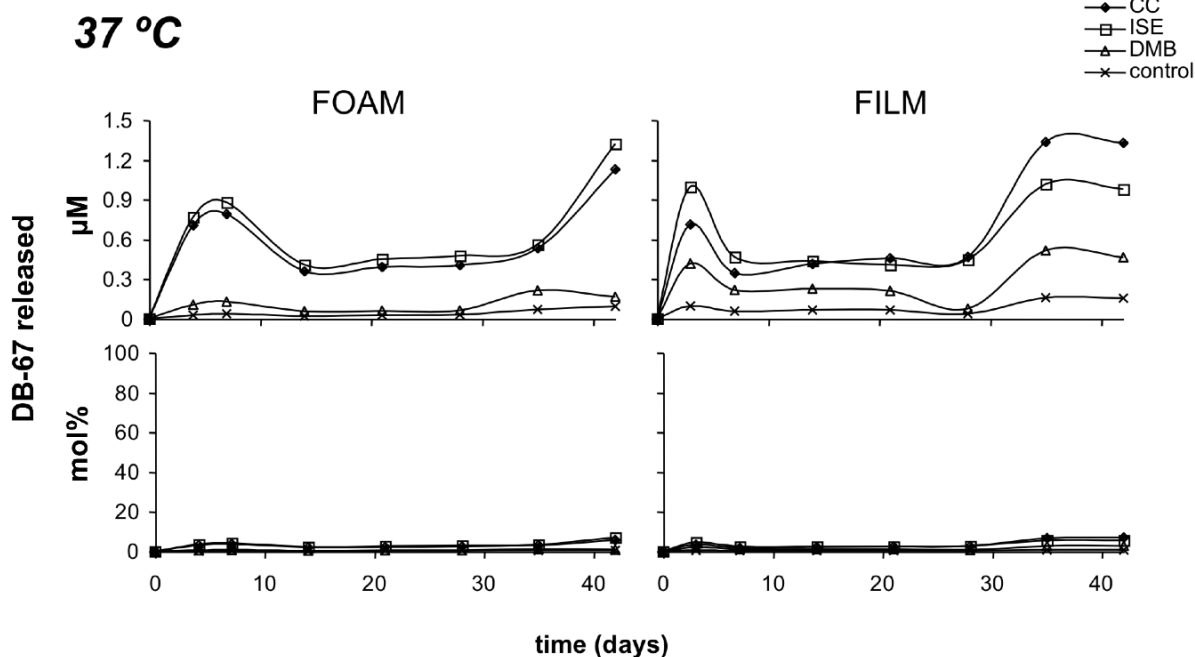


Figure 49 - Release of DB-67 from the ionic films and foams at 37 °C

Release of DB-67 from the ionic foams (CC and ISE) is remarkably similar at 37 °C over the 6-week test period, in terms of the amounts and timing of drug release. The incorporation of ionic ligands was expected to affect the overall network architecture, by decreasing the average hydroxyl functionality of the polymer. However, the incorporation of DMB into the polyurethane foams and films does not appear to have anywhere near the effect that incorporation of an ionic species has. Consistently greater amounts of DB-67 were observed to elute from the ionic materials, while there was only a slight increase due to DMB incorporation.

Similar effects were also observed to occur at 70 °C. Once again, the ionic film and foam materials (ISE and CC) are observed to release significantly greater amounts of DB-67 into solution than their corresponding non-ionic materials (Figure 50).

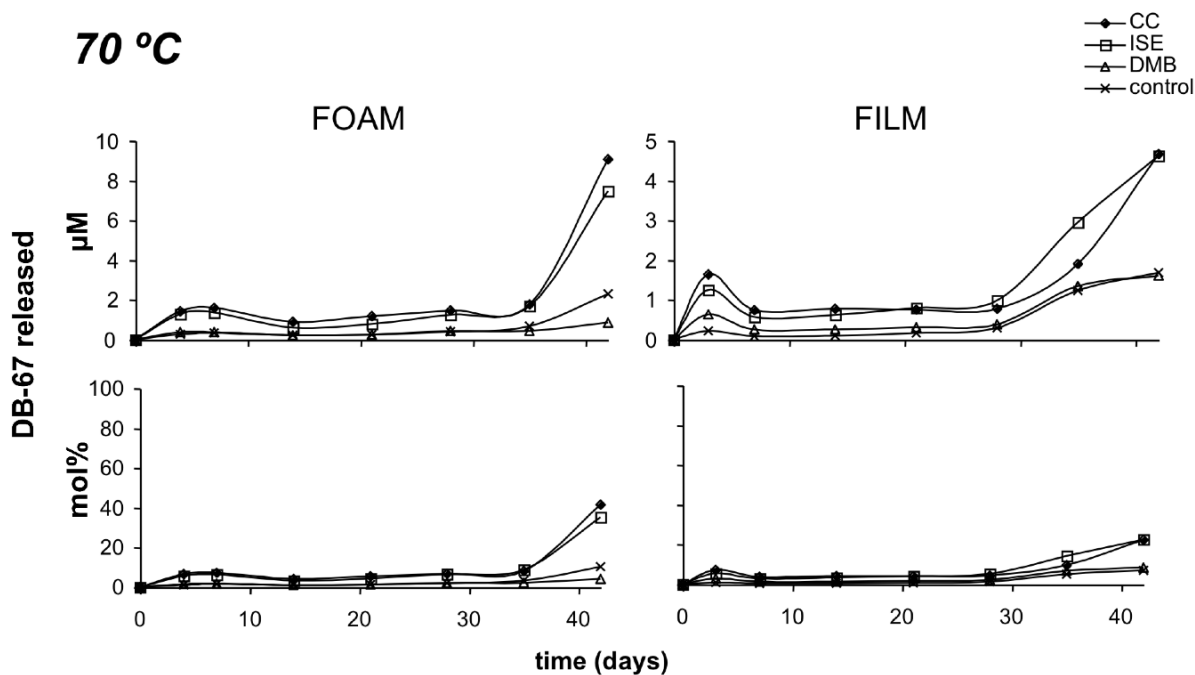


Figure 50 - Release of DB-67 by the ionic materials at 70 °C

The chain termination effect of the ligands is apparent when comparing the DMB foam to the control material. The release rates of DB-67 observed with the CC, ISE, DMB, and especially the control materials are much slower than previously observed for other LDI-glycerol drug

delivery systems. This is due to the need to increase the amount of LDI in the synthetic reaction in order to completely dissolve the ionic species. The additional LDI that was required resulted in an NCO:OH ratio of 1.7 in the synthetic reaction, where previously a value of 1.0 had been used. A much more slowly degrading polymer can be expected due to the increased number of urea bonds in the material, which hydrolyze much more slowly than urethane bonds. Overall, the incorporation of ionic species into LDI-glycerol polyurethane materials was found to increase the rates at which DB-67 is eluted into solution through a material degradation and erosion process.

6.6 CONCLUSIONS

In this study, we have present a means to alter the controlled, long-tem delivery of the camptothecin analogue DB-67 from biocompatible, biodegradable polyurethane films and foams constructed from LDI and glycerol via the incorporation of ionic ligands. We have demonstrated via FT-IR that LDI does not react to any significant degree with sulfonate functional groups. We then incorporated naturally occurring ionic ligands, choline chloride and isethionic acid, and DB-67 into the polymer network via covalent urethane bonds. The ionic ligands were shown to alter the swelling characteristics of the materials to a considerable degree. A non-ionic control ligand, 3,3-dimethyl-butanol, did not demonstrate a similar effect on swelling characteristics of the materials. Scanning electron micrographs revealed substantial differences in morphology between the film materials, but not the foams. Fluorescence microscopy was used to demonstrate substantial differences in the DB-67 distribution throughout the films, but not the foams. Drug release was observed to proceed in a temperature dependent manner via erosive kinetics. The incorporation of ionic ligands hastened the release of DB-67 from the polymer films and foams in a characteristic and predictable manner. These results clearly demonstrate that the controlled release of drugs from LDI-glycerol polyurethanes can be altered with via the incorporation of cationic and anionic ligands.

7.0 GENERAL DISCUSSION

7.1 INTRODUCTION

Humans have always attempted to improve their health by ingesting or administering drugs. Examples appear throughout recorded history, from every continent and culture. Biblical examples include Noah producing alcohol and Christ being offered a sedative to ease the intense pain of crucifixion [190, 191]. The use of opium was described by Theophrastus in the third century B.C., the stimulating powers of methyl-xanthines was exploited by ancient Arabian shepherds, and the paralyzing properties of curare were recognized by native South Americans centuries before the arrival of western civilization [192]. Chemotherapy of cancer, which some consider a modern development, existed in some form or another for more than 400 years [193]. Vaccination, the intentional exposure to minute doses of pathogen, was used in China and India to prevent smallpox and other infections centuries before the birth of Pasteur [194].

Even during the 20th century, drug discovery has often resulted from purely empirical observations and happenstance. The anticancer effects of nitrogen mustard were realized during the development of chemical warfare agents, and penicillin was discovered after the inadvertent contamination of a cell culture experiment [195, 196]. As technology has advanced, particularly after 1970, methods of drug discovery and mass production of therapeutics have become more sophisticated and rational in their approach. The mass production of insulin for the treatment of diabetes is merely one example in which advances in scientific technology resulted in tremendous gains in therapeutic efficacy [197]. In parallel with the rapid rise of modern pharmaceutical technology and biotechnology, the cellular and molecular basis for the action of many drugs has been uncovered. Today drug design benefits from an accumulated base of scientific knowledge. The interactions between neurotransmitters and their receptors, the regulation of hormone secretion, and the sensitivity of tumor cells to specific kinds of chemicals

have resulted in advanced treatments for depression, effective means of birth control, and curative chemotherapy for some select malignancies (i.e. – Hodgkin’s lymphoma), respectively.

New technology and clearer biological insight have led to new classes of therapeutic and prophylactic agents. Consider some of the new products available to patients in the United States over the last few years listed in Table 12 [198].

Table 12 – Newly approved therapeutics available on the US market

AGENT	TRADE NAME	INDICATION
Hepatitis B subunit	Recombivax HB® (Merck & Co., Inc.)	Vaccination against hepatitis B
Human insulin	Humilin® (Eli Lilly)	Treatment of diabetes
Monoclonal antibody against CD3	Orthoclone OKT® (Ortho Biotech)	Prevention of organ rejection
Human growth hormone	Protopin® (Genentech, Inc.)	Growth failure in children
Human interleukin-2	Proleukin® (Chiron Therapeutics)	Metastatic renal cell carcinoma
Erythropoietin	Epogen® (Amgen) Procrit® (Ortho Biotech)	Anemia
Interferon beta-1a	Avonex® (Biogen, Inc.)	Multiple sclerosis
Interferon alpha-n3	Alferon® (Immunex Corp.)	Intralesional treatment of refractory external condylomata acuminata
Tissue plasminogen activator	Activase® (Genentech, Inc.)	Acute myocardial infarction
β -cerebrosidase	Ceredase® (Genzyme, Corp.)	Enzyme deficiency
Deoxyribonuclease (DNase)	Pulmozyme® (Genentech, Inc.)	Cystic fibrosis

Even more complex agents such as chimeric antibodies, gene-based drugs, anti-sense oligonucleotides, and virus-like particles, are emerging as clinically viable entities. New clinical approaches involve cells as well as molecules; the introduction of genetically modified cells into humans has blurred the distinction between conventional pharmacology and transplantation. A revolution in drug development is clearly upon us.

This wealth of new technology and the resulting new armaments in the war against disease will require new strategies for drug and vaccine administration. Most current methods for drug administration are direct descendents of ancient practices, changing little over the past few decades [199]. Egyptian physicians employed pills, ointments, salves, and other forms of treatment over 4,000 years ago. Hippocrates, alluding to modern sterile procedures, warned against the introduction of environmental pathogens into open wounds in the 4th century B.C. Intravenous injections were first performed in humans in 1665, only a few decades after Harvey's description of the circulatory system. Subcutaneous injections were introduced by Wood in 1853 and the modern hypodermic needle was developed by Luer in 1884.

While pills and injections have enabled significant medical advances to be attained, these methods are inadequate for the delivery of new therapies made possible because of the explosion in biotechnology. Recombinant proteins frequently have short half-lives, poor permeability in membranes, and serious toxicity when delivered systemically in large doses. General methods for the delivery of gene-therapy vectors are still unknown, since the uptake, bio-distribution, expression, and toxicity of oligonucleotides have yet to be systematically studied. Similar to new rational approaches to drug and vaccine design, new delivery technologies must exploit findings from basic science. Some of these hurdles may not be overcome for decades, yet the need for advanced therapies persists.

7.2 OLD COMPOUNDS, NEW APPROACHES

The approval of new therapies by the US Food and Drug Administration has slowed over the past few years, in part due to the new challenges encountered with advanced biotechnologies [200, 201]. However, the decline in approvals also stems from a lack of suitable drug candidates. Simply put, drug compounds are not being discovered at rates high enough to continue rapid expansion of the pharmaceutical industry [202]. Numerous large drug companies are beginning to see their blockbuster drug go off patent without any suitable replacement candidates in their developmental pipeline. However, substantial room exists for improvement on currently available and previously identified drug compounds. New clinical indications for drugs can continue to be explored and implemented. In addition, vast numbers of potential drug candidates

have previously been identified, but many were unable to be implemented into any efficacious therapies. Some reasons for this include stability of the drugs active state within the body, susceptibility to physiologic pH changes, rapid clearance via the kidney and liver, and even the manifestation of severe, toxic side effects encountered with the most modest of dosing regimens.

The design of controlled-release drug delivery systems enables one to reexamine previously discarded drug candidates. One of the model drug compounds used in this study, DB-67, is a perfect example of this phenomenon. DB-67 has been reported successful in numerous scientific endeavors, yet its application to any specific disease state has yet to be realized. As previously discussed, DB-67 is subject to rapid inactivation within the body in its native state [5]. The dynamic equilibrium between the lactone and hydroxy-acid is severely shifted due to the drug's ability to bind to serum albumin. As a result, the drug exists almost entirely in its inactive state, with little potential to ever realize its therapeutic potential. The work detailed in this dissertation focuses on the incorporation of DB-67 into various degradable polyurethane drug delivery systems via labile covalent bonds. Yet, this was just a starting point and essentially any compound with pendant hydroxyl or amine groups could easily have served as the model compound. The incorporation of chemotherapeutic agents into implantable reservoirs is a proven strategy in the battle against cancer, and we chose to base our delivery systems on this technology [48, 203-205]. DB-67 was chosen primarily for its fluorescent spectrum, which enabled the detection of the species at minute concentrations in aqueous media. The true focus of this dissertation is to discern how a controlled-release drug delivery system's properties can be modulated via chemical means.

7.3 CONTROLLED RELEASE VIA COVALENT INCORPORATION

The vast majority of degradable controlled release systems rely on diffusion as the primary release strategy [31]. Small molecule drugs are incorporated into a pre-fashioned polymer matrix, usually with the aid of a volatile solvent. The drug is dissolved in the solvent, the matrix is then soaked in the solvent for an extended period, and the solvent is removed. This leaves the drug dispersed throughout the polymer matrix, absorbed onto its surface. These types of systems provide only a transient release phase, and the matrix material remains long after the drug load

has been exhausted. When delivering large drug molecules such as proteins, the compound can be incorporated into porous matrices; the drug becomes entrapped due to small pore size relative to the large drug compound or tortuous routes of diffusion. While long-term release over months and even years has been reported from such systems, the short half-lives of proteins within these matrices often leads to release of inactive drug species [206-208].

It was our goal to design a system capable of releasing small drug molecules over an extended period. If this were to be the case, the release rate would need to be dictated by material erosion, not by diffusion. It was hypothesized that this could be achieved by covalently incorporating a drug moiety via its pendant functional groups into the polymer matrix. The vast majority of drug compounds have either free amine or hydroxyl groups, or both, present somewhere within their chemical structures. These functional groups can easily be converted to urethane bonds in the presence of a suitable catalyst. DB-67 possess two hydroxyl groups, one aromatic and one tertiary, that were used to incorporate the species into a polyurethane network fashioned from LDI and glycerol. We have demonstrated that it is possible to release a small molecule drug over an extended period from such systems, with the release dictated by material erosion rather than drug diffusion.

7.4 CONTROLLED RELEASE VIA ALTERATIONS IN MATERIAL MORPHOLOGY

It has been demonstrated repeatedly through numerous scientific studies that a material's morphology significantly impacts its ability to deliver a drug compound [209-211]. For example, porous polymer matrices release drug at rates significantly different from hydrogels and thin films. Surface to volume considerations become important when designing materials to elute drug at pre-determined rates. If one can accurately control the material morphology, then one can essentially tailor the release properties to meet specific application criteria.

The versatility of polyurethane materials results from their unique chemistry. The material properties correlate to the poly-alcohols, -amines, and -isocyanates used to synthesize them. Once the reactants have been chosen and their relative molar ratios are defined, the blowing, gelling, and cross-linking reactions that condense these agents into urethane and urea

bonds can be selected to occur to differing degrees This gives rise to numerous structural permutations of a solitary reactant mixture. We have utilized these tools to design polyurethane materials with differing material morphology.

The first LDI-glycerol polyurethane drug delivery system described was a small solid disc cut from a cast polymer film. A viscous LDI-glycerol pre-polymer was prepared, incorporating DB-67 into the material via labile urethane linkages. The film was prepared via a non-solvent casting technique, where the polymerization solvent and the polymer non-solvent were miscible. The resulting polymer discs were shown to be relatively uniform in terms of their drug content and morphology. The first permutation on LDI-glycerol polyurethane drug delivery systems was a foam material prepared from the same reactant mixture used in the synthesis of the polyurethane discs. By using a different catalyst and processing techniques, we were able to construct a second drug delivery system with vastly different material morphology. As hypothesized, the drug elution rates from the two systems were vastly different from one another. The foam materials degraded at a much faster rate, delivering more of its drug-load into solution than the corresponding disc materials. The difference in the release rates of the two-systems can be correlated to the material morphology, more specifically, the surface-to-volume ratio. Although exact measurements were not taken, it is clear from scanning electron micrographs that the LDI-glycerol foam materials possess a much greater surface-to-volume ratio than do the polyurethane discs. Considering the crude processing techniques used to fashion these materials in the laboratory, there is substantial opportunity to further refine these materials by utilizing sophisticated synthetic techniques. Once tighter control on material morphology can be gained, materials can begin to be evaluated for their controlled release potential. Further studies will elucidate key structure-release correlations that can be used to develop tightly regulated controlled release systems.

7.5 CONTROLLED RELEASE VIA CATALYST MECHANISM

Polyurethanes are among the most versatile of synthetic materials, and an enormous body of literature exists describing their synthesis and differing material properties. As previously mentioned, the physical properties of polyurethane materials can easily be tailored to specific

material applications. Countless review articles detailing the vast number of processing manufacturing techniques exist and aid the engineer in designing a material for a specific function [212-218]. The synthetic component that is most important in dictating the material properties of the polyurethane is the catalyst. The mechanisms of many urethane catalysts have been deduced, and the selectivity and specificity resulting from the individual mechanisms can be used to control polyurethane synthesis.

In light of these facts, it was hypothesized that the controlled release of DB-67 from LDI-glycerol polyurethane materials could be altered by a change in catalyst alone. To this end, tertiary amine catalysts with different reactivity profiles were selected. The non-selective catalyst 1,4-diazobicyclo[2.2.2]-octane (DABCO), is known to readily catalyze the gelling, blowing, and cross-linking reactions, while 4,4'-(oxydi-2,1-ethane-diyl)bismorpholine (DMDEE) primarily catalyzes the blowing reaction [219]. As a result, of the differences in the catalytic activities of DABCO and DMDEE, the release of DB-67 from the resulting foams should vary. A significant difference in the release of DB-67 from the LDI-glycerol polyurethane foams was detected, proving that controlled release can be modulated via only a change of urethane catalyst. Considering the crude processing techniques used to fashion the foams, there remains considerable room for further investigation.

Using more sensitive processing techniques should result in the ability to actively control material properties and provide finer control of drug release relative to urethane catalyst. In addition, other catalyst systems with different selectivity from either DABCO or DMDEE should be assessed in order to elucidate key catalyst-release correlations. These correlations can then be used in the design and synthesis of highly regulated drug delivery systems. They may even be able to be expanded to other polymer systems besides polyurethanes, such as polyesters.

7.6 CONTROLLED RELEASE VIA DRUG STRUCTURE

It is no surprising fact that drugs delivered from controlled release systems possess differing chemical structures. The chemical structure of the agent ultimately determines the how the interaction with the target biological system occurs. Since the modulation of biological processes is dependent upon the chemical structure of a drug, it is therefore necessary to incorporate

different structures into controlled release systems. Differential release has been observed to occur for a variety of compounds, based primarily on their hydrophobic or hydrophilic character [220-222]. As previously described, drug loading is done in a passive fashion where the drug is absorbed onto but not attached into the polymer. Solubility, diffusive properties, and the drug's affinity for the polymer matrix determine its eventual release characteristics.

However, one can look beyond the hydrophobic and hydrophilic character of a drug, and begin to examine its physical structure. DB-67 and doxorubicin possess unique chemical structures, characterized by two and six functional groups, respectively (Figure 51).

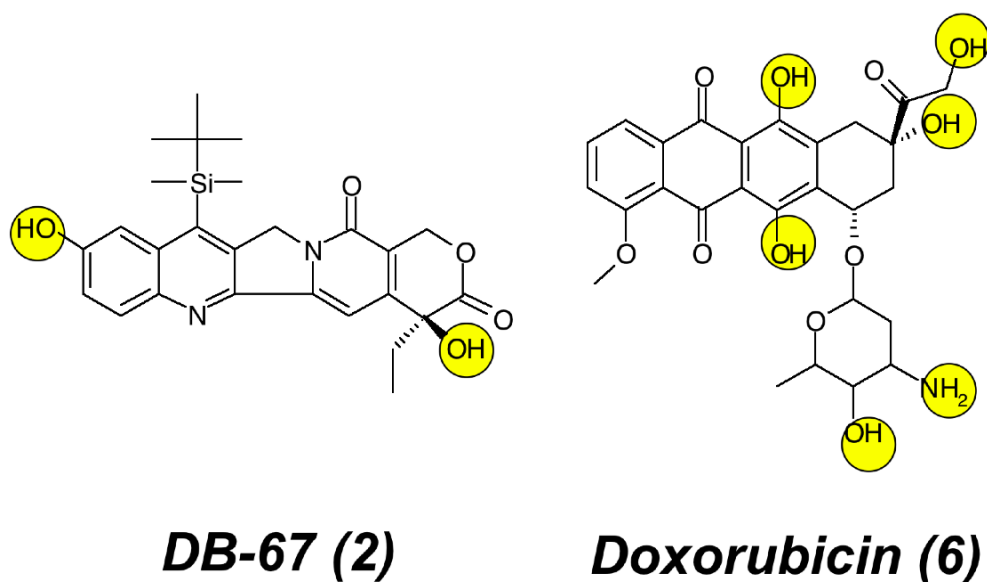


Figure 51 – Structure and attachments of DB-67 and doxorubicin

We have shown that LDI will react with these functional groups to varying degrees in the presence of a urethane catalyst. Since every drug will possess different number and type of functional groups, it is possible to form urethane and urea bonds in differing chemical environments. It was then hypothesized that these differing urethane and urea bond will exhibit different susceptibility to hydrolysis. Since hydrolysis is the primary mechanism governing drug release from the LDI-glycerol polyurethanes, each drug should elute at its own characteristic rate. In essence, the number and type of functional group present on the drug will dictate its controlled release when tethered into the polyurethane network via covalent linkages.

In order to test this hypothesis, a series of naphthalene related compounds were selected to serve as model drug compounds. Mono- and bi-functional hydroxyl and amine derivatives comprising the series were incorporated into LDI-glycerol polyurethane foams in order to assess their release rates. It was subsequently found that material structure plays a key role in dictating the release of these compounds from the polyurethane foams. A “true” drug-delivery LDI-glycerol polyurethane foam was then made, incorporating DB-67, doxorubicin, and paclitaxol. Once again, release rates were shown to correlate to a drug’s chemical structure, presumably due to the differential hydrolysis of urea and urethane bonds.

Typically, when multiple drugs have been released from a single device, it has been accomplished via two separate phases or multiple reservoirs[163, 223-230]. The diffusive properties of the two-phases govern the release of the encapsulated drug compounds. Our approach is different in that multiple drug release has been accomplished from a single-phase material. Not only is the material single-phase, but also it was fashioned in a one-step synthetic reaction. This area of drug delivery has only just begun to be explored, but one can already see the advantages gained in terms of ease of fabrication and versatility with respect to incorporation of different drug species. It is our hope to continue exploration of multiple release systems based on the differential hydrolysis of urethane and urea bonds.

7.7 CONTROLLED RELEASE VIA IONIC LIGANDS

Controlled drug release is a complex process, relying on a precise balance between biology and materials science. We can often look to nature for clues on how to exhibit control over material performance and behavior. For instance, the amphiphilic nature of phospholipids facilitates the ordered structure of cellular membranes, and the precise regulation of ion concentrations underlies brain and kidney function. Ionic substances are indeed important to normal physiologic regulation, maintaining many of the precise balances required for homeostasis. It was of interest to determine if ionic constituents could be used to augment the controlled-release from LDI-glycerol polyurethanes.

The use of ionic species in drug delivery has been limited, mainly augmenting the swelling characteristics of various hydrogel delivery systems [231-233]. It was hypothesized that

the degradation rates of LDI-glycerol polyurethane materials could be enhanced via the incorporation of ionic ligands. The reasons for this are two-fold: (1) the swelling characteristics of the material will change leading to enhanced water uptake and (2) the presence of ions is noted to affect degradation of polyurethanes, enhancing their breakdown [188]. Choline chloride and isethionic acid, two naturally occurring ionic ligands, were chosen to assess ionic effects on LDI-glycerol controlled release systems. The biologic function of these materials has already been discussed in a previous chapter. However, it should be noted again that both ligands contain one primary hydroxyl functional group; choline chloride is cationic and isethionic acid is anionic. Incorporation of these ligands into the polymer network essentially results in chain termination since they are mono-functional. Chain termination will effectively change the overall hydroxyl functionality, changing the network architecture in the process. The non-ionic species, 3,3-dimethyl-butanol, is structurally similar to CC and ISE and was used as a control for the overall change in network architecture

We have decidedly shown that the incorporation of ionic ligands drastically alters the swelling rates and the overall drug delivery characteristics of the LDI-glycerol polyurethane materials. These ligands were mono-functional and represented only two possible ionic groups – quaternary amines and sulfonates. Future work should examine the relative effect of other ionic groups, such as carboxylic acids and phosphate, both of which are known to react to a slight degree with isocyanates. The incorporation of such ligands may result in substantial changes in material properties due to the reactivity of the acid and phosphate group. Multi-functional ionic species should also be examined. Ligands with multiple hydroxyl groups and amine groups, as well as multiple ionizing groups should be evaluated in tandem. The results present here only hint at the potential of ionic ligands to modulate drug delivery.

7.8 CONCLUSION

The results presented in this dissertation lay the groundwork for future endeavors in controlled release drug delivery systems based on LDI-glycerol polyurethane materials. Chemical means of controlling drug-delivery have been investigated, including the following: (1) covalent incorporation of drug species, (2) manipulation of material morphology, (3) catalytic control of

drug elution, (4) differential release based on drug structure, and (5) role of ionic ligands. Covalent incorporation of a number of drug structures was possible, and the release rates corresponded to material erosion, rather than drug diffusion. The polyurethane film systems released materials at a much slower rate than their corresponding foam materials. The film and foam drug delivery systems were shown to exert significant anti-proliferative effects in vitro against malignant glioma cell lines related to the controlled release of DB-67. A simple change in catalyst has been shown to alter release rates from otherwise identical LDI-glycerol polyurethane materials. A drug's chemical structure was able to dictate its release profile following covalent incorporation, making release of multiple drugs at different rates from a single-phase material possible. Finally, the ionic ligands choline chloride and isethionic acid were shown to substantially alter swelling and release characteristics of LDI-glycerol materials. As a result, of this work, a number of key design principles have been elucidated that will aid in the future development of controlled release systems. Significant progress was made with regard to each chemical control method, but in doing so, more questions were posed than could be answered. Drug delivery is truly a complex process, lying at the intersection of three worlds: chemistry, biology, and engineering. For the rational design of biomaterials, an understanding of polymer chemistry and polymer physics is necessary, but not sufficient. Equally important is a quantitative understanding of the principle rates that govern drug transport, interaction, and clearance in both normal physiologic and abnormal pathologic situations. This is not always an easy environment in which to work, but tremendous potential to treat or even cure human disease serves as motivation.

BIBLIOGRAPHY

1. Doyle FP. Medicinal chemistry and current problems in drug development. *Med Chem Adv, Proc Int Symp*, 7th 1981:11-26.
2. Li Q-Y, Zu Y-G, Shi R-Z, Yao L-P. Review camptothecin: current perspectives. *Current Medicinal Chemistry* 2006;13(17):2021-2039.
3. Reddy LH. Drug delivery to tumours: Recent strategies. *Journal of Pharmacy and Pharmacology* 2005;57(10):1231-1242.
4. Luo Y, Prestwich GD. Cancer-targeted polymeric drugs. *Curr Cancer Drug Targets* 2002 Sep;2(3):209-226.
5. Jung LL, Zamboni WC. Cellular, pharmacokinetic, and pharmacodynamic aspects of response to camptothecins: can we improve it? *Drug Resist Updat* 2001 Aug;4(4):273-288.
6. Pommier Y, Pourquier P, Urasaki Y, Wu J, Laco GS. Topoisomerase I inhibitors: selectivity and cellular resistance. *Drug Resist Updat* 1999 Oct;2(5):307-318.
7. Urasaki Y, Laco G, Takebayashi Y, Bailly C, Kohlhagen G, Pommier Y. Use of camptothecin-resistant mammalian cell lines to evaluate the role of topoisomerase I in the antiproliferative activity of the indolocarbazole, NB-506, and its topoisomerase I binding site. *Cancer Res* 2001 Jan 15;61(2):504-508.
8. Hertzberg RP, et al. Modification of the hydroxy lactone ring of camptothecin: inhibition of mammalian topoisomerase I and biological activity. *J Med Chem* 1989 Mar;32(3):715-720.
9. Jaxel C, Kohn KW, Wani MC, Wall ME, Pommier Y. Structure-activity study of the actions of camptothecin derivatives on mammalian topoisomerase I: evidence for a specific receptor site and a relation to antitumor activity. *Cancer Res* 1989 Mar 15;49(6):1465-1469.
10. Burke TG, Mi Z. Preferential binding of the carboxylate form of camptothecin by human serum albumin. *Anal Biochem* 1993 Jul;212(1):285-287.
11. Mi Z, Burke TG. Marked interspecies variations concerning the interactions of camptothecin with serum albumins: a frequency-domain fluorescence spectroscopic study. *Biochemistry* 1994 Oct 25;33(42):12540-12545.

12. Mi Z, Burke TG. Differential interactions of camptothecin lactone and carboxylate forms with human blood components. *Biochemistry* 1994 Aug 30;33(34):10325-10336.
13. Read TA, Thorsen F, Bjerkvig R. Localised delivery of therapeutic agents to CNS malignancies: old and new approaches. *Curr Pharm Biotechnol* 2002 Sep;3(3):257-273.
14. Zagouras NG, Koutinas AA. Processing scheme based on selective dissolution to recycle food packaging and other polymeric wastes and its economic analysis. *Waste Management & Research* 1995;13(4):325-333.
15. Bilban M. Mutagenic testing of workers exposed to toluene-diisocyanates during plastics production process. *Am J Ind Med FIELD Full Journal Title:American journal of industrial medicine* 2004;45(5):468-474.
16. Schnorr TM, Steenland K, Egeland GM, Boeniger M, Egilman D. Mortality of workers exposed to toluene diisocyanate in the polyurethane foam industry. *Occup Environ Med FIELD Full Journal Title:Occupational and environmental medicine* 1996;53(10):703-707.
17. Frisch KC, Klempner D, Editors. *Advances in Urethane Science and Technology*, Vol. 12, 1993.
18. Vratsanos M. Polyurethane Catalysts. In: Salamone JC, editor. *Polymeric Materials Encyclopedia*. New York: CRC Press Inc., 1996. p. 6947-6957.
19. Becker R, Thiele L. Polyurethane Catalysis. In: Salamone JC, editor. *Polymeric Materials Encyclopedia*. New York: CRC Press Inc., 1996. p. 6940-6947.
20. Silva AL, Bordado JC. Recent Developments in Polyurethane Catalysis: Catalytic Mechanisms Review. *Catalysis Reviews - Science and Engineering* 2004;46(1):31-51.
21. Zhang XD, Neff RA, Macosko CW. Foam stability in flexible polyurethane foam systems. *Polymeric Foams* 2004:139-172.
22. Baker JW, Gaunt J. Mechanism of the reaction of aryl isocyanates with alcohols and amines. III. The "spontaneous" reaction of phenyl isocyanate with various alcohols. Further evidence relating to the anomalous effect of dialkylanilines in the base-catalyzed reaction. *Journal of the Chemical Society* 1949:19-24.
23. Baker JW, Gaunt J. Mechanism of the reaction of aryl isocyanates with alcohols and amines. II. The base-catalyzed reaction of phenyl isocyanate with alcohols. *Journal of the Chemical Society* 1949:9-18.
24. Baker JW, Holdsworth JB. Mechanism of aromatic side-chain reactions with special reference to the polar effects of substituents. XIII. Kinetic examination of the reaction of aryl isocyanates with methyl alcohol. *Journal of the Chemical Society* 1947:713-726.

25. Luo S-G, Tan H-M, Zhang J-G, Wu Y-J, Pei F-K, Meng X-H. Catalytic mechanisms of triphenyl bismuth, dibutyltin dilaurate, and their combination in polyurethane-forming reaction. *Journal of Applied Polymer Science* 1997;65(6):1217-1225.
26. Sun H, Zhang L, Szeto K-Y. Bismuth in medicine. *Metal Ions in Biological Systems* 2004;41(Metal Ions and Their Complexes in Medication):333-378.
27. Sadler PJ, Li H, Sun H. Coordination chemistry of metals in medicine: target sites for bismuth. *Coordination Chemistry Reviews* 1999;185-186:689-709.
28. Britain JW, Gemeinhardt PG. Catalysis of the isocyanate-hydroxyl reaction. *Journal of Applied Polymer Science* 1960;4:207-211.
29. Robins J. Structural effects in metal ion catalysis of isocyanate-hydroxyl reactions. *Journal of Applied Polymer Science* 1965;9(3):821-838.
30. Thiele L, Becker R. Catalytic mechanisms of polyurethane formation. *Advances in Urethane Science and Technology* 1993;12:59-85.
31. Ranade VV, Hollinger MA. *Drug Delivery Systems, Second Edition*, 2004.
32. Flynn GL. Considerations in controlled release drug delivery systems. *Pharmaceutical Technology* 1982;6:33-39.
33. Ehrlich P, Bolduan CF. *Collected studies on immunity*. 1st 1st thousand. ed. New York: J. Wiley & Sons; [etc. etc.], 1906.
34. Ghose T, Cerini M, Carter M, Nairn RC. Immunoradioactive agent against cancer. *British medical journal* 1967;1(532):90-93.
35. Bale WF, Spar IL, Goodland RL. Experimental radiation therapy of tumors with I-131-carrying antibodies to fibrin. *Cancer research* 1960;20:1488-1494.
36. Ghose T, Norvell ST, Guclu A, Cameron D, Bodurtha A, MacDonald AS. Immunochemotherapy of cancer with chlorambucil-carrying antibody. *British medical journal* 1972;3(825):495-499.
37. Moolten FL, Capparell NJ, Cooperband SR. Antitumor effects of antibody-diphtheria toxin conjugates. Use of hapten-coated tumor cells as an antigenic target. *Journal of the National Cancer Institute (1940-1978)* 1972;49(4):1057-1062.
38. Li X, Jasti B. *Design of Controlled Release Drug Delivery Systems*. New York: McGraw-Hill, 2006.
39. Yolles S, Eldridge JE, Woodland JHR. Sustained delivery of drugs from polymer/drug mixtures. *Polymer News* 1971;1(4-5):9-15.

40. Ringsdorf H. Structure and properties of pharmacologically active polymers. *Journal of Polymer Science, Polymer Symposia* 1975;51(Int. Symp. Macromol. Honor Professor Herman F. Mark):135-153.
41. Kataoka K. Targetable polymeric drugs. *Controlled Drug Delivery* 1997:49-71.
42. Maeda H, Seymour LW, Miyamoto Y. Conjugates of anticancer agents and polymers: advantages of macromolecular therapeutics in vivo. *Bioconjug Chem* 1992 Sep-Oct;3(5):351-362.
43. Takakura Y, Fujita T, Hashida M, Maeda H, Sezaki H. Control of pharmaceutical properties of soybean trypsin inhibitor by conjugation with dextran. II: Biopharmaceutical and pharmacological properties. *J Pharm Sci* 1989 Mar;78(3):219-222.
44. Matsumura Y, Maeda H. A new concept for macromolecular therapeutics in cancer chemotherapy: mechanism of tumoritropic accumulation of proteins and the antitumor agent smancs. *Cancer Res* 1986 Dec;46(12 Pt 1):6387-6392.
45. Duncan R, Cable HC, Rejmanova P, Kopecek J, Lloyd JB. Tyrosinamide residues enhance pinocytic capture of N-(2-hydroxypropyl)methacrylamide copolymers. *Biochimica et Biophysica Acta, General Subjects* 1984;799(1):1-8.
46. Nishida K, Eguchi Y, Takino T, Takakura Y, Hashida M, Sezaki H. Hepatic disposition characteristics of ¹¹¹In-labeled lactosaminated bovine serum albumin in rats. *Pharm Res* 1991 Oct;8(10):1253-1257.
47. Rauck RL. Intrathecal drug delivery. *Seminars in Pain Medicine* 2004;2(1):2-7.
48. Brem H, Gabikian P. Biodegradable polymer implants to treat brain tumors. *Journal of Controlled Release* 2001;74(1-3):63-67.
49. Guerin C, Olivi A, Weingart JD, Lawson HC, Brem H. Recent Advances in Brain Tumor Therapy: Local Intracerebral Drug Delivery by Polymers. *Investigational New Drugs* 2004;22(1):27-37.
50. Hu L-D, Liu Y, Tang X, Zhang Q. Preparation and in vitro/in vivo evaluation of sustained-release metformin hydrochloride pellets. *European Journal of Pharmaceutics and Biopharmaceutics* 2006;64(2):185-192.
51. Parab PV, Oh CK, Ritschel WA. Release of theophylline from ethyl cellulose microcapsules alone and in conjunction with fat embedded (Precirol) granules and hydroxypropyl methyl cellulose. *Drug Development and Industrial Pharmacy* 1987;13(3):449-472.
52. Luo Y, Kirker KR, Prestwich GD. Cross-linked hyaluronic acid hydrogel films: new biomaterials for drug delivery. *J Control Release* 2000 Oct 3;69(1):169-184.
53. Sinha VR, Khosla L. Bioabsorbable polymers for implantable therapeutic systems. *Drug Development and Industrial Pharmacy* 1998;24(12):1129-1138.

54. Liu J, Chen L, Li L, Hu X, Cai Y. Steady-state fluorescence study on release of camptothecin from agar hydrogel. *International Journal of Pharmaceutics* 2004;287(1-2):13-19.
55. Lai YC. Hydrolytic stabilities of some polyurethane hydrogels. *Journal of Applied Polymer Science* 1991;42(10):2833-2836.
56. Murdan S. Electro-responsive drug delivery from hydrogels. *Journal of Controlled Release* 2003;92(1-2):1-17.
57. Heller J. Bioerodible hydrogels. *Hydrogels Med Pharm* 1987;3:137-149.
58. Martini A, Ciocca C. Drug delivery systems for cancer drugs. *Expert Opinion on Therapeutic Patents* 2003;13(12):1801-1807.
59. Nayak PL. Biodegradable polymers for medical implants. *Popular Plastics & Packaging* 2005;50(1):79-83.
60. West JL. Drug delivery: Pulsed polymers. *Nature Materials* 2003;2(11):709-710.
61. Waldman SD. Implantable drug delivery systems: practical considerations. *Journal of pain and symptom management* 1990;5(3):169-174.
62. Heller J, Trescony PV. Controlled drug release by polymer dissolution. II: Enzyme-mediated delivery device. *Journal of Pharmaceutical Sciences* 1979;68(7):919-921.
63. Heller J, Baker RW, Gale RM, Rodin JO. Controlled drug release by polymer dissolution. I. Partial esters of maleic anhydride copolymers - properties and theory. *Journal of Applied Polymer Science* 1978;22(7):1991-2009.
64. Bodmeier R, Oh KH, Chen H. The effect of the addition of low-molecular weight poly(DL-lactide) on drug release from biodegradable poly(DL-lactide) drug delivery systems. *International Journal of Pharmaceutics* 1989;51(1):1-8.
65. Yoon CS, Ji DS. Effects of in vitro degradation on the weight loss and tensile properties of PLA/LPCL/HPCL blend fibers. *Fibers and Polymers* 2005;6(1):13-18.
66. Lin WJ, Flanagan DR, Linhardt RJ. Accelerated degradation of poly(epsilon-caprolactone) by organic amines. *Pharmaceutical Research* 1994;11(7):1030-1034.
67. Crawford RR, Esmerian OK. Effect of plasticizers on some physical properties of cellulose acetate phthalate films. *Journal of Pharmaceutical Sciences* 1971;60(2):312-314.
68. Pradhan RS, Vasavada RC. Formulation and in vitro release study on poly(DL-lactide) microspheres containing hydrophilic compounds: glycine homopeptides. *Journal of Controlled Release* 1994;30(2):143-154.

69. Rothen-Weinhold A, et al. Injection-molding versus extrusion as manufacturing technique for the preparation of biodegradable implants. *European Journal of Pharmaceutics and Biopharmaceutics* 1999;48(2):113-121.
70. Arshady R. Preparation of biodegradable microspheres and microcapsules: 2. Polyactides and related polyesters. *Journal of Controlled Release* 1991;17(1):1-21.
71. Wang F-J, Wang C-H. Sustained release of etanidazole from spray dried microspheres prepared by non-halogenated solvents. *Journal of Controlled Release* 2002;81(3):263-280.
72. Hatefi A, Amsden B. Camptothecin delivery methods. *Pharm Res* 2002 Oct;19(10):1389-1399.
73. Wall ME, Wani MC, Cook CE, Palmer KH, McPhail AT, Sim GA. Plant antitumor agents. I. Isolation and structure of camptothecin, a novel alkaloidal leukemia and tumor inhibitor from *Camptotheca acuminata*. *Journal of the American Chemical Society* 1966;88(16):3888-3890.
74. Muggia FM, Creaven PJ, Hansen HH, Cohen MH, Selawry OS. Phase I clinical trial of weekly and daily treatment with camptothecin (NSC-100880): correlation with preclinical studies. *Cancer Chemother Rep* 1972 Aug;56(4):515-521.
75. Moertel CG, Schutt AJ, Reitemeier RJ, Hahn RG. Phase II study of camptothecin (NSC-100880) in the treatment of advanced gastrointestinal cancer. *Cancer Chemother Rep* 1972 Feb;56(1):95-101.
76. Gottlieb JA, Guarino AM, Call JB, Oliverio VT, Block JB. Preliminary pharmacologic and clinical evaluation of camptothecin sodium (NSC-100880). *Cancer Chemother Rep* 1970 Dec;54(6):461-470.
77. Hsiang YH, et al. DNA topoisomerase I-mediated DNA cleavage and cytotoxicity of camptothecin analogues. *Cancer Res* 1989 Aug 15;49(16):4385-4389.
78. Hsiang YH, Lihou MG, Liu LF. Arrest of replication forks by drug-stabilized topoisomerase I-DNA cleavable complexes as a mechanism of cell killing by camptothecin. *Cancer Res* 1989 Sep 15;49(18):5077-5082.
79. Bom D, et al. Novel A,B,E-ring-modified camptothecins displaying high lipophilicity and markedly improved human blood stabilities. *J Med Chem* 1999 Aug 12;42(16):3018-3022.
80. Bom D, et al. The novel silatecan 7-tert-butyldimethylsilyl-10-hydroxycamptothecin displays high lipophilicity, improved human blood stability, and potent anticancer activity. *J Med Chem* 2000 Oct 19;43(21):3970-3980.

81. Bom D, et al. The highly lipophilic DNA topoisomerase I inhibitor DB-67 displays elevated lactone levels in human blood and potent anticancer activity. *J Control Release* 2001 Jul 6;74(1-3):325-333.
82. Walter KA, Tamargo RJ, Olivi A, Burger PC, Brem H. Intratumoral chemotherapy. *Neurosurgery* 1995 Dec;37(6):1128-1145.
83. Storm PB, Moriarity JL, Tyler B, Burger PC, Brem H, Weingart J. Polymer delivery of camptothecin against 9L gliosarcoma: release, distribution, and efficacy. *J Neurooncol* 2002 Feb;56(3):209-217.
84. Berrada M, Serreqi A, Dabbarh F, Owusu A, Gupta A, Lehnert S. A novel non-toxic camptothecin formulation for cancer chemotherapy. *Biomaterials* 2005 May;26(14):2115-2120.
85. Zhang Y, Wang C, Yang W, Shi B, Fu S. Tri-component diblock copolymers of poly(ethylene glycol)-poly(epsilon-caprolactone-co-lactide): Synthesis, characterization and loading camptothecin. *Colloid and Polymer Science* 2005;283(11):1246-1252.
86. Hatefi A, Knight D, Amsden B. A biodegradable injectable thermoplastic for localized camptothecin delivery. *Journal of Pharmaceutical Sciences* 2004;93(5):1195-1204.
87. Zhang JY, Beckman EJ, Piesco NP, Agarwal S. A new peptide-based urethane polymer: synthesis, biodegradation, and potential to support cell growth in vitro. *Biomaterials* 2000 Jun;21(12):1247-1258.
88. Zhang JY, Beckman EJ, Hu J, Yang GG, Agarwal S, Hollinger JO. Synthesis, biodegradability, and biocompatibility of lysine diisocyanate-glucose polymers. *Tissue Eng* 2002 Oct;8(5):771-785.
89. Reynolds MM, et al. Nitric Oxide Releasing Polyurethanes with Covalently Linked Diazeniumdiolated Secondary Amines. *Biomacromolecules* 2006;7(3):987-994.
90. Park J-H, Allen MG, Prausnitz MR. Biodegradable polymer microneedles: Fabrication, mechanics and transdermal drug delivery. *Journal of Controlled Release* 2005;104(1):51-66.
91. Mahkam M, Assadi MG, Zahedifar R, Ramesh M, Davaran S. Linear type azo-containing polyurethanes for colon-specific drug delivery. *Journal of Bioactive and Compatible Polymers* 2004;19(1):45-53.
92. Huang J-C, Jennings EM. The effect of temperature on controlled release of heparin from polyurethane and ethylene vinyl acetate copolymer. *International Journal of Polymeric Materials* 2004;53(1):69-78.
93. Mahkam M, Sharifi-Sanjani N. Preparation of new biodegradable polyurethanes as a therapeutic agent. *Polymer Degradation and Stability* 2003;80(2):199-202.

94. Iskakov R, Batyrbekov E, Zhubanov B, Teleuova T, Volkova M. Polyurethanes as carriers of antitumor drugs. *Polymers for Advanced Technologies* 1998;9(4):266-270.
95. Dey J, Warner IM. Spectroscopic and photophysical studies of the anticancer drug: Camptothecin. *Journal of Luminescence* 1997;71(2):105-114.
96. Pollack IF, Erff M, Bom D, Burke TG, Strode JT, Curran DP. Potent topoisomerase I inhibition by novel silatecans eliminates glioma proliferation in vitro and in vivo. *Cancer Res* 1999 Oct 1;59(19):4898-4905.
97. Burke TG, Mishra AK, Wani MC, Wall ME. Lipid bilayer partitioning and stability of camptothecin drugs. *Biochemistry* 1993 May 25;32(20):5352-5364.
98. Coury AJ. Chemical and biochemical degradation of polymers. *Biomaterials Science* (2nd Edition) 2004:411-430.
99. Kohn J, Abramson S, Langer R. Bioresorbable and bioerodible materials. *Biomaterials Science* (2nd Edition) 2004:115-127.
100. Santerre JP, Woodhouse K, Laroche G, Labow RS. Understanding the biodegradation of polyurethanes: From classical implants to tissue engineering materials. *Biomaterials* 2005;26(35):7457-7470.
101. Sampath P, et al. Camptothecin analogs in malignant gliomas: comparative analysis and characterization. *Journal of Neurosurgery* 2003;98(3):570-577.
102. Tyner KM, Giannelis EP. Nanobiohybrids: Novel gene and drug delivery systems. *Materials Research Society Symposium Proceedings* 2004;EXS-1(Architecture and Application of Biomaterials and Biomolecular Materials):449-451.
103. Janss AJ, et al. Synergistic cytotoxicity of topoisomerase I inhibitors with alkylating agents and etoposide in human brain tumor cell lines. *Anti-Cancer Drugs* 1998;9(7):641-652.
104. Helson L, Helsen C, Ainsworth S. Camptothecin cytotoxic effects in vitro: dependency on exposure duration and dose. *Anti-Cancer Drugs* 1995;6(4):612-614.
105. Hinrichsen G. *Polyurethane handbook* (2nd ed.). Edited by G. Oertel, Hanser Publishers, Munich 1993, 770 pp., DM 358, ISBN 3-446-17198-3, 1994.
106. Guelcher SA. Polyurethanes. *Introduction to Biomaterials* 2006:161-183.
107. Walder AJ. Characteristics of medical polyurethanes. *Plastics Engineering* (Brookfield, Connecticut) 1998;54(4):29-31.
108. Szycher M, Siciliano AA, Reed AM. Polyurethane elastomers in medicine. *Polym Biomater* 1994:233-244.
109. Hasirci N. Polyurethanes. *High Perform Biomater* 1991:71-90.

110. Gogolewski S. Selected topics in biomedical polyurethanes. A review. *Colloid and Polymer Science* 1989;267(9):757-785.
111. Lee S-H, Kim S-R, Kim JS, Bae H-R, Lee C-H, Kim D-D. In-vitro and in-vivo antibacterial activity evaluation of a polyurethane matrix. *Journal of Pharmacy and Pharmacology* 2003;55(4):559-566.
112. Park JH, Lee KB, Kwon IC, Bae YH. PDMS-based polyurethanes with MPEG grafts: mechanical properties, bacterial repellency, and release behavior of rifampicin. *Journal of Biomaterials Science, Polymer Edition* 2001;12(6):629-645.
113. Yamaoka T, Makita Y, Sasatani H, Kim SI, Kimura Y. Linear type azo-containing polyurethane as drug-coating material for colon-specific delivery: its properties, degradation behavior, and utilization for drug formulation. *Journal of Controlled Release* 2000;66(2-3):187-197.
114. Ouchi T, Hagihara Y, Takahashi K, Takano Y, Igarashi I. Synthesis and antitumor activity of poly(ethylene glycol)s linked to 5-fluorouracil via a urethane or urea bond. *Drug Design and Discovery* 1992;9(1):93-105.
115. Huang SJ, Wang JM, Tseng SC, Wang LF, Chen JS. Controlled immobilization of chondroitin sulfate in polyacrylic acid networks. *J Biomater Sci Polym Ed* 2007;18(1):17-34.
116. Jaeger RJ, Plugge H, Szabo S. Acute urinary bladder toxicity of a polyurethane foam catalyst mixture: a possible new target organ for a propionitrile derivative. *Journal of Environmental Pathology and Toxicology* 1980;4(2-3):555-562.
117. Gad SC. A neuromuscular screen for use in industrial toxicology. *J Toxicol Environ Health FIELD Full Journal Title:Journal of toxicology and environmental health* 1982;9(5-6):691-704.
118. Artavia LD, Macosko CW. Polyurethane flexible foam formation. *Low Density Cell Plast* 1994:22-55.
119. Hartley FD, Cross MM, Lord FW. Mechanism of polyurethane foam formation. *Advan Polyurethane Technol* 1968:127-140.
120. Grabner G, Rechthaler K, Mayer B, Koehler G, Rotkiewicz K. Solvent Influences on the Photophysics of Naphthalene: Fluorescence and Triplet State Properties in Aqueous Solutions and in Cyclodextrin Complexes. *Journal of Physical Chemistry A* 2000;104(7):1365-1376.
121. Zuma H, Toyota M, Asakawa Y, Kawano S. Naphthalene - A constituent of Magnolia flowers. *Phytochemistry* 1996;42(4):999-1004.
122. Gabos S, et al. Polycyclic aromatic hydrocarbons in water, fish, and deer liver samples following forest fires. *Organohalogen Compounds* 1999;43:329-333.

123. Gassett JW, et al. Volatile compounds from the forehead region of male white-tailed deer (*Odocoileus virginianus*). *Journal of Chemical Ecology* 1997;23(3):569-578.
124. Szalanski AL, Austin JW, Scheffrahn RH, Messenger MT. Molecular diagnostics of the formosan subterranean termite (Isoptera: Rhinotermitidae). *Fla Entomol* 2004 JUN;87(2):145-151.
125. Niewiadomski T, Wiszniowski K. Technical progress in the manufacture of naphthalene. *Chemik* 1958;11:209-213.
126. Woolhouse TG. Manufacture of naphthalene of crystallizing point 78 Deg. *Journal of Applied Chemistry* 1957;7:573-583.
127. Wainwright MS, Foster NR. Catalysts, kinetics, and reactor design in phthalic anhydride synthesis. *Catalysis Reviews - Science and Engineering* 1979;19(2):211-292.
128. Sinha DN, Sen B, Bhattacharyya NB. Catalytic manufacture of phthalic anhydride in the national context - a retrospective survey. Part I. *Chemical Industry Developments* 1978;12(4):7-14.
129. Freeman HS, Hsu WN, Esancy JF, Esancy MK. Proton magnetic resonance spectra of some naphthalene derivatives. *Dyes and Pigments* 1988;9(1):67-82.
130. Zheng Y, Yanful EK, Bassi AS. A review of plastic waste biodegradation. *Critical Reviews in Biotechnology* 2005;25(4):243-250.
131. Lelah MD. *Polyurethanes in Medicine*, 1986.
132. Stokes K, McVenes R, Anderson JM. Polyurethane elastomer biostability. *Journal of Biomaterials Applications* 1995;9(4):321-354.
133. Akutsu-Shigeno Y, et al. Isolation of a bacterium that degrades urethane compounds and characterization of its urethane hydrolase. *Applied Microbiology and Biotechnology* 2006;70(4):422-429.
134. Labow RS, Tang Y, McCloskey CB, Santerre JP. The effect of oxidation on the enzyme-catalyzed hydrolytic biodegradation of poly(urethane)s. *Journal of Biomaterials Science, Polymer Edition* 2002;13(6):651-665.
135. Hautala RR, Schore NE, Turro NJ. Novel fluorescent probe. Use of time-correlated fluorescence to explore the properties of micelle-forming detergent. *Journal of the American Chemical Society* 1973;95(17):5508-5514.
136. Abuin E, Lissi E. Partition coefficient of naphthalene between water and cetyltrimethylammonium bromide micelles. *Journal of Physical Chemistry* 1980;84(20):2605-2607.

137. Nadal M, Wargent JJ, Jones KC, Paul ND, Schuhmacher M, Domingo JL. Influence of UV-B Radiation and Temperature on Photodegradation of PAHs: Preliminary Results. *Journal of Atmospheric Chemistry* 2006;55(3):241-252.
138. Garcia-Martinez MJ, Canoira L, Blazquez G, Da Riva I, Alcantara R, Llamas JF. Continuous photodegradation of naphthalene in water catalyzed by TiO₂ supported on glass Raschig rings. *Chemical Engineering Journal (Amsterdam, Netherlands)* 2005;110(1-3):123-128.
139. Cvrckova O, Ciganek M. Photostability of polycyclic aromatic hydrocarbons (PAHs) and nitrated polycyclic aromatic hydrocarbons (NPAHs) in dichloromethane and isooctane solutions. *Polycyclic Aromatic Compounds* 2005;25(2):141-156.
140. Lane DA, Tang H. Photochemical degradation of polycyclic aromatic compounds. I. Naphthalene. *Polycyclic Aromatic Compounds* 1994;5(1-4):131-138.
141. Lu Q-W, Hoyer TR, Macosko CW. Reactivity of common functional groups with urethanes: models for reactive compatibilization of thermoplastic polyurethane blends. *Journal of Polymer Science, Part A: Polymer Chemistry* 2002;40(14):2310-2328.
142. Kieffer A, Hartwig A. Interphase reaction of isocyanates with epoxy resins containing functional groups of different reactivity. *Macromolecular Materials and Engineering* 2001;286(4):254-259.
143. Brennan DJ, Tinetti SM. Reactions of the secondary hydroxyl groups of phenoxy-type thermoplastics: model studies and polymer derivatization. *Polymer Preprints (American Chemical Society, Division of Polymer Chemistry)* 1998;39(2):367-368.
144. Smith HA. Effect of urethane groups on the reaction of alcohols with isocyanates. *Journal of Polymer Science, Polymer Chemistry Edition* 1968;6(5):1299-1306.
145. Farkas A, Strohm PF. Mechanism of the amine-catalyzed reaction of isocyanates with hydroxyl compounds. *Industrial & Engineering Chemistry Fundamentals* 1965;4(1):32-38.
146. Chen AY, Shih S-J, Garriques LN, Rothenberg ML, Hsiao M, Curran DP. Silatecan DB-67 is a novel DNA topoisomerase I-targeted radiation sensitizer. *Molecular Cancer Therapeutics* 2005;4(2):317-324.
147. Bence AK, Mattingly CA, Burke TG, Adams VR. The effect of DB-67, a lipophilic camptothecin derivative, on topoisomerase I levels in non-small-cell lung cancer cells. *Cancer Chemotherapy and Pharmacology* 2004;54(4):354-360.
148. Lee YC, Byfield JE. Induction of DNA degradation in vivo by adriamycin. *J Natl Cancer Inst FIELD Full Journal Title:Journal of the National Cancer Institute* 1976;57(1):221-224.

149. Momparler RL, Karon M, Siegel SE, Avila F. Effect of adriamycin on DNA, RNA, and protein synthesis in cell-free systems and intact cells. *Cancer Res* FIELD Full Journal Title:Cancer research 1976;36(8):2891-2895.
150. Tewey KM, Rowe TC, Yang L, Halligan BD, Liu LF. Adriamycin-induced DNA damage mediated by mammalian DNA topoisomerase II. *Science* FIELD Full Journal Title:Science (New York, NY) 1984;226(4673):466-468.
151. Zwelling LA, Michaels S, Erickson LC, Ungerleider RS, Nichols M, Kohn KW. Protein-associated deoxyribonucleic acid strand breaks in L1210 cells treated with the deoxyribonucleic acid intercalating agents 4'-(9-acridinylamino) methanesulfon-m-anisidide and adriamycin. *Biochemistry* FIELD Full Journal Title:Biochemistry 1981;20(23):6553-6563.
152. Rowinsky EK, Cazenave LA, Donehower RC. Taxol: a novel investigational antimicrotubule agent. *J Natl Cancer Inst* FIELD Full Journal Title:Journal of the National Cancer Institute 1990;82(15):1247-1259.
153. Manfredi JJ, Horwitz SB. Taxol: an antimetabolic agent with a new mechanism of action. *Pharmacol Ther* FIELD Full Journal Title:Pharmacology & therapeutics 1984;25(1):83-125.
154. Dvorak J, et al. Liposomal doxorubicin combined with regional hyperthermia: reducing systemic toxicity and improving locoregional efficacy in the treatment of solid tumors. *Journal of Chemotherapy (Firenze, Italy)* 2004;16(Suppl. 5):34-36.
155. Mazue G, et al. Anthracyclines: A review of general and special toxicity studies. *International Journal of Oncology* 1995;7(4):713-726.
156. Donehower RC, Rowinsky EK. An overview of experience with TAXOL (paclitaxel) in the U.S.A. *Cancer Treat Rev* FIELD Full Journal Title:Cancer treatment reviews 1993;19 Suppl C:63-78.
157. Rowinsky EK, Eisenhauer EA, Chaudhry V, Arbuck SG, Donehower RC. Clinical toxicities encountered with paclitaxel (Taxol). *Semin Oncol* FIELD Full Journal Title:Seminars in oncology 1993;20(4 Suppl 3):1-15.
158. Gopferich A, Tessmar J. Polyanhydride degradation and erosion. *Advanced Drug Delivery Reviews* 2002;54(7):911-931.
159. Gopferich A. Polymer degradation and erosion. Mechanisms and applications. *European Journal of Pharmaceutics and Biopharmaceutics* 1996;42(1):1-11.
160. Volpicelli JR, Fenton M. Sustained-release naltrexone formulations for the treatment of alcohol and opioid dependence. *Future Neurology* 2006;1(4):389-398.
161. DiMeco F, Brem H, Weingart JD, Olivi A. Gliadel: a new method for the treatment of malignant brain tumors. *Drug Delivery Systems in Cancer Therapy* 2004:215-228.

162. Anon, inventor. Porous, time-release mechanism for silicon-coated, drug-eluting stent. RD Patent No. 472017, 2003.
163. Zhou T, Lewis H, Foster RE, Schwendeman SP. Development of a multiple-drug delivery implant for intraocular management of proliferative vitreoretinopathy. *Journal of Controlled Release* 1998;55(2,3):281-295.
164. Noble CO, et al. Novel Nanoliposomal CPT-11 Infused by Convection-Enhanced Delivery in Intracranial Tumors: Pharmacology and Efficacy. *Cancer Research* 2006;66(5):2801-2806.
165. Konishi M, et al. In vivo anti-tumor effect of dual release of cisplatin and adriamycin from biodegradable gelatin hydrogel. *Journal of Controlled Release* 2005;103(1):7-19.
166. Richardson TP, Peters MC, Ennett AB, Mooney DJ. Polymeric system for dual growth factor delivery. *Nature Biotechnology* 2001;19(11):1029-1034.
167. Lee BJ, Ryu SG, Cui JH. Controlled release of dual drug-loaded hydroxypropyl methyl cellulose matrix tablet using drug-containing polymeric coatings. *International Journal of Pharmaceutics* 1999;188(1):71-80.
168. Ye W-P, Chien YW. Dual-controlled drug delivery across biodegradable copolymer. I. Delivery kinetics of levonorgestrel and estradiol through (caprolactone/lactide) block copolymer. *Pharmaceutical Development and Technology* 1996;1(1):1-9.
169. Ye W-P, Chien YW. Dual-controlled drug delivery across biodegradable copolymer. II. Delivery kinetics of levonorgestrel and estradiol from (matrix/matrix) laminate drug delivery system. *Journal of Controlled Release* 1996;41(3):259-269.
170. Zhang J, Doll BA, Beckman EJ, Hollinger JO. A biodegradable polyurethane-ascorbic acid scaffold for bone tissue engineering. *J Biomed Mater Res A* 2003 Nov 1;67(2):389-400.
171. Hovorka O, et al. Differences in the intracellular fate of free and polymer-bound doxorubicin. *Journal of Controlled Release* 2002;80(1-3):101-117.
172. Crivellato E, et al. Efficiency of doxorubicin handling by isolated hepatocytes is a valuable indicator for restored cell function. *Histochemical Journal* 2000;32(9):534-543.
173. Chambon MH, Viratelle OM. Interaction of doxorubicin with ATP: quantification of complexes and effect on its diffusion into DNA-loaded liposomes - implication for ATP-driven transport studies. *Analytical Biochemistry* 1998;263(2):198-207.
174. Balasubramanian SV, Straubinger RM. Taxol-lipid interactions: taxol-dependent effects on the physical properties of model membranes. *Biochemistry* 1994 Aug 2;33(30):8941-8947.

175. Wood MJ, Irwin WJ, Scott DK. Photodegradation of doxorubicin, daunorubicin and epirubicin measured by high-performance liquid chromatography. *Journal of Clinical Pharmacy and Therapeutics* 1990;15(4):291-300.
176. Beijnen JH, Van der Houwen OAGJ, Underberg WJM. Aspects of the degradation kinetics of doxorubicin in aqueous solution. *International Journal of Pharmaceutics* 1986;32(2-3):123-131.
177. Cyrankiewicz M, Ziomkowska B, Kruszewski S. Membranes affinity of hydroxycamptothecins, anticancer agents, determined by fluorescence spectra analysis. *Optica Applicata* 2006;36(2-3):209-215.
178. Bom D, et al. The Novel Silatecan 7-tert-Butyldimethylsilyl-10-hydroxycamptothecin Displays High Lipophilicity, Improved Human Blood Stability, and Potent Anticancer Activity. *Journal of Medicinal Chemistry* 2000;43(21):3970-3980.
179. Brenner GMaS, C.W. *Pharmacology*, 2nd Edition. Philadelphia, PA: Saunders Company (Elsevier), 2006.
180. Warren R, et al. Human in vitro and in vivo cutaneous responses to soap suspensions: role of solution behavior in predicting potential irritant contact dermatitis. *In Vitro & Molecular Toxicology* 1999;12(2):97-107.
181. Welty JD, Read WO. Studies On Some Cardiac Effect Of Taurine. *J Pharmacol Exp Ther* 1964 Apr;144:110-115.
182. Welty JD, Read WO, Shaw EH, Jr. Isolation of 2-hydroxyethanesulfonic acid (isethionic acid) from dog heart. *J Biol Chem* 1962 Apr;237:1160-1161.
183. Banister J, Whittaker VP. Pharmacological activity of the carbon analog of acetylcholine. *Nature (London, United Kingdom)* 1951;167:605-606.
184. Hasan FB, Elkind JL, Cohen SG, Cohen JB. Cationic and uncharged substrates and reversible inhibitors in hydrolysis by acetylcholinesterase (EC 3.1.1.7). The trimethyl subsite. *The Journal of biological chemistry* 1981;256(15):7781-7785.
185. Skarja GA, Woodhouse KA. In vitro degradation and erosion of degradable, segmented polyurethanes containing an amino acid-based chain extender. *J Biomater Sci Polym Ed FIELD Full Journal Title:Journal of biomaterials science Polymer edition* 2001;12(8):851-873.
186. Matuszak ML, Frisch KC, Reegen SL. Hydrolysis of linear polyurethanes and model monocarbamates. *Journal of Polymer Science, Polymer Chemistry Edition* 1973;11(7):1683-1690.
187. Zhang JY, Doll BA, Beckman EJ, Hollinger JO. Three-dimensional biocompatible ascorbic acid-containing scaffold for bone tissue engineering. *Tissue Eng* 2003 Dec;9(6):1143-1157.

188. Lamba NMK, Woodhouse KA, Cooper SL. Polyurethanes in Biomedical Applications, 1997.
189. Marcus Y. A simple empirical model describing the thermodynamics of hydration of ions of widely varying charges, sizes, and shapes. *Biophysical Chemistry* 1994;51(2-3):111-127.
190. Genesis 9:20-21, The Bible. New Revised Standard Version ed. Grand Rapids, MI: Zondervan Publishing House.
191. Matthew 27:33-34, The Bible. New Revised Standard Version ed. Grand Rapids, MI: Zondervan Publishing House.
192. Gilman AG. Goodman and Gilman's Pharmacological Basis of Therapeutics. 7th ed, 1985.
193. Pratt WB, Ruddon RW. The Anticancer Drugs [with Reference to Pharmacology], 1979.
194. Payette PJ, Davis HL. History of vaccines and positioning of current trends. *Current Drug Targets: Infectious Disorders* 2001;1(3):241-247.
195. Tsukada H, Inoue A, Nomiya T, Kan A, Koseki Y. Metabolism of cancer cells and its relation to anti-cancer chemicals. I. Influences of nitrogen mustard and its N-oxide upon metabolism of Ehrlich ascites tumor cells. *Gan FIELD Full Journal Title:Gan Gann; the Japanese journal of cancer research* 1957;48(4):415-417.
196. Bentley R. The development of penicillin: Genesis of a famous antibiotic. *Perspectives in Biology and Medicine* 2005;48(3):444-452.
197. Forsham PH. Milestones in the 60-year history of insulin (1922-1982). *Diabetes Care FIELD Full Journal Title:Diabetes care* 1982;5 Suppl 2:1-3.
198. Saltzman WM. Drug Delivery: Engineering, Principles for Drug Therapy, 2001.
199. Banker GS, Rhodes CT. *Modern Pharmaceutics*, Vol. 7, 1979.
200. Manuel SM, Piascik P. How FDA approves biotechnology drugs. *Am Pharm FIELD Full Journal Title:American pharmacy* 1995;NS35(5):14-15.
201. Santell JP. Projecting future drug expenditures--1993. *Am J Hosp Pharm FIELD Full Journal Title:American journal of hospital pharmacy* 1993;50(1):71-77.
202. Munos B. Can open-source R&D reinvigorate drug research? *Nature Reviews Drug Discovery* 2006;5(9):723-729.
203. Blackshear PJ. Implantable drug-delivery systems. *Scientific American* 1979;241(6):66-73.
204. Dash AK, Cudworth GC, 2nd. Therapeutic applications of implantable drug delivery systems. *Journal of pharmacological and toxicological methods* 1998;40(1):1-12.

205. Langer R, Urquhart J, Blackshear PJ. Implantable drug delivery systems. Transactions - American Society for Artificial Internal Organs 1981;27:648-654.
206. Torchilin VP, Lukyanov AN. Peptide and protein drug delivery to and into tumors: challenges and solutions. Drug Discovery Today 2003;8(6):259-266.
207. Lee VHL. Problems and solutions in peptide and protein drug delivery. Pharmacokinet Pharmacodyn 1991;3:80-92.
208. Lee VHL. Peptide and protein drug delivery - problems and some solutions. Pept: Target New Drug Dev 1991:120-134.
209. Nair R-H. Cocrystals: Molecular Design of Pharmaceutical Materials. Molecular Pharmaceutics 2007;4(3):299-300.
210. Okamoto H, Takeda K. Molecular design and morphology of peptide nanotubes: Towards the novel drug delivery materials. Journal of Drug Delivery Science and Technology 2005;15(1):97-107.
211. Silva GA, Costa FJ, Neves NM, Reis RL. Microparticulate release systems based on natural origin materials. Advances in Experimental Medicine and Biology 2004;553(Biomaterials):283-300.
212. Taverna M. Polyurethane processing: Recent developments. Advances in Urethane Science and Technology 2001:113-155.
213. Housel T. Flexible polyurethane foam. Handbook of Polymer Foams 2004:85-122.
214. Eaves D. Rigid polyurethane foams. Handbook of Polymer Foams 2004:55-84.
215. Haberstroh E, Kleba I. Bladder reaction injection molding: Manufacturing of low polyurethane foam parts using flexible mold cores. Journal of Polymer Engineering 2001;21(2-3):147-165.
216. Schmelzer HG, Kumpf RJ. Reactive processing of polymers: A) Reactive processing of engineering thermoplastics; B) Reaction injection molding of polyurethanes. Journal of Macromolecular Science, Pure and Applied Chemistry 1997;A34(10):2085-2101.
217. Jeffs M. Polyurethane: A polymer addressing the environmental issues of the 21st century. Cellular Polymers 1996;15(2):117-129.
218. Kowligi RR, Calcotte RW. Vascular prostheses from polyurethanes: methods for fabrication and evaluation. High Perform Biomater 1991:425-442.
219. Florio JJ. Catalysis of urethane systems. Handbook of Coatings Additives (2nd Edition) 2004:1-30.

220. Tang Y-D, Venkatraman SS, Boey FYC, Wang L-W. Sustained release of hydrophobic and hydrophilic drugs from a floating dosage form. *International Journal of Pharmaceutics* 2007;336(1):159-165.
221. Trikeriotis M, Ghanotakis DF. Intercalation of hydrophilic and hydrophobic antibiotics in layered double hydroxides. *International Journal of Pharmaceutics* 2007;332(1-2):176-184.
222. Nounou MM, El-Khordagui LK, Khalafallan NA, Khalil SA. In vitro release of hydrophilic and hydrophobic drugs from liposomal dispersions and gels. *Acta Pharmaceutica (Zagreb, Croatia)* 2006;56(3):311-324.
223. Prescott JH, et al. Chronic, programmed polypeptide delivery from an implanted, multireservoir microchip device. *Nature Biotechnology* 2006;24(4):437-438.
224. Matsumoto A, Matsukawa Y, Horikiri Y, Suzuki T. Rupture and drug release characteristics of multi-reservoir type microspheres with poly(DL-lactide-co-glycolide) and poly(DL-lactide). *International Journal of Pharmaceutics* 2006;327(1-2):110-116.
225. Zhou HY, Chen XG, Liu CS, Meng XH, Liu CG, Yu LJ. Release characteristics of three model drugs from chitosan/cellulose acetate multimicrospheres. *Biochemical Engineering Journal* 2006;31(3):228-233.
226. Douaihy CM, Koka V, Mingotaud C, Gauffre F. Tunable sustained release properties of "onion-like" phospholipids multilamellar vesicles. *Journal of Colloid and Interface Science* 2006;303(1):280-287.
227. Lynch I, de Gregorio P, Dawson KA. Simultaneous Release of Hydrophobic and Cationic Solutes from Thin-Film "Plum-Pudding" Gels: A Multifunctional Platform for Surface Drug Delivery? *Journal of Physical Chemistry B* 2005;109(13):6257-6261.
228. Abdul S, Poddar SS. A flexible technology for modified release of drugs: multi layered tablets. *Journal of Controlled Release* 2004;97(3):393-405.
229. Streubel A, Siepmann J, Peppas NA, Bodmeier R. Bimodal drug release achieved with multi-layer matrix tablets: transport mechanisms and device design. *Journal of Controlled Release* 2000;69(3):455-468.
230. Iwata M, Nakamura Y, McGinity JW. In vitro and in vivo release properties of brilliant blue and tumor necrosis factor-alpha (TNF-alpha) from poly(DL-lactic-co-glycolic acid) multiphase microspheres. *Journal of Microencapsulation* 1999;16(6):777-792.
231. Satish CS, Satish KP, Shivakumar HG. Hydrogels as controlled drug delivery systems: synthesis, crosslinking, water and drug transport mechanism. *Indian Journal of Pharmaceutical Sciences* 2006;68(2):133-140.

232. Caykara T, Aycicek I. pH-responsive ionic poly(N,N-diethylaminoethyl methacrylate-co-N-vinyl-2-pyrrolidone) hydrogels: Synthesis and swelling properties. *Journal of Polymer Science, Part B: Polymer Physics* 2005;43(19):2819-2828.
233. Peppas N, Khare AR. Preparation, structure and diffusional behavior of hydrogels in controlled release. *Advanced Drug Delivery Reviews* 1993;11(1-2):1-35.